Land-Atmosphere Interactions over the Indonesian Maritime Continent

by

Andi S. Muttaqin

A dissertation submitted in partial fulfillment of

the requirements for the degree of

Doctor of Philosophy

(Atmospheric and Oceanic Sciences)

at the

UNIVERSITY OF WISCONSIN-MADISON

2023

Date of final oral examination: 05/03/2023

The dissertation is approved by the following members of the Final Oral Committee:
    Ankur R. Desai, Professor, Atmospheric and Oceanic Sciences
    Ángel Adames-Corraliza, Assistant Professor, Atmospheric and Oceanic Sciences
    Stephanie Henderson, Assistant Professor, Atmospheric and Oceanic Sciences
    Jingyi Huang, Assistant Professor, Soil Science
    Christopher Kucharik, Professor, Agronomy

Abstract

The "Maritime Continent" (MC) is the largest archipelago in the tropical region, consisting of over 22,000 islands and inhabited by more than 400 million people. This region has a significant impact on global atmospheric circulation, especially during the strong interannual climate variability events, such as El Niño Southern Oscillation (ENSO) and Indian Ocean Dipole (IOD) events, which can have far-reaching effects on global climate patterns. The region is also affected by seasonal variations, such as monsoons (Australian and Indian Monsoons), intraseasonal variations, such as the Madden-Julian Oscillation (MJO), and diurnal variations due to Sea Breeze Circulation (SBC).

These multiscale variabilities influence the livelihood of the inhabitant through weather extremes and affect the practice and sustainability of agriculture in the region, which produces globally essential crops and agricultural commodities. Unfortunately, state-of-the-art global climate and weather prediction models suffer from persistent systematic bias in precipitation and limited prediction skills over the MC, also known as the "MC prediction barrier." Additionally, the MC often disrupts the propagation of MJO, also called the "MC barrier effect." Furthermore, the monsoon transition and onset over the region are challenging to precisely predict due to the "false onset," which affects the planting time of the primary crops, eventually threatening food security. Recent studies hint that land surface properties might contribute to these problems.

This dissertation investigates the role of land-atmosphere interactions over the Indonesian Maritime Continent. Specifically, the study explores the contribution of land-atmosphere feedback to the diurnal cycle of precipitation over the coastal regions of the Maritime Continent. This study also examines the role of land-atmosphere interactions in MJO propagation across the MC. Finally, this study investigates how land-atmosphere feedback modulates the onset of the wet season in the region during the years without significant large-scale circulations. By pursuing these lines of inquiry, the dissertation aims to enhance our understanding of the complex interactions between land and atmosphere, increase resilience to the impacts of climate variability, and improve food security for the millions of people living on the Maritime Continent.

Acknowledgments

I am deeply grateful to everyone who contributed to the successful completion of this work. Above all, I would like to express my heartfelt appreciation to my advisor, Prof. Ankur Desai, for his exceptional guidance, support, and generous funding through his research, professorship, and personal grants. He has been an exemplary mentor, advisor, and friend, and I feel fortunate to have worked under his supervision. In addition, I would like to thank my committee members, Prof. Christopher Kucharik, Dr. Jingyi Huang, Dr. Stephanie Henderson, and Dr. Ángel Adames, for their invaluable feedback and insightful suggestions. I also extend my thanks to the IIE and the AMINEF advisors, who have been instrumental in providing Fulbright fellowship support since the early stage of PhD application. Finally, I appreciate the support and camaraderie of everyone in the Ecometeorology Lab and in the Atmospheric, Oceanic, and Space Science (AOSS) community, who have created a welcoming and stimulating environment for me to grow and learn.

Throughout my time as a Ph.D. student at the University of Wisconsin-Madison, I have been incredibly grateful and blessed to have the love and unwavering support of my wife, Rysda Nurharmelya, and my daughter, Aafiyah Muttaqin. Additionally, I would like to extend my deepest love and appreciation to my mother, Juju Juniah; my late father, Ade Subadio, who passed away during my second year of PhD; my sister, Amalia Nurjanah; my parents-in-law, Harmadji and Kustiati; my families-in-law; colleagues from Universitas Gadjah Mada, Bandung Institute of Technology, and IPB University; and to all of my teachers and friends, who always provided prayer, excellent support, motivations, and endless long-distance encouragement from Indonesia.

Contents

3 The Role of Land-Atmosphere Interactions on the Propagation of Madden-Julian Oscillation Across the Maritime Continent   **41**

List of Figures

List of Tables

Chapter 1

Introduction

The Indonesian Maritime Continent (MC), located between the Indian and Pacific Oceans, is an area of immense importance for global weather and climate patterns. Coined by Ramage (1968), the term 'Maritime Continent' emphasizes the pivotal role played by the Indonesian archipelago in global climate dynamics. The word 'mar·i·time' denotes the close association with the sea or ocean, while 'con·ti·nent' signifies the vast expanse of continuous land, highlighting the unique nature of this region characterized by countless islands interconnected over the shallow seas. This extensive archipelago releases substantial latent heat energy compared to other tropical regions, influencing extratropical circulation.

Furthermore, the position of MC at the intersection of major ocean basins and its complex topography, characterized by widespread islands connected by tropical warm seas, makes it a unique and challenging area for atmospheric and hydrologic research. In particular, land-ocean-atmosphere interactions over the Maritime Continent are crucial in regulating the regional and global climate (Yamanaka et al., 2018). Understanding these interactions and their impacts on weather patterns is essential for improving our ability to forecast extreme events, such as droughts and floods, and advancing our understanding of Earth's climate system.

Of these interactions, ocean-atmosphere interactions over the Maritime Continent elucidate the 'slowly varying' climate variabilities, such as the Indian Ocean Dipole (IOD) and El Niño Southern Oscillation (ENSO), through sea surface temperature and precipitation relationship (McBride et al.,

2003; Nur'utami & Hidayat, 2016). However, ocean-atmosphere interactions alone are insufficient to explain the recent challenges over the Maritime Continent (e.g., Wu et al., 2018; T. Zhang et al., 2019); therefore, more detailed investigations are needed on the land surface role of the Maritime Continent.

Recent modeling and observational studies highlight the essential role of land surface conditions on rainfall characteristics over the Asian monsoon (Takahashi & Polcher, 2019) and on the onset of the Indian monsoon (Barton et al., 2019) through the role of surface fluxes on the planetary boundary layer (PBL). These recent findings and reviews provide a hint that the Maritime Continent land surface dynamics and its interactions with the overlying atmosphere might play a more decisive role on weather and climate variabilities over the region than previously thought, which warrants further investigations.

Therefore, this dissertation focuses on several key aspects of land-atmosphere interactions over the Indonesian Maritime Continent and their implications for regional and global weather and climate patterns, including the effect of land surface properties on sea-breeze circulations, propagation of the Madden-Julian Oscillation (MJO), and monsoon onset variation. Additionally, the implications of these interactions for agriculture in the region are explored, as the local climate variability significantly influences crop productivity and food security.

In this chapter, we will delve into more specific details regarding the global and local importance of the Maritime Continent and the current challenges faced over the region. These challenges include the "MC Prediction Barrier," which hampers accurate weather predictions in the region, the "MC Barrier Effect on MJO Propagation," which contributes to the altered behavior of the MJO over the MC, and local-spatiotemporal monsoon onset variations. Additionally, we will explore the potential importance of land surface properties and their interaction with the overlaying atmosphere in addressing these problems.

1.1   The Maritime Continent: Global and Local Importance

The Maritime Continent holds immense significance on both global and local scales. Encompassing the largest archipelago within the tropics, it spans between $90°E$–$160°E$ longitude and $15°S$–$15°N$ latitude, comprising nearly 22,000 islands of varying sizes, from the smallest island of 0.002 km^2 to the largest island of 785,753 km^2 (Figure 1.1). This complex geography includes high mountain ranges, dense tropical rainforests, and large river systems, fostering a multitude of microclimates across the region.

Serving as a geographical bridge between the Asian and Australian continents, the MC represents a unique climatic and geographical zone. Home to over 400 million people, it houses a rich spectrum of cultural diversity across populations from the Malay Peninsula, the islands of Indonesia, Brunei, the Philippines, and East Timor, as well as Papua New Guinea and the northern tip of Australia. These communities are deeply intertwined with the region's climate, relying on its predictability for agriculture, fishing, and other climate-dependent livelihoods.

The MC plays a pivotal role in global atmospheric circulation. Ramage (1968) first recognized its significant role by modulating meridional latent-heat transport from the tropical heat sources towards higher latitude heat sinks through the upper branch of the Hadley cell that moves poleward (Dhaka & Kumar, 2023). This finding has been further supported by subsequent modeling and observational studies (e.g., Neale & Slingo, 2003; Henderson & Maloney, 2018). The significant latent heat energy over the Indonesian maritime continent determines the intensity of meridional heat transport to higher latitudes, which in turn affects the jet streams (Woollings et al., 2023) and ultimately influences global weather patterns, as the jet streams have a major impact on the subtropical belt over mid-latitudes (Moon et al., 2022).

The climate of the Maritime Continent is characterized by a variety of factors that interact on different spatial and temporal scales, which not only influence the region itself but also have far-reaching global effects. From low to high frequency, the climate variabilities over the region operate in interannual, seasonal, intraseasonal, and diurnal cycles. These climate and weather variabilities are driven by large and small circulations such as the East Walker Cell (EWC), which

is responsible for the El Niño Southern Oscillation (ENSO) in the Pacific Ocean (Trenberth et al., 1998), and the West Walker Cell (WWC), which drives the Indian Ocean Dipole (IOD) in the Indian Ocean (Hamada et al., 2002; Meehl & Arblaster, 2011; Iskandar et al., 2018; Lin & Qian, 2019). Interhemispheric circulations that drive monsoons also play a significant role in the seasonal variation over the region (Chang et al., 2016).

The climate variability over MC is further influenced by the tropical zonal wave and oscillation that drives the Madden-Julian Oscillation (MJO) (Madden & Julian, 1971, 1972), and sea breeze circulation (SBC) over the extensive land-ocean interfaces throughout the maritime continent responsible for the diurnal cycles (Yamanaka, 2016). These multiscale variabilities influence the practice and sustainability of agriculture and farming in the region (Muttaqin et al., 2019; Apriyana et al., 2021).

The low-frequency interannual variabilities, such as ENSO and IOD, are affected by the large-scale ocean-atmosphere interactions (Jin, 1996). However, the ocean-atmosphere perspective alone (e.g., Xue et al., 2020) could not explain some recent challenges over the Maritime Continent, such as the MC "Prediction Barrier" (Wang et al., 2019; Yang et al., 2019), MC "Barrier Effect on MJO Propagation" (Kerns & Chen, 2016; C. Zhang & Ling, 2017; Kerns & Chen, 2020) and local-spatiotemporal Monsoon onset variations over the Maritime Continent (Marjuki et al., 2016). Furthermore, the unique features of the Maritime Continent, such the spatial distribution of its landmasses and land surface properties around the region, introduce additional complexities to these problems, which eventually contribute to the region's influence on the global climate system. Consequently, understanding land-atmosphere interactions in the MC is crucial to link the local processes over the region with its role in global circulations. Fortunately, recent research provides hints that land surface properties and their interaction with the overlaying atmosphere might have potential importance to answer the current problems.

The complex interactions and feedback between the terrestrial land surface and the atmosphere are determined by the mass and energy fluxes between the two systems (Gerken et al., 2019). These interactions are local in space, i.e., the interaction is considered to be between the land surface and the column of air above it, which mutually influence the state variables of the land surface, planetary

boundary layer, and the free atmosphere that allows for modulation of clouds and precipitation (Misra, 2020). The connection from land surface states to atmospheric responses can be considered two segments, i.e., 1) soil state to surface fluxes, and 2) surface fluxes to atmospheric states and precipitation (Dirmeyer, 2011; Santanello et al., 2011). Key variables in the first segment involve soil moisture and its correlation with evapotranspiration (SM-ET) (Betts et al., 1996; Betts, 2004), while the second segment involves evapotranspiration and its correlation with precipitation (ET-P) (Wei & Dirmeyer, 2012). Although the MC is not considered the "hot spot" for land-atmosphere coupling (Koster et al., 2006), the importance of the maritime continent's landmasses is captured in modeling studies (Neale & Slingo, 2003; Zhou et al., 2021) and needs further observational investigations.

1.2 Multi-scale Challenges over the Maritime Continent

1.2.1 MC Prediction Barrier

State-of-the-art global climate models and weather prediction models suffer from persistent systematic bias in precipitation and limited prediction skills over the Indo-Pacific Maritime Continent (MC), also known as the "MC prediction barrier" (Neale & Slingo, 2003; Wang et al., 2019; Yang et al., 2019). MC is a complex system of tropical islands surrounded by shallow-warm seas between the Indian and Pacific oceans, and it is affected by multiscale weather and climate variabilities (Yoneyama & Zhang, 2020). Over this region, models cannot reproduce the observed diurnal precipitation cycle. The timing of the diurnal rainfall peak deviates from the observation (Li et al., 2017). Also, the seasonal prediction skills are low, especially during the wet season and over the western MC (T. Zhang et al., 2016). Despite the effort to increase model resolution and explicitly resolve convection in the model, a recent study shows that such model improvement insignificantly enhances model performance (Argüeso et al., 2020).

Neale and Slingo (2003) suggested that MC rainfall bias, which further develops the idea of the prediction barrier, is sourced from the incapability of the model to capture MC diurnal cycle. Consequently, the diurnal cycle representation in models needs to be improved so the model output

captures the amplitude and timing of rainfall peaks as those appear in observations. However, the most advanced models still cannot correctly reproduce the observed diurnal cycle (Li et al., 2017; Argüeso et al., 2020; Watters et al., 2021). Although models better capture the phase of the diurnal precipitation cycle, the amplitude of the model output is overestimated over MC landmasses. Therefore, understanding MC diurnal cycle is a potential key to improving predictability.

1.2.2   MC Barrier Effect on MJO Propagation

The Madden-Julian Oscillation (MJO) is the dominant mode of intraseasonal variations in the tropics, propagating to the east with a phase speed of around 5 m s^{-1} from the Indian Ocean to the west Pacific Ocean (Madden & Julian, 1971, 1972). The eastward propagation of the MJO observed over the MC demonstrates two characteristics distinct from that observed over the open waters: 1) the MJO center tends to "detour" the equatorial MC islands southward during boreal winter, passing over the oceanic region between Indonesia and Australia, and 2) MJO propagation is frequently halted in the MC region (C. Zhang & Ling, 2017). Indo-Pacific Maritime Continent also often disrupts the propagation of Madden-Julian Oscillation (MJO) from the Indian Ocean to the West Pacific, better known as the "MC barrier effect." Almost half of the MJO propagation failed to cross the MC (C. Zhang & Ling, 2017). The MC barrier effect has been the subject of several recent observational, modeling, and theoretical studies (Hirata et al., 2013; Ling et al., 2013; Kim et al., 2014; Feng et al., 2015; Kerns & Chen, 2016; C. Zhang & Ling, 2017; Adames et al., 2020; Ahn et al., 2020; Abhik et al., 2023). However, the exact role of MC landmasses in the propagation of the MJO through the MC region needs to be better understood and remain a topic of intense research (Kim et al., 2020).

Previous research has examined the function of topography and land-sea contrast on MC islands. Their findings indicate that topography, land-sea contrast, and convection in the MC area interact with large-scale circulation, i.e., Hadley and Walker cells, to define the mean state (Ahn et al., 2020). Furthermore, Ahn et al. (2020) focus on isolating the role of convection in the MC islands on MJO propagation by setting the updraft plume radius to its minimum and maximum, and their findings show that MC land convection (vertical and meridional moisture gradient) is heavily

affecting the basic state and MJO propagation. The study provides insight into how MJO inhibited or grew further by parameterizing convection types; however, the mechanistic role of land surface response to determine those convection types is ruled out.

1.2.3 Monsoon Onset Variations

The Maritime Continent lies between the Asian and Australian summer monsoons, with monsoon rainfall typically peaking in Austral summer. Seasonal asymmetries are highly variable geographically and reflect interactions on multiple scales (Robertson et al., 2011). The onset date of the rainy season is crucial for agriculture in the region (Naylor et al., 2002; Naylor et al., 2007). It determines the suitable time for planting crops, while delayed onset can lead to crop failure (Boer & Wahab, 2007). Unexpectedly, interannual climate variability explains only a tiny fraction (0–15%) of rice yield variation (Ray et al., 2015). However, a common and significant problem for small farmers cultivating this staple food in the region is the variation of wet-season onset, which affects planting time (Moron et al., 2009). A delayed rainy-season onset typically leads to rice yield reduction, decreased rice planting, and increased risk of annual rice deficits (Naylor et al., 2007). Furthermore, the rainy-season onset is often challenging to establish in the field due to "false onset" or "false rain"—an isolated rainfall event preceding the expected onset date but followed by a dry spell (Marjuki et al., 2016).

There are numerous definitions of the onset of the wet season. A popular definition relates the onset date to the first day of a wet spell with a given amount of accumulated precipitation without being followed by a dry spell in the subsequent weeks. The thresholds are empirically derived or parameterized to make them uniquely suitable to the local climate (Marjuki et al., 2016). Marjuki et al. (2016) also calculated trends in onset delay for 1971–2012 and found that monsoon onset delayed ten days per decade over a particular region of MC, i.e., Java—dominant rice-producing area in MC. Furthermore, the probability of 30-day delay onset is projected to increase (Naylor et al., 2007) and threaten food security. Despite the general trend and projection of the onset delay, false onset is made more loss due to the incapability of detecting the actual onset and should be addressed. Recent research found that monsoon dynamics were constrained by land surface

moisture, including onset (Smyth & Ming, 2021). Meanwhile, a recent review on the monsoon onset highlights the importance of exploring the mechanism of how land-atmosphere interactions play an essential role in determining monsoon onset (Bombardi et al., 2019). However, further research is required to evaluate how land-atmosphere interaction affects the timing of monsoons and vice-versa.

1.3 Research Questions and Hypotheses

As highlighted in the preceding sections, existing knowledge gaps in the understanding of the Maritime Continent's complex system present both fundamental and applied challenges. This dissertation explores the processes of land-atmosphere interactions and their implication on sea-breeze circulations, propagation of the Madden-Julian Oscillation, and monsoon onset variations. The following three research questions have been formulated based on the unresolved issues identified earlier, and each question will be addressed in a separate chapter of this dissertation:

1. How do variations in land surface properties—specifically land surface temperature, soil moisture, and near-surface latent heat—across the Maritime Continent's coastal regions influence the intensity of sea-breeze (quantified by low-level onshore wind speed) and consequent diurnal precipitation patterns? *The following sub-questions further specify the various aspects of this main research question:*

   1.1. What is the relationship between variations in land surface temperature and the intensity of sea breeze in the Maritime Continent's coastal region?

   1.2. How does surface soil moisture in the coastal regions of the Maritime Continent affect the sea-breeze intensity and the associated precipitation?

   1.3. To what extent does near-surface latent heat across the Maritime Continent's coastal lands contribute to changes in sea-breeze intensity and resulting diurnal precipitation patterns?

2. How do the land surface properties over the maritime continent impact the propagation of

the Madden-Julian Oscillation?

3. How do the land surface properties over the maritime continent modulate the variation of monsoon onset?

For each research question, we develop a set of hypotheses, which serve as proposed mechanisms to provide a structured approach to our investigation.

1. Land surface properties and their exchange with the atmosphere have a causal relationship with the sea breeze circulation over the coastal regions of the Maritime Continent. *More detailed hypotheses are provided as follows:*

   1.1. Land-sea surface temperature gradient is the first order that drives sea breeze circulation. Land surface temperature affects the land-sea gradient temperature and low-level pressure gradient force, which further affect the sea-breeze intensity measured by low-level onshore wind speed.

   1.2. Surface soil moisture content determines the availability of moisture for evapotranspiration, which adds up moisture that is brought by the sea breeze from the adjacent sea, enhancing the available moisture in the atmosphere.

   1.3. Near-surface latent heat represents the energy due to evapotranspiration, which adds up atmospheric moisture. This leads to the intensification of precipitation if the available moisture can be converted to clouds depending on the atmospheric stability.

2. The land convection intensities over the main islands of the Maritime Continent redistribute the MJO convection center, further dissipating and disrupting MJO, resulting in MJO blocked over the Maritime Continent.

3. Large variation of the onset is due to the large-scale climate variabilities. The land surface properties over the main islands over the Maritime Continent a couple of weeks ahead of the monsoon onset modify the onset variation within

1.4   Overview of Dissertation Research

By systematically investigating these research questions, the subsequent chapters of this dissertation (Chapters 2, 3, and 4) will endeavor to provide a deeper understanding of the complex interactions within the maritime continent system. For the sea breeze analysis (Chapter 2), we will use the Granger causality test to identify the causality between land surface properties and sea breeze intensity. In the MJO analysis (Chapter 3), we will apply the Large-scale Precipitation Tracking (LPT) method from Kerns and Chen (2016, 2020) to track MJO's centroid and path and compare those that are blocked versus those that cross the maritime continent, examining the land surface conditions during each scenario to determine which factors might lead to MJO blocking. For the monsoon onset analysis (Chapter 4), we will compare delayed versus early onset years without significant large-scale climate variability, using a certain threshold to determine the effect of local land surface conditions on monsoon onset variations. While this study may not address all existing knowledge gaps, it aspires to contribute to the understanding of land-atmosphere interactions over the region. The final chapter (Chapter 5) of this dissertation will synthesize the findings, discuss their broader implications, and suggest potential avenues for future research in this domain.

Figures
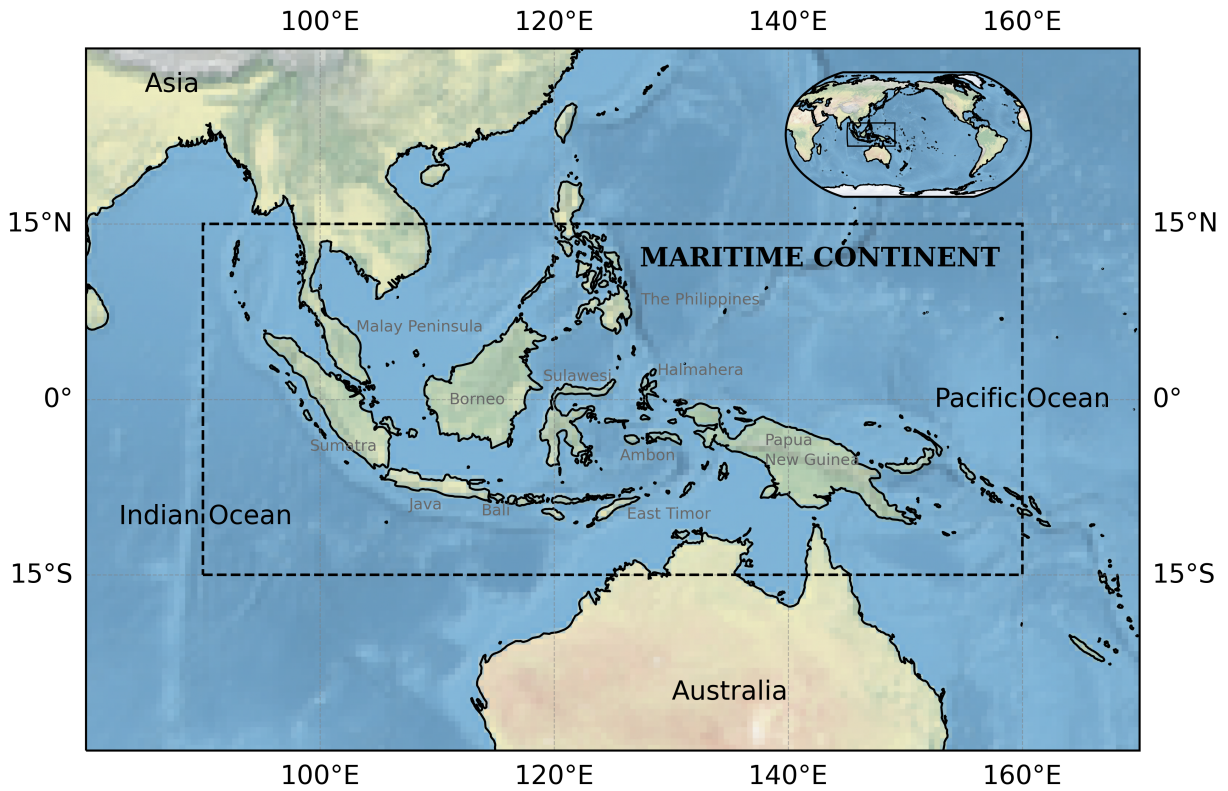
Figure 1.1: The map of the Maritime Continent that spans between 90°E–160°E longitude and 15°S–15°N latitude, covering parts of Southeast Asia, the Malay Peninsula, the islands of Indonesia, the Philippines, New Guinea, and northern tip of Australia. The study area is marked by a dashed rectangle. This study focuses on the Indonesian part of the Maritime Continent. An inset map in the top right corner shows the globe in Robinson projection with the study area box.

References

Abhik, S., Hendon, H. H., & Zhang, C. (2023). The Indo-Pacific Maritime Continent Barrier Effect on MJO Prediction. *Journal of Climate*, *36*(3), 945–957. https://doi.org/10.1175/JCLI-D-22-0010.1

Adames, Á. F., Kim, D., Maloney, E. D., & Sobel, A. H. (2020). The Moisture Mode Framework of the Madden-Julian Oscillation. In C.-P. Chang, K.-J. Ha, R. H. Johnson, D. Kim, G. N. C. Lau, & B. Wang (Eds.), *The Multiscale Global Monsoon System* (pp. 273–287). World Scientific. https://doi.org/10.1142/9789811216602_0022

Ahn, M.-S., Kim, D., Ham, Y.-G., & Park, S. (2020). Role of Maritime Continent Land Convection on the Mean State and MJO Propagation. *Journal of Climate*, *33*(5), 1659–1675. https://doi.org/10.1175/JCLI-D-19-0342.1

Apriyana, Y., Surmaini, E., Estiningtyas, W., Pramudia, A., Ramadhani, F., Suciantini, S., Susanti, E., Purnamayani, R., & Syahbuddin, H. (2021). The Integrated Cropping Calendar Information System: A Coping Mechanism to Climate Variability for Sustainable Agriculture in Indonesia. *Sustainability*, *13*(11). https://doi.org/10.3390/su13116495

Argüeso, D., Romero, R., & Homar, V. (2020). Precipitation Features of the Maritime Continent in Parameterized and Explicit Convection Models. *Journal of Climate*, *33*(6), 2449–2466. https://doi.org/10.1175/JCLI-D-19-0416.1

Barton, E. J., Taylor, C. M., Parker, D. J., Turner, A. G., Belušić, D., Böing, S. J., Brooke, J. K., Harlow, R. C., Harris, P. P., Hunt, K., Jayakumar, A., & Mitra, A. K. (2019). A Case-Study of Land-Atmosphere Coupling during Monsoon Onset in Northern India. *Quarterly Journal of the Royal Meteorological Society*, *146*(731), 2891–2905. https://doi.org/10.1002/qj.3538

Betts, A. K. (2004). Understanding Hydrometeorology using Global Models. *Bulletin of the American Meteorological Society*, *85*(11), 1673–1688. https://doi.org/10.1175/BAMS-85-11-1673

Betts, A. K., Ball, J. H., Beljaars, A. C. M., Miller, M. J., & Viterbo, P. A. (1996). The Land Surface-Atmosphere Interaction: A Review Based on Observational and Global Modeling Perspectives. *Journal of Geophysical Research: Atmospheres*, *101*(D3), 7209–7225. https://doi.org/10.1029/95JD02135

Boer, R., & Wahab, I. (2007). Use of Sea Surface Temperature for Predicting Optimum Planting Window for Potato at Pengalengan, West Java, Indonesia. In M. V. K. Sivakumar & J. Hansen (Eds.), *Climate Prediction and Agriculture: Advances and Challenges* (pp. 135–141). Springer Berlin Heidelberg. https://doi.org/10.1007/978-3-540-44650-7_14

Bombardi, R. J., Moron, V., & Goodnight, J. S. (2019). Detection, Variability, and Predictability of Monsoon Onset and Withdrawal Dates: A Review. *International Journal of Climatology*, *40*(2), 641–667. https://doi.org/10.1002/joc.6264

Chang, C.-P., Lu, M.-M., & Lim, H. (2016). Monsoon Convection in the Maritime Continent: Interaction of Large-Scale Motion and Complex Terrain. *Meteorological Monographs*, *56*, 6.1–6.29. https://doi.org/10.1175/AMSMONOGRAPHS-D-15-0011.1

Dhaka, S., & Kumar, V. (2023). Chapter 1 - Composition and Thermal Structure of the Earth's Atmosphere. In A. Kumar Singh & S. Tiwari (Eds.), *Atmospheric remote sensing* (pp. 1–18). Elsevier. https://doi.org/10.1016/B978-0-323-99262-6.00023-7

Dirmeyer, P. A. (2011). The Terrestrial Segment of Soil Moisture–Climate Coupling. *Geophysical Research Letters*, *38*(16). https://doi.org/10.1029/2011GL048268

Feng, J., Li, T., & Zhu, W. (2015). Propagating and Nonpropagating MJO Events over Maritime Continent. *Journal of Climate*, *28*(21), 8430–8449. https://doi.org/10.1175/JCLI-D-15-0085.1

Gerken, T., Ruddell, B. L., Yu, R., Stoy, P. C., & Drewry, D. T. (2019). Robust Observations of Land-to-Atmosphere Feedbacks using the Information Flows of FLUXNET. *npj Climate and Atmospheric Science*, *2*. https://doi.org/10.1038/s41612-019-0094-4

Hamada, J.-I., Yamanaka, M. D., Matsumoto, J., Fukao, S., Winarso, P. A., & Sribimawati, T. (2002). Spatial and Temporal Variations of the Rainy Season over Indonesia and their Link to ENSO. *Journal of the Meteorological Society of Japan Ser II*, *80*(2), 285–310. https://doi.org/10.2151/jmsj.80.285

Henderson, S. A., & Maloney, E. D. (2018). The Impact of the Madden–Julian Oscillation on High-Latitude Winter Blocking during El Niño–Southern Oscillation Events. *Journal of Climate*, *31*(13), 5293–5318. https://doi.org/10.1175/JCLI-D-17-0721.1

Hirata, F. E., Webster, P. J., & Toma, V. E. (2013). Distinct Manifestations of Austral Summer Tropical Intraseasonal Oscillations. *Geophysical Research Letters*, *40*(12), 3337–3341. https://doi.org/10.1002/grl.50632

Iskandar, I., Lestari, D. O., Utari, P. A., Supardi, Rozirwan, Khakim, M. Y. N., Poerwono, P., & Setiabudidaya, D. (2018). Evolution and Impact of the 2016 Negative Indian Ocean Dipole. *Journal of Physics: Conference Series*, *985*(1), 012017. https://doi.org/10.1088/1742-6596/985/1/012017

Jin, F.-F. (1996). Tropical Ocean-Atmosphere Interaction, the Pacific Cold Tongue, and the El Niño-Southern Oscillation. *Science*, *274*(5284), 76–78. https://doi.org/10.1126/science.274.5284.76

Kerns, B. W., & Chen, S. S. (2016). Large-Scale Precipitation Tracking and the MJO over the Maritime Continent and Indo-Pacific Warm Pool. *Journal of Geophysical Research: Atmospheres*, *121*(15), 8755–8776. https://doi.org/10.1002/2015JD024661

Kerns, B. W., & Chen, S. S. (2020). A 20-Year Climatology of Madden-Julian Oscillation Convection: Large-Scale Precipitation Tracking from TRMM-GPM Rainfall. *Journal of Geophysical Research: Atmospheres*, *125*(7), 1–21. https://doi.org/10.1029/2019JD032142

Kim, D., Kug, J.-S., & Sobel, A. H. (2014). Propagating versus Nonpropagating Madden-Julian Oscillation Events. *Journal of Climate*, *27*(1), 111–125. https://doi.org/10.1175/JCLI-D-13-00084.1

Kim, D., Maloney, E. D., & Zhang, C. (2020). Review: MJO Propagation over the Maritime Continent. In C.-P. Chang, K.-J. Ha, R. H. Johnson, D. Kim, G. N. C. Lau, & B. Wang (Eds.), *The Multiscale Global Monsoon System* (pp. 261–272). World Scientific. https://doi.org/10.1142/9789811216602_0021

Koster, R. D., Sud, Y. C., Guo, Z., Dirmeyer, P. A., Bonan, G., Oleson, K. W., Chan, E., Verseghy, D., Cox, P., Davies, H., Kowalczyk, E., Gordon, C. T., Kanae, S., Lawrence, D., Liu, P., Mocko, D., Lu, C.-H., Mitchell, K., Malyshev, S., ... Xue, Y. (2006). GLACE: The Global Land–Atmosphere Coupling Experiment. Part I: Overview. *Journal of Hydrometeorology*, *7*(4), 590–610. https://doi.org/10.1175/JHM510.1

Li, Y., Jourdain, N. C., Taschetto, A. S., Gupta, A. S., Argüeso, D., Masson, S., & Cai, W. (2017). Resolution Dependence of the Simulated Precipitation and Diurnal Cycle over the Maritime Continent. *Climate Dynamics*, *48*, 4009–4028. https://doi.org/10.1007/s00382-016-3317-y

Lin, J., & Qian, T. (2019). A New Picture of the Global Impacts of El Nino-Southern Oscillation. *Scientific Reports*, *9*(17543). https://doi.org/10.1038/s41598-019-54090-5

Ling, J., Zhang, C., & Bechtold, P. (2013). Large-Scale Distinctions between MJO and Non-MJO Convection Initiation over the Tropical Indian Ocean. *Journal of the Atmospheric Sciences*, *70*(9), 2696–2712. https://doi.org/10.1175/JAS-D-13-029.1

Madden, R. A., & Julian, P. R. (1971). Detection of a 40–50 Day Oscillation in the Zonal Wind in the Tropical Pacific. *Journal of the Atmospheric Sciences*, *28*(5), 702–708. https://doi.org/10.1175/1520-0469(1971)028⟨0702:DOADOI⟩2.0.CO;2

Madden, R. A., & Julian, P. R. (1972). Description of Global-Scale Circulation Cells in the Tropics with a 40–50 Day Period. *Journal of the Atmospheric Sciences*, *29*(6), 1109–1123. https://doi.org/10.1175/1520-0469(1972)029⟨1109:DOGSCC⟩2.0.CO;2

Marjuki, van der Schrier, G., Tank, A. M. G. K., van den Besselaar, E. J. M., Nurhayati, & Swarinoto, Y. S. (2016). Observed Trends and Variability in Climate Indices Relevant for Crop Yields in Southeast Asia. *Journal of Climate*, *29*(7), 2651–2669. https://doi.org/10.1175/JCLI-D-14-00574.1

McBride, J. L., Haylock, M. R., & Nicholls, N. (2003). Relationships between the Maritime Continent Heat Source and the El Niño-Southern Oscillation Phenomenon. *Journal of Climate*, *16*(17), 2905–2914. https://doi.org/10.1175/1520-0442(2003)016⟨2905:RBTMCH⟩2.0.CO;2

Meehl, G. A., & Arblaster, J. M. (2011). Decadal Variability of Asian-Australian Monsoon-ENSO-TBO Relationships. *Journal of Climate*, *24*(18). https://doi.org/10.1175/2011JCLI4015.1

Misra, V. (2020). Land-Atmosphere Interactions. In *Regionalizing Global Climate Variations: A Study of the Southeastern US Regional Climate* (pp. 17–46). Elsevier. https://doi.org/10.1016/B978-0-12-821826-6.00002-3

Moon, W., Kim, B.-M., Yang, G.-H., & Wettlaufer, J. S. (2022). Wavier Jet Streams Driven by Zonally Asymmetric Surface Thermal Forcing. *Proceedings of the National Academy of Sciences*, *119*(38), e2200890119. https://doi.org/10.1073/pnas.2200890119

Moron, V., Robertson, A. W., & Boer, R. (2009). Spatial Coherence and Seasonal Predictability of Monsoon Onset over Indonesia. *Journal of Climate*, *22*(3), 840–850. https://doi.org/10.1175/2008JCLI2435.1

Muttaqin, A. S., Suarma, U., Nurjani, E., Kurniadhini, F., Prabaningrum, R., & Wulandari, R. (2019). The Impact of Climate Variability on Tobacco Productivity over Temanggung Regency, Indonesia. *E3S Web of Conferences*, *76*(04003). https://doi.org/10.1051/e3sconf/20197604003

Naylor, R. L., Battisti, D. S., Vimont, D. J., Falcon, W. P., & Burke, M. B. (2007). Assessing Risks of Climate Variability and Climate Change for Indonesian Rice Agriculture. *Proceedings of the National Academy of Sciences*, *104*(19), 7752–7757. https://doi.org/10.1073/pnas.0701825104

Naylor, R. L., Falcon, W., Wada, N., & Rochberg, D. (2002). Using El Niño Southern Oscillation Climate Data to Improve Food Policy Planning in Indonesia. *Bulletin of Indonesian Economic Studies*, *38*(1), 75–91. https://doi.org/10.1080/000749102753620293

Neale, R., & Slingo, J. (2003). The Maritime Continent and Its Role in the Global Climate: A GCM Study. *Journal of Climate*, *16*(5), 834–848. https://doi.org/10.1175/1520-0442(2003)016⟨0834:TMCAIR⟩2.0.CO;2

Nur'utami, M. N., & Hidayat, R. (2016). Influences of IOD and ENSO to Indonesian Rainfall Variability: Role of Atmosphere-Ocean Interaction in the Indo-Pacific Sector. *Procedia Environmental Sciences*, *33*, 196–203. https://doi.org/10.1016/j.proenv.2016.03.070

Ramage, C. S. (1968). Role of a tropical "Maritime Continent" in the Atmospheric Circulation. *Monthly Weather Review*, *96*(6), 365–370. https://doi.org/10.1175/1520-0493(1968)096⟨0365:ROATMC⟩2.0.CO;2

Ray, D. K., Gerber, J. S., MacDonald, G. K., & West, P. C. (2015). Climate Variation Explains a Third of Global Crop Yield Variability. *Nature Communications*, *6*(5989). https://doi.org/10.1038/ncomms6989

Robertson, A. W., Moron, V., Qian, J.-H., Chang, C.-P., Tangang, F., Alrdian, E., Koh, T. Y., & Liew, J. (2011). The Maritime Continent Monsoon. In C.-P. Chang, Y. Ding, N.-C. Lau,

R. H. Johnson, B. Wang, & T. Yasunari (Eds.), *The Global Monsoon System, Research and Forecast 2nd Edition* (pp. 85–98). World Scientific. https://doi.org/10.1142/9789814343411_0006

Santanello, J. A., Peters-Lidard, C. D., & Kumar, S. V. (2011). Diagnosing the Sensitivity of Local Land–Atmosphere Coupling via the Soil Moisture–Boundary Layer Interaction. *Journal of Hydrometeorology*, *12*(5), 766–786. https://doi.org/10.1175/JHM-D-10-05014.1

Smyth, J. E., & Ming, Y. (2021). Investigating the Impact of Land Surface Characteristics on Monsoon Dynamics with Idealized Model Simulations and Theories. *Journal of Climate*, *34*(19), 7943–7958. https://doi.org/10.1175/JCLI-D-20-0954.1

Takahashi, H. G., & Polcher, J. (2019). Weakening of Rainfall Intensity on Wet Soils over the Wet Asian Monsoon Region using a High-Resolution Regional Climate Model. *Progress in Earth and Planetary Science*, *6*(26). https://doi.org/10.1186/s40645-019-0272-3

Trenberth, K. E., Branstator, G. W., Karoly, D., Kumar, A., Lau, N.-C., & Ropelewski, C. (1998). Progress during TOGA in Understanding and Modeling Global Teleconnections Associated with Tropical Sea Surface Temperatures. *Journal of Geophysical Research Oceans*, *103*(C7), 14291–14324. https://doi.org/10.1029/97JC01444

Wang, S., Sobel, A. H., Tippett, M. K., & Vitart, F. (2019). Prediction and Predictability of Tropical Intraseasonal Convection: Seasonal Dependence and the Maritime Continent Prediction Barrier. *Climate Dynamics*, *52*, 6015–6031. https://doi.org/10.1007/s00382-018-4492-9

Watters, D., Battaglia, A., & Allan, R. P. (2021). The Diurnal Cycle of Precipitation According to Multiple Decades of Global Satellite Observations, Three CMIP6 Models, and the ECMWF Reanalysis. *Journal of Climate*, *34*(12), 5063–5080. https://doi.org/10.1175/JCLI-D-20-0966.1

Wei, J., & Dirmeyer, P. A. (2012). Dissecting Soil Moisture-Precipitation Coupling. *Geophysical Reseach Letters*, *39*(19). https://doi.org/10.1029/2012GL053038

Woollings, T., Drouard, M., O'Reilly, C. H., Sexton, D. M. H., & McSweeney, C. (2023). Trends in the Atmospheric Jet Streams are Emerging in Observations and Could be Linked to Tropical Warming. *Communications Earth and Environment*, *4*(125). https://doi.org/10.1038/s43247-023-00792-8

Wu, P., Mori, S., & Syamsudin, F. (2018). Land-Sea Surface Air Temperature Contrast on the Western Coast of Sumatra Island during an Active Phase of the Madden-Julian Oscillation. *Progress in Earth and Planetary Science*, *5*(4). https://doi.org/10.1186/s40645-017-0160-7

Xue, P., Malanotte-Rizzoli, P., Wei, J., & Eltahir, E. A. B. (2020). Coupled Ocean-Atmosphere Modeling over the Maritime Continent: A Review. *JGR Oceans*, *125*(6). https://doi.org/10.1029/2019JC014978

Yamanaka, M. D. (2016). Physical Climatology of Indonesian Maritime Continent: An Outline to Comprehend Observational Studies. *Atmospheric Research*, *178–179*, 231–259. https://doi.org/10.1016/j.atmosres.2016.03.017

Yamanaka, M. D., Ogino, S.-Y., Wu, P.-M., Hamada, J.-I., Mori, S., Matsumoto, J., & Syamsudin, F. (2018). Maritime Continent Coastlines Controlling Earth's Climate. *Progress in Earth and Planetary Science*, *5*(21). https://doi.org/10.1186/s40645-018-0174-9

Yang, S., Zhang, T., Li, Z., & Dong, S. (2019). Climate Variability over the Maritime Continent and Its Role in Global Climate Variation: A Review. *Journal of Meteorological Research*, *33*(6), 993–1015. https://doi.org/10.1007/s13351-019-9025-x

Yoneyama, K., & Zhang, C. (2020). Years of the Maritime Continent. *Geophysical Research Letters*, *47*(12), e2020GL087182. https://doi.org/10.1029/2020GL087182

Zhang, C., & Ling, J. (2017). Barrier Effect of the Indo-Pacific Maritime Continent on the MJO: Perspectives from Tracking MJO Precipitation. *Journal of Climate*, *30*(9), 3439–3459. https://doi.org/10.1175/JCLI-D-16-0614.1

Zhang, T., Tam, C.-Y., Jiang, X., Yang, S., Lau, N.-C., Chen, J., & Laohalertchai, C. (2019). Roles of Land-Surface Properties and Terrains on Maritime Continent Rainfall and its Seasonal Evolution. *Climate Dynamics*, *53*, 6681–6697. https://doi.org/10.1007/s00382-019-04951-6

Zhang, T., Yang, S., Jiang, X., & Zhao, P. (2016). Seasonal-Interannual Variation and Prediction of Wet and Dry Season Rainfall over the Maritime Continent: Roles of ENSO and Monsoon Circulation. *Journal of Climate*, *29*(10), 3675–3695. https://doi.org/10.1175/JCLI-D-15-0222.1

Zhou, Y., Fang, J., & Wang, S. (2021). Impact of Islands on the MJO Propagation Across the Maritime Ccontinent: A Numerical Modeling Study of an MJO Event. *Climate Dynamics*, *57*, 2921–2935. https://doi.org/10.1007/s00382-021-05849-y

Chapter 2

The Role of Land Surface Properties and Fluxes on Sea-Breeze Circulations over the Maritime Continent

Abstract

Over the Maritime Continent (MC), the timing of the diurnal cycle of precipitation is poorly resolved by numerical models, regardless of the improvement of the model's spatial and temporal resolution. This suggests an incomplete understanding of the physical processes driven by the complex interactions between landmasses, the atmosphere, and the ocean. Accurate representation of these processes is crucial for regional climate modeling and weather forecasting. In this region, diurnal precipitation is closely related to land-sea breeze circulation, promoted by the onshore-offshore surface temperature gradient. We investigated the added effect of variability in land surface properties on sea-breeze intensity over the coastal region of the Indonesian Maritime Continent, encompassing the five main MC islands, such as Sumatra, Java, Borneo, Sulawesi, and Papua New Guinea. Sea surface temperature data were obtained from ERA5 at an hourly frequency and $0.25° \times 0.25°$ spatial resolution. The influence of land surface properties on sea-breeze intensity was investigated using the high-resolution ERA5-Land dataset by ECMWF. These datasets were analyzed using Granger Causality analysis to quantify the relationships among land surface properties and sea-breeze circu-

lation along pre-defined transects aligned perpendicular to the coastline over the study area. Our findings indicate that the strength of land-sea breeze circulations varies within the study region, with some transects revealing that land surface properties moderate sea-breeze circulations. Land-atmosphere interactions over the coastal region of the Indonesian Maritime Continent are partly responsible for controlling land-sea breeze circulations, depending on land surface characteristics. Current analyses relied on the global reanalysis dataset, which means that incorporating more observations and variables can help improve our understanding of the land-atmosphere feedback over the Maritime Continent.

Plain Language Summary

This study examines the sea-breeze intensity over the Indonesian Maritime Continent, a region that includes Sumatra, Java, Borneo, Sulawesi, and Papua New Guinea. We want to understand how changes in the land surface, such as temperature and soil moisture, affect the strength and patterns of the sea-breeze intensities. To do this, we used data on sea surface temperature, land surface temperature, and near-surface soil moisture from various sources. We found that the strength of land-sea breezes can vary in different regions and that changes in land surface properties can impact these breezes. The interactions between land and atmosphere play a crucial role in controlling these weather patterns, and they can depend on factors like the land's physical features. By collecting more data from specific locations, we can improve our understanding of how these interactions affect rainfall in this region, which is important for agriculture, water resources management, and weather forecasting.

2.1   Introduction

Sea breeze circulation (SBC) is a local and mesoscale wind phenomenon that occurs in many coastal locations around the world, including over the Indonesian Maritime Continent (MC). SBC develops when solar radiation and the differing rates at which land and water change temperature create a pressure gradient force pointing toward the land (Miller et al., 2003). This circulation

has a significant impact on the local wind field, air quality, convective activity, and precipitation patterns. The sea breeze circulation has been extensively studied for more than a century, with numerous investigations focusing on its various features, such as the sea breeze gravity current, sea breeze frontal zone, Kelvin-Helmholtz billows, and interactions with other atmospheric instabilities. In recent years, practical applications of sea breeze research have emerged, including sea breeze geoengineering techniques aimed at increasing rainfall over coastal plains (Mostamandi et al., 2022).

The Maritime Continent (MC), a region characterized by a complex array of islands, seas, and straits, lies at the heart of the tropics and serves as a critical component of the Earth's climate system. Encompassing countries such as Indonesia, Malaysia, the Philippines, Brunei Darussalam, Timor Leste, and Papua New Guinea, the MC acts as a bridge between the Indian and Pacific Oceans, linking climate variabilities over both of the basins. This unique geography, combined with the diverse distribution of land and sea surfaces, gives rise to intricate atmospheric and oceanic processes that significantly influence regional weather patterns and global climate dynamics (Ramage, 1968).

Numerical models have consistently struggled to accurately simulate the observed diurnal cycle of precipitation timing, especially over the Indonesian Maritime Continent coastal regions (Li et al., 2017). This inability to reproduce the precipitation patterns is indicative of underlying issues in the representation of crucial physical processes within the models. One such process, surface fluxes, has been identified as a primary factor contributing to the rainfall biases over the Maritime Continent (Yang et al., 2019). These biases in surface fluxes can result from inadequate parameterizations or inaccurate representation of factors such as land surface properties, vegetation cover, and soil moisture. As a consequence, the misrepresented processes in models can lead to significant errors in the simulation of land-sea interactions, sea-breeze circulations, and the diurnal precipitation patterns over the Indonesian Maritime Continent. A better understanding of the role of land surface fluxes and their interactions with other atmospheric processes is, therefore, crucial for improving the accuracy and reliability of weather and climate predictions in this region.

In this study, we explore the potential influence of land surface properties on modifying sea breeze circulations over the coastal regions of the Indonesian Maritime Continent. An accurate

representation of these interactions is essential for improving weather and climate predictions in the region. Given the recognized biases in numerical models due to misrepresented surface fluxes, our investigation focuses on understanding the role of land surface properties and fluxes in modulating sea breeze circulations and their associated precipitation patterns. By examining the relationship between land surface fluxes and sea breeze circulations, we aim to identify the key factors and processes that contribute to the dynamics of sea-breeze circulations over the region. This analysis provides valuable insights into the underlying mechanisms driving land-sea interactions and helps improve the representation of these processes in models, ultimately enhancing the accuracy of weather and climate forecasts for the Indonesian Maritime Continent and its surrounding regions.

2.2   Methodology

This study examines the impact of land surface properties on sea-breeze circulations across coastal regions of the Indonesian Maritime Continent (MC) (15°N–15°S and 90°E–160°E) over 30 years (1991–2020). The investigation encompasses coastal regions of the five largest islands over the MC, including Sumatra, Java, Borneo, Sulawesi, and Papua New Guinea. Key land surface properties and fluxes of interest include land surface skin temperature (°C) and soil moisture (m^3 m^{-3}) from ERA5-Land (Muñoz-Sabater et al., 2021). While soil moisture is overestimated in ERA5-Land, however, it has a strong positive correlation with observation for tropical regions based on the comparison with Soil Moisture Active Passive (SMAP) 9 km gridded product (Lal et al., 2022; Lal et al., 2023).

Meanwhile, sea surface temperature (°C) is also included in calculating the land-sea gradient temperature, i.e., the sea-breeze driving mechanism, which was retrieved from ERA5 (Hersbach et al., 2020). The ERA5-Land and ERA5 datasets can be accessed via the C3S Climate Data Store (CDS) at https://cds.climate.copernicus.eu/. These hourly variables are crucial for understanding diurnal variations in land-atmosphere interactions and their effect on sea-breeze circulations.

The comparison analysis between ERA5-Land soil moisture and SMAP 9 km gridded product on a global scale indicates a prevalent overestimation of moisture levels while exhibiting a strong

positive correlation in tropical and temperate regions (Lal et al., 2022). Furthermore, the west of the Maritime Continent region is considered the persistent hotspot, i.e., areas with consistently high values and no significant change over 40 years. Meanwhile, the east of the maritime continent shows intensifying hotspots (i.e., areas with high values showing significant, p¡0.05, increasing trend over 40 years) (Lal et al., 2023).

2.2.1 Sampling Locations: Segments and Transects

With a coastline spanning over 99,000 kilometers, the Indonesian Maritime Continent possesses the world's second-longest coastline, surpassed only by Canada. The intricate configuration of this coastline poses a significant challenge for conducting a thorough analysis of the sea-breeze circulation. Consequently, a sampling methodology has been developed to facilitate the study of sea-breeze circulation over the region. In this study, we develop 'segments' and 'transects' as the sampling locations to obtain values of the variables for sea-breeze analysis from the gridded dataset. Furthermore, we focus on the large islands over the Indonesian Maritime Continent, i.e., Sumatra $(473, 481$ km$^2)$, Java $(128, 793$ km$^2)$, Borneo $(743, 329$ km$^2)$, Sulawesi $(180, 681$ km$^2)$, and Papua New Guinea $(785, 753$ km$^2)$.

In simple terms, a segment is a straight line along the coast that will be used to identify and observe the sea-breeze circulation to a certain extent of its landward and seaward sides. The length of the segment is constrained by the shape of the coastline. To determine a segment line, we manually traced the coastline of the medium-resolution coastlines (`resolution='50m'`) from the cartographic Python library, Cartopy (Met Office, 2010–2015). Then, we drew virtual lines that aligned with the straight coastlines and recorded the coordinates at each tip of the segment line. The coordinate of segments is presented in Tables 2.1–2.5, grouped by the main islands. The length of each segment is calculated from tip to tip using the geodesic distance function from the GeoPy library (https://github.com/geopy/geopy). Consequently, the length and orientation of each line segment vary depending on the complexity of the coastline (Figure 2.1). As a result, $N = 81$ lines were determined as the segments with an average of 146.9 km (Figure 2.2). When added together, the total length of the segments ($N = 81$) is 11,894.87 km, around 12% of the total coastline of the

Indonesian Maritime Continent.

Meanwhile, the transect is defined as perpendicular lines (cross-shore) along the segments. Each segment can have at least one transect or N transects, depending on the segment's length and transect spacing. Using the land-sea mask data from ERA5-Land, the transects provide coordinates over the sea (lat_1, lon_1) and land (lat_2, lon_2) for the extraction of the gridded dataset. The land-sea mask value is 1 for a point over land and 0 for a point over the sea, with the values in-between representing the mixture of land and water bodies. In this study, we perform sensitivity analysis on the transect length to explore the optimum distance between two points to extract land-sea surface temperature differences in observing the extent of sea-breeze circulation at each segment. The sensitivity analysis includes four transect lengths, i.e., $0.4°$ (44.4 km), $0.8°$ (88.8 km), $1.2°$ (133.2 km), and $1.6°$ (177.6 km), with the total number of transects, are $N = 175, 176, 170$, and 158, for each transect length, respectively (Figure 2.3). The number of transects decreased as the transect length increased since longer transects exceeded the width of the narrow parts of the island, e.g., on the northern part of Sulawesi.

To derive transects from the segments, we developed a Python function (i.e., `seg2trans`), and it is available on https://gist.github.com/amuttaqin/e08fe055359d074810edf0aa93595a9c. The `seg2trans` function allows us to adjust the transect length (i.e, length to the coastline, `dist2coast`) and transect spacing (spacing between transects, `dist2trans`). In this study, we make the transect spacing distance fixed to $0.5°$ or 55.5 km (`dist2trans=0.5`). Furthermore, each transect represents the onshore-offshore direction of sea-breeze wind flows, important to determine the sea-breeze events. This onshore direction ($\theta_{bearing}$, $0°$ or $360°$ means North, $90°$ is East, $180°$ is South, and $270°$ is West) varies depending on transect orientation and land-sea distribution, and can be calculated from transects coordinates:

$$\theta_{bearing} = \operatorname{atan2}(\sin \Delta\lambda \cdot \cos \phi_2, \cos \phi_1 \cdot \sin \phi_2 - \sin \phi_1 \cdot \cos \phi_2 \cdot \cos \Delta\lambda) \qquad (2.1)$$

where ϕ_1, λ_1 is the transect tip coordinate over sea (lat_1, lon_1), ϕ_2, λ_2 is the transect tip coordinate over land (lat_2, lon_2), and $\Delta\lambda$ is the difference in longitude $(lon_2 - lon_1)$. Then, to get the onshore-

offshore wind magnitude, the wind vector is projected onto the transect bearing:

$$P = A \cdot \cos(\theta_{wind} - \theta_{bearing}) \tag{2.2}$$

where $A = \sqrt{u^2 + v^2}$ is the magnitude of the wind (u and v is the horizontal wind component) and $\Delta\theta = \theta_{wind} - \theta_{bearing}$ is the angle difference between the direction of the wind and the desired projection (onshore direction). Onshore wind magnitude is represented by positive values of P, while offshore wind magnitude is represented by its negative values.

2.2.2   Identification and Classification of Sea-Breeze Circulations

Sea-breeze circulation is driven by the near-surface temperature gradient between land and the adjacent sea due to the differential heating and land-sea heat capacity contrast. This temperature gradient modifies the distribution of atmospheric pressure that causes the wind to flow onshore during the day (sea breeze) and offshore during the night (land breeze). The land-sea temperature difference can be considered the primary driving force of sea-breeze circulations, while other factors may contribute to this circulation that might enhance or suppress sea-breeze circulations. One factor that might interfere with the development of sea-breeze circulation is synoptic disturbance. Several studies used 5 m s^{-1} as the threshold of wind to filter out synoptic disturbance (Savijärvi & Alestalo, 1988; Arritt, 1993; Porson et al., 2007). However, it might be local in nature (Hughes & Veron, 2018). An insight into the 1000 hPa wind speed from ERA5 for 30 years shows that 75% of the observed wind speed falls below 4.6 m s^{-1}, and these statistics sourced from $N = 176$ sampling locations (transects). Assuming that synoptic wind mostly occurred above the 75th percentile, we use the value as a threshold to remove the synoptic disturbance.

In this study, we identify the strength of sea-breeze circulations by investigating the relationship between differential heating of land vs. sea and the onshore-offshore component of wind speed (from ERA5-Land and ERA5, respectively). We expect that the breeze speed is directly proportional to the land-sea temperature contrast; steeper temperature gradients lead to a faster wind breeze. Therefore, we might expect a high correlation coefficient between these variables. In this study,

the onshore-offshore wind component is the horizontal wind that is projected to the orientation of the onshore-offshore direction of each transect at each segment as stated in Equation (2.2). Higher temperature differences may lead to a stronger wind breeze, although it also might be interrupted by other circumstances.

Coastal regions with sea-breeze signals are identified if there is a positive correlation between land-sea surface temperature difference and onshore-offshore wind speed using a selected transect length with the optimum length for observing the extent of sea-breeze circulations. Furthermore, the sea-breeze signal is classified by the magnitude of the correlation, with the 'weak' sea-breeze signal characterized by a correlation coefficient of less than 0.5 ($r < 0.5$), while $r \geq 0.5$ identifies the 'strong' sea-breeze signals.

2.2.3   Causality Between Land Surface Fluxes and SBCs

The connection between land surface properties, i.e., land surface temperature and soil moisture, on sea-breeze intensity is calculated using the Pearson correlation and Granger causality analysis. The Granger causality analysis (Granger, 1969) is used in this study to investigate the causal relationship between land surface properties and sea-breeze circulation (SBC). The Granger causality approach is useful in determining the directionality of causation between two variables by assessing whether past values of one variable help in forecasting future values of another variable. In this study, the Granger causality analysis aims to answer the question of whether the land surface properties, i.e., soil moisture, have an added impact on the intensity of sea-breeze circulation over the Indonesian Maritime Continent. This analysis identifies regions with strong and weak land-atmosphere feedback in shaping sea-breeze intensity.

Historically, Granger causality analysis was initially used in Economic research (Granger, 1969). However, this method has gained more popularity in climate science (McGraw & Barnes, 2018). In this study, Granger causality is used to determine whether surface properties (soil moisture, $m^3 \ m^{-3}$) are useful for determining the sea-breeze intensity, which is identified by the intensity of onshore wind speed ($m \ s^{-1}$) at the tip of each transect. We hypothesized that land surface flux of soil moisture can 'Granger-cause' sea-breeze intensity by modifying latent heat, which eventually

slows or improve the intensity of sea-breeze circulations.

The Granger causality tests are performed using `grangercausalitytests`. It will test whether the time series y Granger causes the time series x. The Null hypothesis is that the series y does not Granger cause the time series x. Granger causality means that past values of y have a statistically significant effect on the current value of x, taking past values of x into account as a regressor. We reject the null hypothesis that y does not Granger cause x if the p-values are below the desired size of the test. The null hypothesis is that the coefficients corresponding to past values of y are zero. In this study, variables that are tested for their causality on sea-breeze intensity are near-surface soil moisture content (m^3 m^{-3}). Granger causality is a hypothesis testing method that can check whether each of the factors significantly affects sea breeze intensity (onshore-offshore wind speed). We hypothesized that 3 hours lag (in advance) of land surface properties could significantly affect the sea-breeze intensity ($p < 0.05$). Using the sampled segments $N = 5$ that span over the Indonesian Maritime Continent, we can see the variation of this causality by location.

2.3 Results

2.3.1 Sensitivity Analysis on the Sampling Method: Transect Length

Sensitivity analysis on transect length is performed by calculating the coefficient of correlation between land-sea temperature difference and onshore-offshore wind speed at each transect length for each segment. There are four different transect lengths, i.e., 44 km, 88 km, 133 km, and 177 km. These numbers come from the distance in latitude longitude, i.e., $0.4°$, $0.8°$, $1.2°$, and $1.6°$, respectively.

Combining the two factors, i.e., four transect lengths and $N = 176$ transects, we calculated the correlation coefficient from $N = 704$ time series. The resulting correlation coefficient is presented as a heatmap plot in Figure 2.4, grouped by islands. The result shows that there is no significant difference in the correlation coefficient among the varying transect lengths. However, it is noticeable that some segments exhibit strong sea-breeze signals (high correlation coefficient, blue cells), while others only have weak SBC signals (low correlation coefficient, red cells).

From the same figure (Figure 2.4), it can be inferred that 60% of segments over Sumatra are considered to have strong sea-breeze signals ($r \geq 0.5$). The 40% of the remaining weak SBC signals are mostly located over the western part of Sumatra, which faces many small islands onshore. The presence of many small islands near the coast might interfere with the sea breeze signals as multiple islands might have their own smaller and local circulation. In contrast, the segments over Borneo are dominated by weak SBC signals. The only segments that have strong signals were located over the southern and northern parts of Borneo, i.e., segments number 34 and 41 (see Figure 2.4 and refer to Figure 2.1). Overall, Sulawesi has the most common strong SBC segment (86%), followed by Java (75%), Sumatra (60%), Papua (53%), and Borneo (16%).

For further analysis, one transect length is selected, i.e., 88 km ($0.8°$). At this length, the total transect reaches the maximum sample coverage, i.e., $N = 176$ transects (see Figure 2.3). As it can be observed, a longer transect length might reduce the sampling numbers due to narrow parts of the island that is not fit for a longer transect length.

2.3.2 Sea-breeze Identification and Classification

Sea-breeze circulations are identified over the five main islands over the Indonesian Maritime Continent using 30 years of land-sea surface temperature and 1000 hPa wind dataset. The five main islands are Sumatra, Java, Borneo, Sulawesi, and Papua New Guinea. The coastlines over these islands are sampled using segments and transects. The number of segments is $N = 80$, and it varies between islands. The map of segments is presented in Figure 2.1. Furthermore, transects are derived from segments. The transects, i.e., transect tips over land and sea, are used to extract the variables from the gridded dataset. We derived four different transect lengths to explore the optimum length for the transect to observe sea-breeze circulation over the Indonesian Maritime Continent. The lengths of the transects include 44 km, 88 km, 133 km, and 177 km. This is derived based on the transect length in latitude/longitude degrees, i.e., $0.4°$, $0.8°$, $1.2°$, and $1.6°$. The estimated length in km is calculated using geodesic distance. The map of the transects is presented in Figure 2.3.

Correlation between land-sea temperature difference vs. onshore-offshore wind speed on the

selected transect length (88 km) shows several sampling locations with statistically significant correlation, indicating signals on sea breeze circulation (Figure 2.5). This analysis also can be used to see the classification of SBC intensity over the Indonesian Maritime Continent.

2.3.3 Land-Atmosphere Feedback on Sea-Breeze Circulations

Furthermore, we examine the effect of land surface properties on sea breeze intensity using Granger causality analysis. Taking one sample at each of the main islands, we tested the hypothesis that soil moisture Granger-cause the sea-breeze intensity (1000 hPa onshore-offshore wind speed) with a lag of 3 hours ($p < 0.05$). The results of the Granger causality analysis are presented in Table 2.6. The table consists of the island name, segment number, F-test, and p-value. The lag for this test is set as 3 hours, which means that we test whether the information of soil moisture 3 hours in advance will help to predict the sea-breeze intensity. From the table, we found that the past value of surface soil moisture (3 hours) should contain information that helps predict SBC intensity above and beyond the information contained in past values of SBC alone. In simple terms, we observe that soil moisture condition is Granger-cause the sea-breeze intensity.

2.4 Discussion

This study explores the potential influence of land surface properties (i.e., land surface temperature and near-surface soil moisture) on shaping and modifying sea breeze circulations over the Indonesian Maritime Continent, which is characterized by the complex interactions between the land-sea-atmosphere. Numerical models hint that surface properties and fluxes might contribute to modulating sea breeze and diurnal circulation (Li et al., 2017). We investigate this particular suggestion using the ERA5 and ERA5-Land datasets. We hypothesize that land surface properties could help predict sea-breeze intensities.

The first step to accomplish this is the identification of sea-breeze signals along the coastal region of the Indonesian Maritime Continent. First, we define the "segments" and "transects" as the sampling method. Segments are the straight line along the coast. Therefore, the length of the

segment depends on the coastline shape. The most extended segment is located northeast of the Papua New Guinea coastline due to the straight nature of the coastline. Anywhere else, the coastal formation is complex, and segments are broken down into smaller lengths. Then, using simple arithmetic, transects are calculated from the available segments to get the perpendicular line along the coast. The transects aim to extract the values of land surface variables at one end and to extract the values of sea surface variables at the other end. These values will then be used to calculate the temperature gradient at each transect since sea-breeze circulation is governed primarily by the temperature gradient (Miller et al., 2003). The other essential variable to obtain at each transect is the 1000 hPa wind speed to explain the intensity of the sea breeze circulation.

We further quantify the sea breeze signals using the correlation between land-sea temperature difference and the projected wind, the wind that is projected onto the transect line to represent onshore-offshore wind breeze intensity. From this approach, we can identify regions in the Indonesian Maritime Continent with weak and strong sea-breeze signals (Figure 2.5). The bubble plot shows bubble size and color to represent the correlation coefficient between land-sea temperature difference vs. near-surface onshore-offshore wind. Coastal regions with strong sea-breeze signals are identified by a correlation coefficient larger than 0.5 ($r > 0.5$), while weak sea-breeze signals are identified by $r < 0.5$.

Furthermore, we examined the impact of land surface properties and fluxes, i.e., sea surface temperature and soil moisture, toward sea-breeze intensity (onshore-offshore wind speed). Soil moisture availability on the surface can be a source of near-surface latent heat. This will impact the availability of moisture in the atmosphere due to evapotranspiration. In terms of the sea-breeze system, it will affect the available moisture for cloud formation and diurnal inland precipitation.

The hypothesis was tested using Granger causality analysis on the sample location of the five main islands over the Indonesian Maritime Continent with a strong sea breeze signal. We found that land surface temperature and soil moisture can Granger-cause the sea breeze intensity with a lag of 3 hours (Table 2.6). It means that the past values of surface fluxes up to certain lag hours should contain information to predict sea breeze intensity in the later time. In summary, using the Granger causality analysis, we found that land surface fluxes (i.e., soil moisture) three

hours in advance significantly contribute to the intensity of sea breeze intensity over the Indonesian Maritime Continent.

2.5   Conclusions

In conclusion, our study reveals that the seaward and landward extend from 40–177 km can be utilized to observe the sea-breeze intensity using land-sea surface temperature and near-surface wind speed. Furthermore, sea-breeze signals along the coastline of the Indonesian Maritime Continent can also be explored using the correlation coefficient between the surface temperature gradient and the projected wind. Some regions exhibit strong sea breeze signals, i.e., the southwest coast of Sumatra, most of the coastline of Java, and most parts of Sulawesi, while Borneo and Papua mostly have weak sea-breeze signals. Our findings also highlight the importance of land surface properties in influencing sea breeze intensity. Using Granger causality analysis, we discovered a statistically significant causality between soil moisture and sea breeze intensity. It means that past values of soil moisture, in this case, 3 hours in advance, contain information that is useful for predicting sea breeze circulation intensity, providing a better understanding of the land-atmosphere interactions that drive sea breeze circulations over the Indonesian Maritime Continent.

Tables

Table 2.1: Coordinates of segments for sea-breeze analysis along the coastline of Sumatra. The coordinates indicate the locations of the tips of each segment. The estimated segment lengths (**len_km**) are calculated in kilometers. Representation of these segments on the map is shown on Figure 2.1.

segment	mainland	lat1	lon1	lat2	lon2	len_km
1	Sumatra	4.8500	95.4000	3.7500	96.5000	172.35
2	Sumatra	3.7000	96.8000	2.8000	97.6000	133.45
3	Sumatra	2.4000	97.7000	1.9000	98.6000	114.37
4	Sumatra	1.5000	98.8000	0.4000	99.1000	126.13
5	Sumatra	-0.1353	99.7852	-1.9247	100.8829	232.54
6	Sumatra	-2.2500	100.8600	-3.6400	102.2000	214.05
7	Sumatra	-3.9500	102.3000	-5.9000	104.7000	342.56
8	Sumatra	-2.9500	106.0000	-5.7000	105.8000	304.91
9	Sumatra	-1.0200	104.3800	-1.9000	104.5000	98.29
10	Sumatra	-0.7500	103.3000	-1.1500	104.3000	119.77
11	Sumatra	0.0210	103.8162	0.5620	103.3926	76.17
12	Sumatra	2.1906	100.5620	2.6828	100.2093	67.09
13	Sumatra	4.0750	98.3160	2.9300	99.9600	222.26
14	Sumatra	5.1500	97.6000	4.4000	98.2500	109.90
15	Sumatra	5.2500	96.3000	5.2500	97.4000	121.94

Table 2.2: Similar to Table 2.1, except for sea-breeze analysis along Java coastline.

segment	mainland	lat1	lon1	lat2	lon2	len_km
16	Java	-6.772	105.536	-6.085	105.925	87.31
17	Java	-6.838	105.636	-6.931	106.461	91.76
18	Java	-7.314	106.480	-7.781	108.407	218.85
19	Java	-7.550	108.796	-8.200	110.900	242.90
20	Java	-8.241	111.227	-8.386	112.739	167.33
21	Java	-8.280	113.227	-8.640	114.194	113.68
22	Java	-6.609	111.052	-6.914	112.483	161.75
23	Java	-6.948	110.471	-6.462	110.721	60.44
24	Java	-6.770	108.600	-6.932	110.532	214.30
25	Java	-6.299	108.320	-6.796	108.625	64.49
26	Java	-5.952	107.099	-6.297	108.233	131.19
27	Java	-6.000	106.100	-6.084	107.029	103.26

Table 2.3: Similar to Table 2.1, except for sea-breeze analysis along Borneo coastline.

segment	mainland	lat1	lon1	lat2	lon2	len_km
28	Borneo	-0.5330	109.2040	1.1000	108.9500	182.77
29	Borneo	-1.2970	110.0210	-2.8890	110.2640	178.10
30	Borneo	-2.9670	110.2940	-2.9380	111.6660	152.56
31	Borneo	-3.4576	111.8675	-3.2064	112.9847	127.23
32	Borneo	-2.9960	113.0740	-3.4700	114.4500	161.67
33	Borneo	-4.1970	114.6640	-3.6000	115.9000	152.32
34	Borneo	-2.9754	116.2298	-1.8069	116.3810	130.30
35	Borneo	-1.6590	116.3840	-0.9020	117.2200	125.15
36	Borneo	-0.2620	117.3820	0.8560	117.7880	131.62
37	Borneo	1.9850	117.7310	1.1910	118.7520	143.58
38	Borneo	3.1360	117.3340	2.3750	117.9930	111.58
39	Borneo	4.1854	117.8245	4.3468	118.3507	61.08
40	Borneo	5.9520	117.9470	5.3730	118.9880	131.90
41	Borneo	5.5130	115.7830	6.7130	116.6500	163.77
42	Borneo	4.5240	114.0350	5.0160	114.9920	119.29
43	Borneo	3.2440	113.0560	4.5030	114.0720	179.21
44	Borneo	2.7910	111.5010	3.1710	113.1220	185.04
45	Borneo	1.7590	111.1180	2.6880	111.4370	108.68
46	Borneo	1.8470	109.6190	1.4790	110.9620	154.88

Table 2.4: Similar to Table 2.1, except for sea-breeze analysis along Sulawesi coastline.

segment	mainland	lat1	lon1	lat2	lon2	len_km
47	Sulawesi	-1.2410	119.3200	-0.7990	119.6290	59.76
48	Sulawesi	-2.4030	119.0930	-1.8890	119.3530	63.77
49	Sulawesi	-5.3480	119.3680	-4.3090	119.6400	118.79
50	Sulawesi	-5.4190	119.3520	-5.7050	119.7440	53.73
51	Sulawesi	-5.2615	120.3080	-3.2382	120.3892	223.92
52	Sulawesi	-2.9555	120.2218	-2.6108	120.7506	70.07
53	Sulawesi	-4.0689	121.5911	-3.5262	120.8476	102.09
54	Sulawesi	-3.6423	122.2103	-4.0863	122.7252	75.37
55	Sulawesi	-2.2002	121.6893	-3.1723	122.3994	133.38
56	Sulawesi	-1.3324	122.5162	-1.8880	121.6966	109.96
57	Sulawesi	-0.9830	121.6660	-0.7820	122.6150	107.94
58	Sulawesi	-1.3560	120.6030	-1.4420	121.1450	61.06
59	Sulawesi	0.5240	121.6960	0.4100	120.9100	88.40
60	Sulawesi	0.3040	123.4910	0.4460	124.3800	100.20
61	Sulawesi	0.9320	122.9820	0.8330	123.9300	106.08
62	Sulawesi	1.3120	120.9400	0.9000	122.7730	209.04

Table 2.5: Similar to Table 2.1, except for sea-breeze analysis along the coastline of Papua.

segment	mainland	lat1	lon1	lat2	lon2	len_km
63	Papua	-1.37000	131.43000	-2.20000	132.27400	131.31
64	Papua	-3.67950	133.94850	-4.44840	135.19960	162.88
65	Papua	-4.50000	135.86350	-5.28300	137.84780	236.51
66	Papua	-5.74660	138.19500	-6.68760	138.68440	117.31
67	Papua	-8.14897	139.96780	-9.08450	140.90340	145.98
68	Papua	-9.12050	141.02000	-9.23860	142.47340	160.27
69	Papua	-9.34280	142.60260	-8.97140	143.29860	86.83
70	Papua	-7.76020	144.86380	-8.07210	146.06000	136.34
71	Papua	-8.15760	146.11460	-10.03500	147.70640	271.54
72	Papua	-10.04760	147.72480	-10.32350	149.67650	216.03
73	Papua	-8.13820	148.08840	-9.07560	148.58480	117.19
74	Papua	-7.44650	147.18480	-8.09110	148.00190	114.91
75	Papua	-6.70790	147.06560	-6.69750	147.79470	80.62
76	Papua	-5.45830	145.75900	-5.96335	147.25943	175.34
77	Papua	-4.83690	145.76350	-5.45370	145.73700	68.27
78	Papua	-2.85675	141.44175	-4.20000	145.00000	422.33
79	Papua	-1.51350	137.88350	-2.85675	141.44175	422.76
80	Papua	-2.35580	136.37660	-3.48000	135.36080	167.95
81	Papua	-0.36710	132.46230	-0.77440	133.87120	163.17

Table 2.6: Granger causality analysis over five sampled segments for the five main islands over the Indonesian Maritime Continent. Only one transect is sampled at each selected segment. Segment is selected based on the correlation coefficient between land-sea temperature difference vs. wind speed as shown in Figure 2.4. This hypothesis testing is determined at 95% confidence level with the `mlag=[3]` or 3-hour lag. In addition, `df_denom=262980` for each of the sampled segments, showing the total time (hourly) over 30 years of analysis.

Island	Segment number	ssr based F-test	p-value	df_denom
Sumatra	2	1902.566	0.0000	262980
Java	21	2341.890	0.0000	262980
Borneo	41	733.857	0.0000	262980
Sulawesi	47	4547.172	0.0000	262980
Papua	72	1216.368	0.0000	262980

Figures
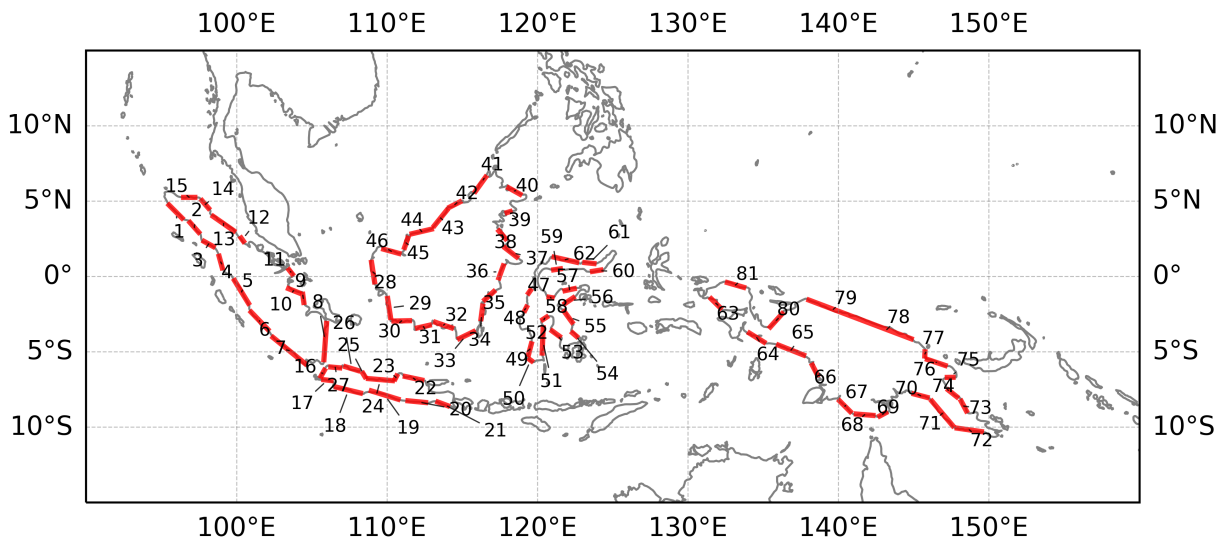
Figure 2.1: Spatial distribution of segments (depicted as red lines) used as sampling locations for sea-breeze analysis over the Indonesian Maritime Continent (MC). The segments is numbered ($N = 81$) over the five MC main islands: Sumatra, Java, Borneo, Sulawesi, and Papua New Guinea. Labeled islands is provided in Figure 1.1.
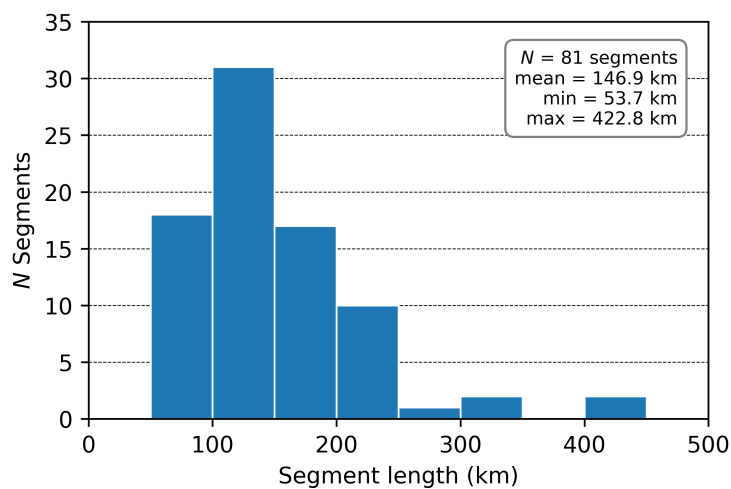
Figure 2.2: Length distribution of segments for sea-breeze analysis over the five main islands of the Indonesian Maritime Continent.
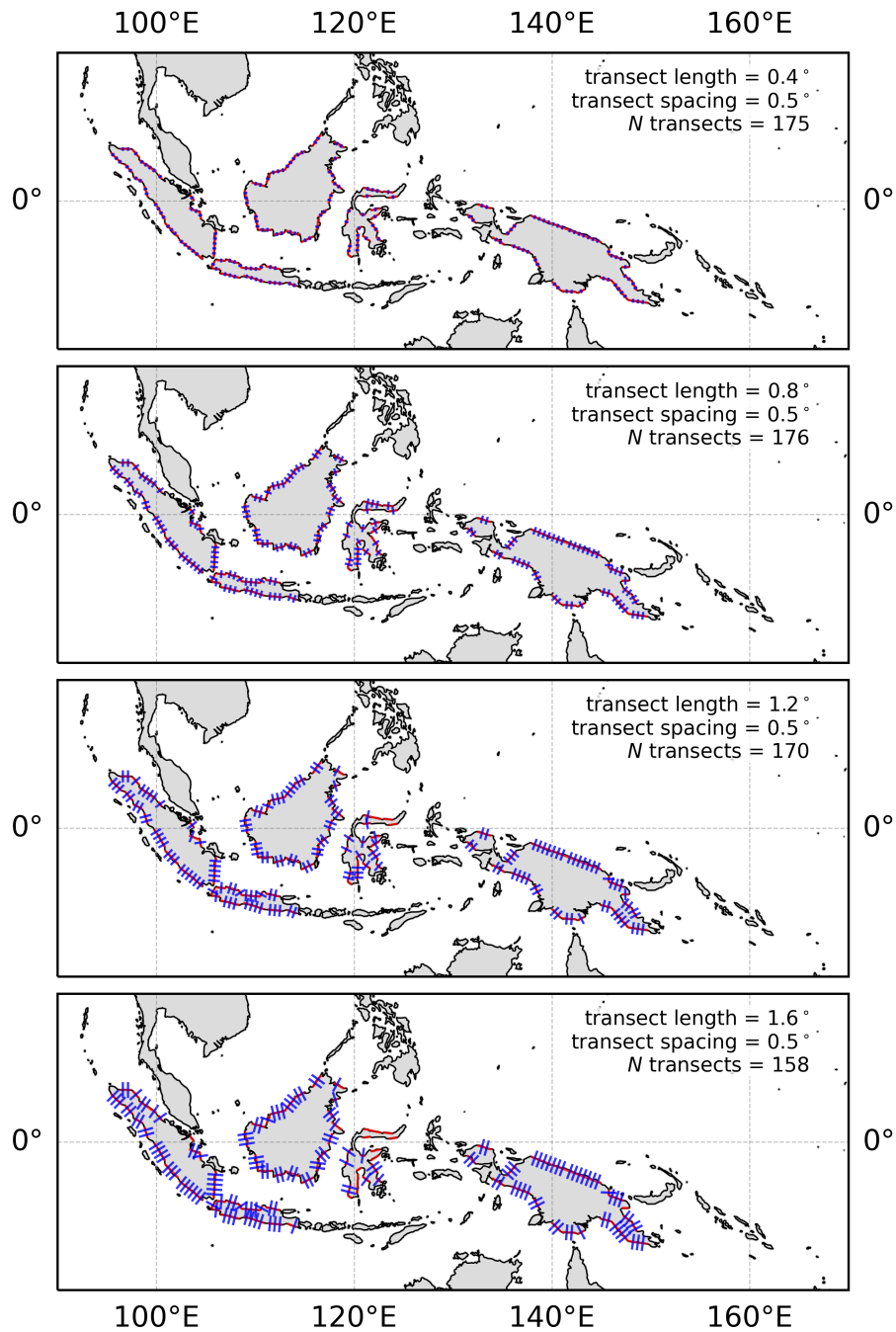
Figure 2.3: Spatial distribution of transects (depicted as blue lines) used as sampling locations for sea-breeze analysis across the Indonesian Maritime Continent (MC). The transects are divided into four lengths: 0.4° (equivalent to 44.4 km), 0.8° (88.8 km), 1.2° (133.2 km), and 1.6° (177.6 km), respectively, with a consistent transect spacing of 0.5°. The number of transects varies depending on the length of each transect.
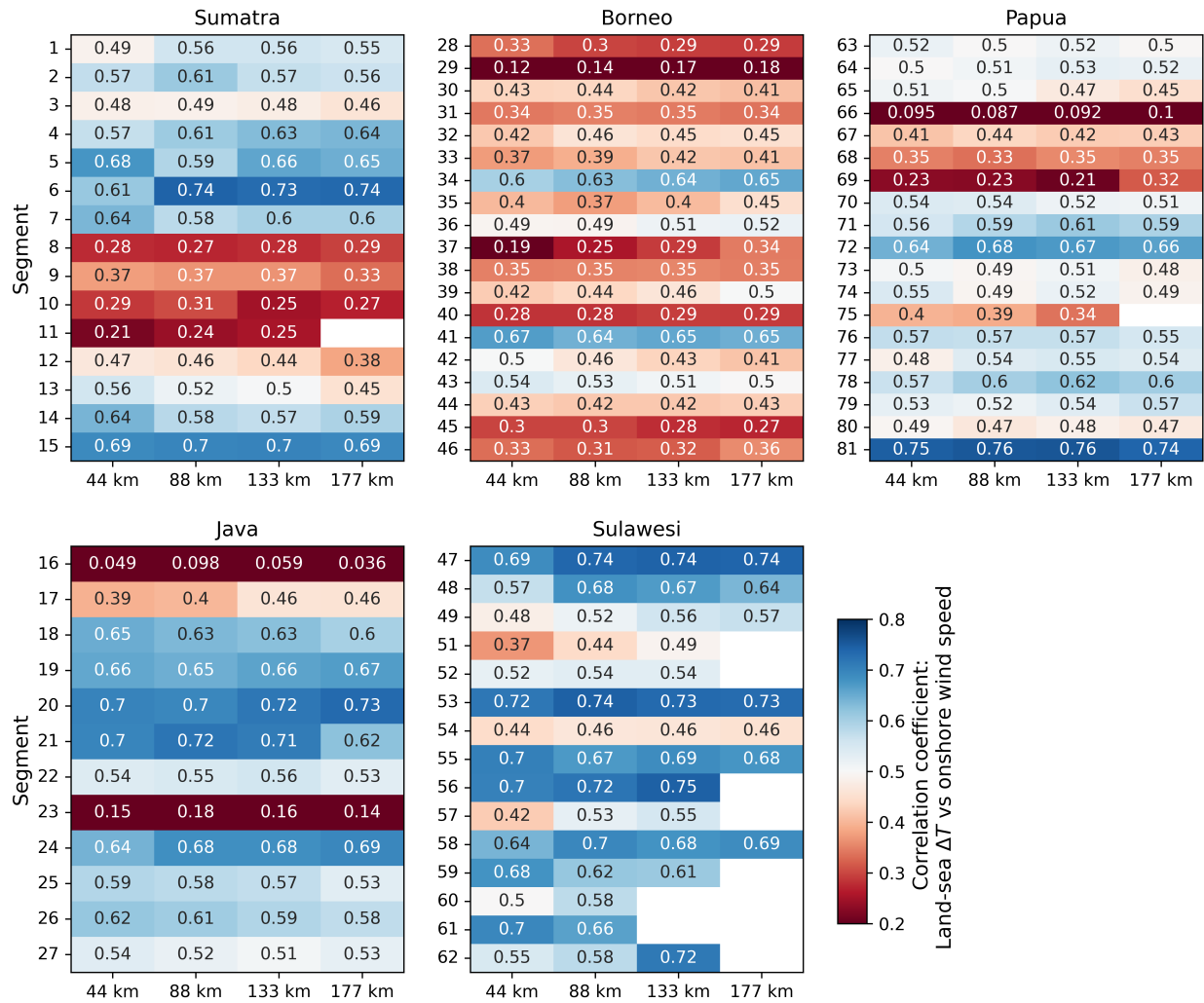
Figure 2.4: Correlation coefficient between land-sea surface temperature difference and onshore-offshore wind speed for each segment (y-axis) at four different transect lengths (44 km, 88 km, 133 km, and 177 km) on the x-axis. The correlation is calculated from 30 years of hourly data, from 1991–2020. The plot is grouped by the main islands over the Indonesian Maritime Continent.
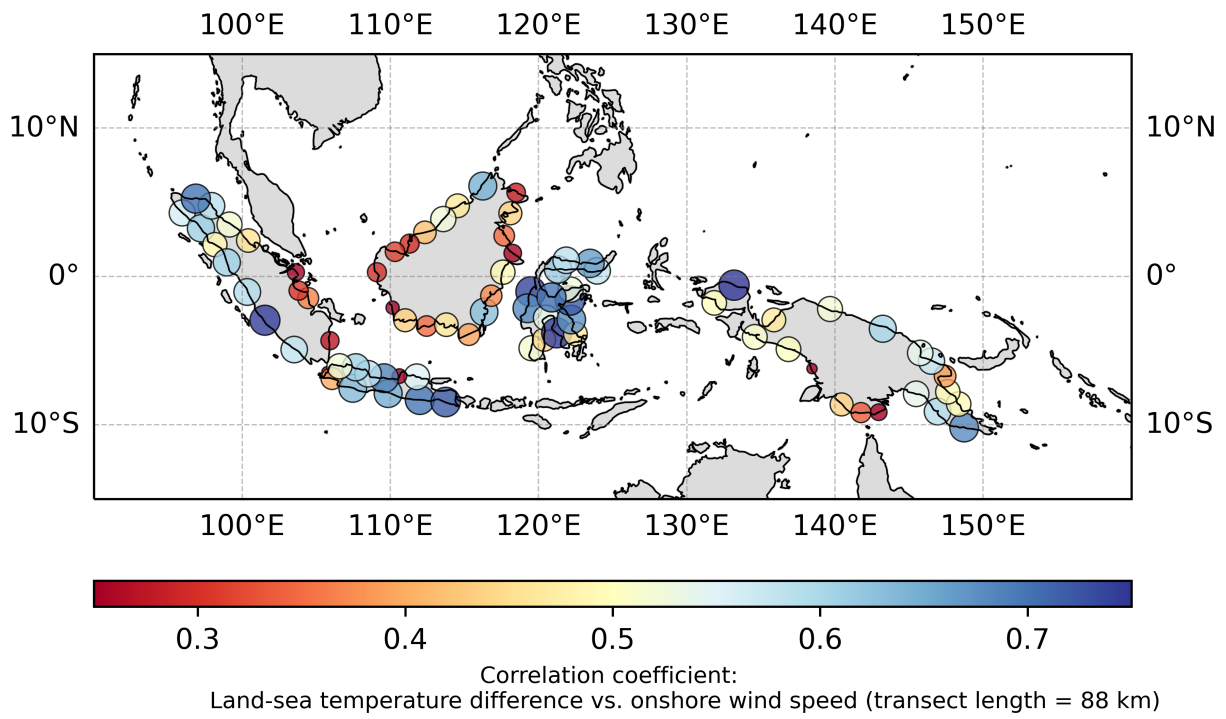
Figure 2.5: Sea-breeze intensity identification based on the correlation coefficient between land-sea temperature difference vs. onshore-offshore wind at each transect (averaged at each segment) at the transect length of 88 km.

References

Arritt, R. W. (1993). Effects of the large-scale flow on characteristic features of the sea breeze. *Journal of Applied Meteorology and Climatology*, *32*(1), 116–125. https://doi.org/10.1175/1520-0450(1993)032⟨0116:EOTLSF⟩2.0.CO;2

Granger, C. W. J. (1969). Investigating causal relations by econometric models and cross-spectral methods. *Econometrica*, *37*(3), 424–438. https://doi.org/10.2307/1912791

Hersbach, H., Bell, B., Berrisford, P., Hirahara, S., Horányi, A., Muñoz-Sabater, J., Nicolas, J., Peubey, C., Radu, R., Schepers, D., Simmons, A., Soci, C., Abdalla, S., Abellan, X., Balsamo, G., Bechtold, P., Biavati, G., Bidlot, J., Bonavita, M., . . . Thépaut, J.-N. (2020). The ERA5 global reanalysis. *Quarterly Journal of the Royal Meteorological Society*, *146*(730), 1999–2049. https://doi.org/10.1002/qj.3803

Hughes, C. P., & Veron, D. E. (2018). A characterization of the Delaware sea breeze using observations and modeling. *Journal of Applied Meteorology and Climatology*, *57*(7), 1405–1421. https://doi.org/10.1175/JAMC-D-17-0186.1

Lal, P., Shekhar, A., Gharun, M., & Das, N. N. (2023). Spatiotemporal evolution of global long-term patterns of soil moisture. *Science of the Total Environment*, *867*(161470). https://doi.org/10.1016/j.scitotenv.2023.161470

Lal, P., Singh, G., Das, N. N., Colliander, A., & Entekhabi, D. (2022). Assessment of ERA5-Land volumetric soil water layer product using in situ and SMAP soil moisture observations. *IEEE Geoscience and Remote Sensing Letters*, *19*(2508305), 1–5. https://doi.org/10.1109/LGRS.2022.3223985

Li, Y., Jourdain, N. C., Taschetto, A. S., Gupta, A. S., Argüeso, D., Masson, S., & Cai, W. (2017). Resolution Dependence of the Simulated Precipitation and Diurnal Cycle over the Maritime Continent. *Climate Dynamics*, *48*, 4009–4028. https://doi.org/10.1007/s00382-016-3317-y

McGraw, M. C., & Barnes, E. A. (2018). Memory matters: A case for Granger Causality in climate variability studies. *J. Clim*, *31*(8), 3289–3300. https://doi.org/10.1175/JCLI-D-17-0334.1

Met Office. (2010–2015). *Cartopy: A cartographic python library with a matplotlib interface.* Exeter, Devon. http://scitools.org.uk/cartopy

Miller, S. T. K., Keim, B. D., Talbot, R. W., & Mao, H. (2003). Sea breeze: Structure, forecasting, and impacts. *Reviews of Geophysics*, *41*(3). https://doi.org/10.1029/2003RG000124

Mostamandi, S., Predybaylo, E., Osipov, S., Zolina, O., Gulev, S., Prajuli, S., & Stenchikov, G. (2022). Sea breeze geoengineering to increase rainfall over the arabian red sea coastal plains. *Journal of Hydrometeorology*, *23*(1). https://doi.org/10.1175/JHM-D-20-0266.1

Muñoz-Sabater, J., Dutra, E., Agustí-Panareda, A., Albergel, C., Arduini, G., Balsamo, G., Boussetta, S., Choulga, M., Harrigan, S., Hersbach, H., Martens, B., Miralles, D. G., Piles, M.,

Rodríguez-Fernández, N. J., Zsoter, E., Buontempo, C., & Thépaut, J.-N. (2021). ERA5-Land: A state-of-the-art global reanalysis dataset for land applications. *Earth Syst. Sci. Data*, *13*(9), 4349–4383. https://doi.org/10.5194/essd-13-4349-2021

Porson, A., Steyn, D. G., & Schayes, G. (2007). Sea-breeze scaling from numerical model simulations, part I: Pure sea breezes. *Boundary-Layer Meteorology*, *122*, 17–29. https://doi.org/10.1007/s10546-006-9090-4

Ramage, C. S. (1968). Role of a tropical "Maritime Continent" in the Atmospheric Circulation. *Monthly Weather Review*, *96*(6), 365–370. https://doi.org/10.1175/1520-0493(1968)096⟨0365:ROATMC⟩2.0.CO;2

Savijärvi, H., & Alestalo, M. (1988). The sea breeze over a lake or gulf as the function of the prevailing flow. *Contributions to Atmospheric Physics*, *61*, 98–104.

Yang, S., Zhang, T., Li, Z., & Dong, S. (2019). Climate Variability over the Maritime Continent and Its Role in Global Climate Variation: A Review. *Journal of Meteorological Research*, *33*(6), 993–1015. https://doi.org/10.1007/s13351-019-9025-x

Chapter 3

The Role of Land-Atmosphere Interactions on the Propagation of Madden-Julian Oscillation Across the Maritime Continent

Abstract

The Indo-Pacific Maritime Continent (MC) often disrupts the propagation of the Madden-Julian Oscillation (MJO) from the Indian Ocean to the western Pacific Ocean, a phenomenon known as the "MC barrier effect." Recent studies have shown that almost half of propagating MJO events fail to cross the MC, making this phenomenon the subject of several recent observational, modeling, and theoretical studies. However, the role of MC landmasses, particularly its land-atmosphere interactions, in the propagation of the MJO through the MC region needs to be better understood. In this study, we assess the potential of land-atmosphere feedback that might impede or allow the propagation of the MJO over the MC. Specifically, we contrast the composite land surface properties leading to two MJO event types: "MJO-C," i.e., MJO event that initiated over the Indian Ocean and managed to cross the MC latitudes and longitudes into the western Pacific Ocean, and "MJO-B," i.e., MJO event that initiated over the Indian Ocean but completely dissipated over or nearby the MC, after interacting with the MC landmasses. The analysis primarily focuses on MJO events that interacted with the MC region and excluded MJO events that detoured around the MC. We

retrieved the land surface properties over the MC from the ERA5-Land dataset at high temporal (hourly) and spatial (0.1°×0.1°) resolutions. The list of MJO events and trajectories from the Large-scale Precipitation Tracking (LPT) method were utilized to obtain the MJO propagation characteristics, such as its initiation location and time, termination, intensity, and centroid track in longitudes and latitudes. Lagged land-to-atmosphere feedback analysis was used to identify which and how land surface variables primarily affect the MJO propagation behavior over the MC region. Our results indicate that anomalously low land surface temperatures of the central and western MC islands led to the blocking or weakening of the MJO over the Indonesian Maritime Continent. Therefore, our study highlights the importance of land-atmosphere interactions and the role of the MC landmasses in the propagation of the MJO through the MC region.

Plain Language Summary

The Madden-Julian Oscillation (MJO) is a sub-seasonal eastward-moving climatic disturbance that brings convection and heavy rainfall over much of the tropics. Often, in tropical Southeast Asia, MJO fails to reach the western Pacific Ocean from the Indian Ocean. Recent studies observed that around half of MJO disturbances dissipate or fail to cross this scattered island region, known as the Maritime Continent (MC). Many researchers have put their effort into investigating this phenomenon, looking for a common explanation, yet it remains a substantial challenge. This study focuses on the role of land surface properties from a land-atmosphere interaction perspective. We compared land surface conditions and energy exchange with the atmosphere before two groups of MJO events hit the Maritime Continent: MJO-C and MJO-B. MJO-C events are MJOs that pass through the Maritime Continent and eventually reach the western Pacific Ocean. In contrast, MJO-B events are MJOs that completely halted over or nearby the Maritime Continent due to their interaction with the region. This study uses an MJO identification method (i.e., Large-scale Precipitation Tracking or LPT) that can track the longitudinal and latitudinal shift of the MJO precipitation centroid; hence it can be particularly useful to identify MJOs that interact with or pass through the MC region and exclude MJOs that detour around the MC. This study

reveals that cooler land surface temperature and drier soil moisture over parts of the MC tend to block MJO propagation over the region, implying a significant land-atmosphere component to this phenomenon. Therefore, understanding the role of land surface properties on MJO behavior over the MC is important for improving its predictability and mitigating problems that MJO-induced heavy rainfall can bring to the region.

3.1   Introduction

Over half a century ago, Roland Madden and Paul Julian discovered the "tropic's pulse"—a pattern of atmospheric variability that shifted eastward along the equator, which we now recognize as the Madden-Julian Oscillation (MJO) (Madden & Julian, 1971, 1972; Hand, 2015). This intraseasonal oscillation is well-known for bringing convection and heavy rainfall that moves eastward along the tropics with a cycle of roughly 20–90 days and a speed range of 1–9 m s^{-1} (Chen & Wang, 2020). The MJO is associated with extreme rainfall and contributed to flooding events over Southeast Asia (e.g., Baranowski et al., 2020; Da Silva & Matthews, 2021) and northern Australia (e.g., Wheeler et al., 2009; Cowan et al., 2019). It also has extensive extratropical impacts by significantly modulating the frequency of high-latitude blocking that alter the global circulation (e.g., Henderson et al., 2016; Henderson & Maloney, 2018), exposing its global-scale societal impact. Over the Maritime Continent (MC), the MJO significantly increases the probability of extreme precipitation by up to 70%, with the magnitude of the impact varying across regions (Muhammad et al., 2020). However, the unique behavior of the MJO over the Maritime Continent remains a topic of intense research (Kim et al., 2020).

The Maritime Continent, consisting of fractions of islands scattered along the equator from around $100°E$–$150°E$ and $10°N$–$10°S$, frequently hinders the propagation of MJO events, also called the "MC barrier effect." This is evidenced by Kerns and Chen (2016) and Zhang and Ling (2017), who found that 40–50% of MJO events that originated over the Indian Ocean fail to propagate across the MC, while the MJO events that propagate across the MC are mostly attenuated. This barrier effect has received more attention after consecutive initial studies comparing propagating versus

nonpropagating MJO events (Hirata et al., 2013; Kim et al., 2014; Feng et al., 2015). Later, the terms propagating and nonpropagating MJO events with respect to the MC were replaced mainly by MJO-C (MJO that crosses the MC) and MJO-B (MJO that is blocked by the MC), respectively (e.g., Ling et al., 2019; Zhou et al., 2022). Another peculiar behavior of MJO propagation is that it tends to detour southward around the MC during austral summer (December to February) and northward during boreal summer (June to August) (Kim et al., 2017). Since our focus here is on land-atmosphere interactions, we solely emphasize the direct interaction between MC land surface properties and fluxes and MJO propagation in the context of the MC barrier effect, thereby filtering out MJOs that deviate around the region.

Recent studies on the MC barrier effect and its proposed key mechanisms can be grouped into four main hypotheses: land vs. oceanic convection, moisture mode thinking, air-sea coupling, and transient dry precursor (Kim et al., 2020). The first group proposed that the development of oceanic convection is critical to the propagation of the MJO across the MC and that MJO convection over the ocean is occasionally disrupted by anomalously strong land convection (Zhang & Ling, 2017). The third group partially aligns with this idea, proposing that warmer ocean conditions favor eastward propagation of the MJO by promoting the development of convection but providing more emphasis on ocean-atmosphere coupling (Hirata et al., 2013). Meanwhile, the second and fourth groups concurrently support the idea that MJO propagation over MC relies on moisture distribution over MC surroundings (Kim et al., 2014; Feng et al., 2015; Adames et al., 2020). Taken together, these four main hypotheses have provided valuable insights into the multiple factors that contribute to the distinctive behavior of MJO propagation over the Maritime Continent. However, among these hypotheses, there are reinforcing as well as competing ideas indicating that the understanding of this particular issue still needs to be improved (Kim et al., 2020). Furthermore, these four main ideas are concerned mostly with the role of atmospheric and oceanic parameters, leaving the potential impact of MC land surface properties and fluxes on MJO propagation less explored. In this study, building upon the first main hypothesis and focusing on the land-atmosphere aspect, we investigated the contribution of MC land surface properties and energy exchange with the atmosphere on the MC barrier effect on MJO propagation over the

Maritime Continent.

Land surface properties, such as soil surface temperature and moisture, play a role in how energy from radiation is divided between heat that is released into the air (sensible heat) and phase change that leads to evapotranspiration (latent heat). This energy partition can affect the formation of local convection, suggesting feedback mechanisms between the land surface and the atmosphere (Eltahir, 1998), yet it is challenging to observe (Taylor et al., 2012). Gerken et al. (2019) used emergent methods, such as information flows, to reveal robust global hotspots of land-atmosphere coupling using the global network of micrometeorological flux measurement sites (FLUXNET) database (Baldocchi et al., 2001). However, land-atmosphere feedback over non-continental and geographically unique regions, such as the Maritime Continent, is still inconclusive and less documented, yet it is essential (e.g., Zhang & Ling, 2017) and warrants more investigations. Therefore, this study investigated the contribution of land-to-atmosphere feedback over the Maritime Continent on the intraseasonal variability of the MJO. We hypothesize that the leading condition of MC land surface properties (e.g., soil surface temperature and moisture) and near-surface energy fluxes before MJO reaches the Maritime Continent can affect the behavior of the subsequent MJO propagation over the region, particularly through the modification of the planetary boundary layer and local convection over MC landmasses.

3.2 Methodology

3.2.1 Types of MJO Events and the MC Barrier Effect

To investigate the effect of the Maritime Continent's land surface properties and fluxes on the Madden-Julian Oscillation (MJO) propagation from the Indian Ocean to the western Pacific Ocean in the context of the "MC barrier effect," we compare and contrast the composite land surface properties and fluxes over the Maritime Continent (MC) islands between two types of MJO events: MJO-C and MJO-B. The "MC barrier effect" refers to the phenomenon whereby the Maritime Continent's region can act as a barrier to MJO propagation, preventing it from reaching the western Pacific. In this study, we define MJO-C (or MJO-Crossed) as the MJO event that originated from

the Indian Ocean, propagated eastward, crossed over the Maritime Continent region, and eventually reached and terminated over the Pacific Ocean. Meanwhile, MJO-B (or MJO-Blocked) is defined as the MJO event that originated over the Indian Ocean and propagated eastward, but dissipated over or near the Maritime Continent after interacting with the landmasses in the region. Furthermore, MJOs that only persist in less than one day over the Maritime Continent are mostly located in the vicinity of the MC and do not locate over the land. Also, if this filter is not applied, the MJO that is detoured will falsely be considered as MJO crossed or MJO blocked. Therefore, an MJO event will be determined if it persists ¿ 1 day over the MC.

Figure 3.1 provides a schematic illustration of two types of MJO events, MJO-C (Fig. 3.1a) and MJO-B (Fig. 3.1b). The figure shows the trajectory of the MJO precipitation centroid as lines with arrows originating from the Indian Ocean and directing eastward and interacting with the Maritime Continent region ($100°$E–$150°$E and $10°$N–$10°$S) before it passes through to the western Pacific Ocean ($>160°$E) to be defined as MJO-C, or before it dissipated over the Maritime Continent or its immediate surrounding to be defined as MJO-B. For our analysis, it is important to note that both MJO-C and MJO-B events should interact with the Maritime Continent region to ensure that they reflect the influence of land-atmosphere interaction on MJO propagation, and to eliminate other effects, such as the impact of ocean-atmosphere interaction. This is critical to provide meaningful insights into the role of land-atmosphere interactions on MJO propagation over the Maritime Continent.

3.2.2   Selection of MJO Tracking Methods

To classify MJO-C and MJO-B, as illustrated in 3.1, we need to track the MJO heavy-precipitation center (or centroid), and its propagation in three dimensions, i.e., time, longitude, and latitude, to particularly observe the latitudinal shift of the MJO centroid and differentiate the MJO event that has interaction with the Maritime Continent and those that detoured around the MC. Commonly available MJO indices offer MJO tracking in two dimensions (time and zonal phases). For example, the Realtime Multivariate MJO (RMM) index provides progression and intensities of MJO convective center based on the first two empirical orthogonal functions (EOFs) of the daily outgoing

longwave radiation (OLR) anomalies and zonal winds, which are used to construct the RMM phase-space diagram that divided into eight MJO phases/regions (Wheeler & Hendon, 2004). The RMM index is beneficial for navigating the progression of MJO and is widely used for climate variability monitoring and prediction. However, since the OLR and zonal winds to calculate this index are averaged from 15°N to 15°S, the resulting MJO index could not pinpoint the latitudinal variation of the propagation of the MJO centroid, which is required in this study.

Another MJO index, i.e., the Outgoing Longwave Radiation MJO index (or OMI), primarily focuses on the OLR to diagnose the circulation feature of the MJO (Kiladis et al., 2014). The advantage of OMI over RMM is that OLR is a more direct measure of the MJO convection center than the wind anomalies used in the RMM index. However, the OMI index provides a phase-space diagram similar to the RMM index without providing latitudinal information. Additionally, instead of using OLR and winds, another method developed by (Ling et al., 2014) and improved by Zhang and Ling (2017) uses rainfall anomalies to track MJO time-longitude evolution, which is known as the Precipitation Tracking method. This method is straightforward to find the locus of heavy precipitation related to the MJO convection center. Nevertheless, this method could not provide latitudinal-shift information on the precipitation center, making the above-mentioned three methods, i.e., RMM, OMI, and Precipitation Tracking, unsuitable for this study.

Fortunately, Kerns and Chen (2016, 2020) provide a Lagrangian object-oriented method to locate and trace MJO convection center progression in three dimensions, which is called Large-scale Precipitation Tracking (LPT). Briefly, LPT tracks MJO precipitation centroid with a minimum size of 300,000 km^2 and time continuity of at least 10 days using spatially smoothed 3-day rainfall accumulation. This method provides the MJO trajectory that represents the meandering of the MJO centroid over time, making it suitable for the objective of this study to differentiate the mode of interactions between MJO and the Maritime Continent. Kerns and Chen (2020) made the MJO LPT tracks dataset available at https://orca.atmos.washington.edu/data/lpt/index.html.

3.2.3 MJO Classification

This study utilizes the MJO LPT events and tracks dataset from Kerns and Chen (2020) to develop an objective classification algorithm that classifies the MJO events into MJO-C, MJO-B, or MJO that has no interaction with the Maritime Continent. To accomplish this objective, a classification algorithm is constructed using the parameter settings in Table 3.1. In the classification algorithm, MJO that only persists ¡ 1 day is mostly located in the vicinity of the Maritime Continent and does not locate over the land. Therefore, this filter is important to remove MJO that detoured around the Maritime Continent.

3.2.4 Land-to-Atmosphere Feedback Analysis

To understand how MC land surface properties affect MJO propagation, we analyze the lagged land-to-atmosphere feedback during MJO-C and MJO-B and the difference between these two events. Specifically, we investigate the role of land surface properties a few days before the MJO convection center enters the Indonesian Maritime Continent region at $100°$E. These land surface properties include soil surface temperature and top-layer soil moisture from the ERA5-Land dataset (Muñoz-Sabater et al., 2021). The effect of seasonality on land surface properties was removed by subtracting the values from its long-term mean. Additionally, a statistical significance test was performed to observe the significant difference between the two land surface conditions during MJO-C and MJO-B, and stippling is used to mark the significant values.

3.3 Results

3.3.1 MJO Precipitation Trajectories: LPT Method

In this study, we select the Large-scale Precipitation Tracking (LPT) method (Kerns & Chen, 2016, 2020) to track each Madden-Julian Oscillation (MJO) precipitation trajectory due to its ability to capture the MJO centroid propagation in three dimensions, including time, longitude, and latitude. LPT method provides MJO propagation track by performing the Gaussian spatial

smoothing of 3-day accumulation of rain for every 3-hour timestep using a precipitation threshold, e.g., 8–16 mm d^{-1}. We use the 12-mm d^{-1} precipitation threshold as it has proven reasonable based on the sensitivity analysis performed by Kerns and Chen (2016). We utilize the LPT running output from https://orca.atmos.washington.edu/data/lpt/kc2020/20_72h/thresh12/systems/mjo_lpt_list.txt and select only the eastward propagating trajectories from the list. As a result, from June 1998 to June 2018, a total of 220 global eastward-propagating MJO events were identified (Fig. 3.2). Around 11 percent of the MJO LPT was observed over the western Hemisphere, which is consistent with the OLR composites for phase 8 of the RMM index (Kerns & Chen, 2020).

Figure 3.2a is similar to figure 4b in Kerns and Chen (2020) and shown here with additional details to provide a global context of MJO LPT, and served as an essential step before discussing the MJO behavior over the Maritime Continent (rectangular dashed line) and its land-atmosphere interactions. In Fig. 3.2a, each MJO trajectory is depicted in color, and blue circles represent the initial location of eastward-propagating MJO events, while red crosses represented the end location when the MJO dissipated. The initiation location of MJO can be anywhere between 40°E (coast of Madagascar) all the way to 40°W (over the Amazon rainforest), while the termination location spread from 90°E to 0°. The varying circle sizes along the track represent the MJO's intensity, allowing the visualization of MJO intensity dynamics along the path.

The majority of the MJO events were found to have spent their lifetime over the Indian Ocean, Maritime Continent, and Pacific Oceans. Interestingly, the Large-scale Precipitation Tracking (LPT) method also captured a few MJO events over tropical America and the Atlantic Ocean. When comparing these events to the canonical MJO propagation, which describes MJO propagation from phase 1 to phase 8, only a few of the total events exhibited the canonical MJO, i.e., initiation in phases 1-3 and dissipation in phases 7-8. The locations of western Hemisphere MJO LPT systems are consistent with the OLR composites for phase 8 of the RMM index (Kerns & Chen, 2020).

We observed deflections of the MJO track off the equator line, particularly in the Western North Pacific and to the south of the Pacific Ocean. These off-equator deflections can be attributed to various factors, such as air-sea interactions and background atmospheric conditions, which can alter the propagation and characteristics of MJO events. This finding underscores the complex

nature of MJO propagation, emphasizing the importance of studying MJO events globally and also regionally.

Furthermore, the LPT method revealed that the global MJO speed range was between 0–14 m s^{-1}, with 90% of the events having a speed range of 1–9 m s^{-1} (Fig. 3.2b). More than half (57%) of the MJO events lasted only between 5–15 days (Fig. 3.2c).

3.3.2   Objective Classification of MJO Propagation

From a total of 220 global MJO events observed during the study period using the MJO LPT method, 119 events, representing 54% of the total, were filtered out during the objective classification process. The reason for this exclusion was that these events were not initiated over the Indian Ocean, which is prescribed in this study to have an MJO system that had been established before hitting the Maritime Continent. The remaining 101 MJO events were subjected to further analysis using the objective classification method.

Upon analysis, as an aggregate, we found that approximately 39% of these remaining MJO events belonged to the MJO-B category, while about 15% were classified as MJO-C (Fig. 3.3). It is important to note that the MJO-B and MJO-C categories represent distinct types of MJO events that are characterized by the interaction with the MC landmasses and the results of that interaction. If the interaction made the MJO dissipate over the MC region, it is classified as MJO-B. Meanwhile, if the interaction did not hinder the MJO from propagating through to the Pacific Ocean, it is classified as MJO-C. The remaining 46% MJO events, although originating from the Indian Ocean, did not interact with the Maritime Continent landmasses, which is the key aspect considered in this study.

The results of the object classification were then compared to the expert judgment, which involved visual observation and careful tracking of each MJO event to determine its interaction with the MC landmasses. This comparison aimed to validate the performance of the objective classification method and evaluate its accuracy in classifying MJO events, specifically that relates to the MC barrier effect. In this comparison, depicted in Fig. 3.4, the objective classification method demonstrate high skill levels in detecting MJO events, with a success rate of over 80% in

identifying MJO-C event and 90% in detecting MJO-B events. These numbers indicate that the method can effectively classify MJO events and reliably distinguish between the different categories based on their interaction with the MC landmasses.

Furthermore, the f-score, which is a metric that combines both precision and recall to provide a single measure of classification performance, was found to be greater than 90% for all classes (Table 3.2). This high f-score indicates that the objective classification method performed well in terms of both correctly identifying MJO events and avoiding false positives or negatives. Overall, the comparison between the objective classification results and expert judgment highlights the effectiveness of the method in capturing the key features of MJO events and their interaction with the Maritime Continent, and the validation process serves to increase confidence in the method's applicability for future application.

3.3.3   Land Surface Composite and the Composite Difference

MJO classification algorithm provided details on MJO types, i.e., MJO-C or MJO-B. Then, leading to each of the events, the land surface properties were composited. For each land surface variable, i.e., land surface temperature and surface soil moisture, there were two composites. The difference can be obtained from the composite by subtracting the MJO-C composite from the MJO-B composite. Furthermore, a t-test at a 95% confidence level is performed to highlight the significant difference between the two composite means. The results showed that the composite mean mostly significantly differed over the Indonesian Maritime Continent (Figures 3.10, 3.11, 3.12, 3.13, 3.14, 3.15, 3.16, and 3.17). The stippling shows significant differences that are presented for each island to provide more detailed representations.

3.4   Discussion

This study assesses the potential of land-atmosphere interaction to affect the propagation and behavior of the Madden-Julian Oscillation over the Indonesian Maritime Continent. MJO normally initiated over the Indian Ocean and moved to the east, bringing heavy rainfall along the path.

Interestingly, the behavior of MJO is unique over the MC region. Previous studies investigate this by exploring the possible mechanism of ocean-atmosphere interaction. However, since the MC is a combination of land fractions, we need to look at the effect of land surface conditions on this intraseasonal propagation.

We begin by designing a filter, or a classification method, for MJO propagation (Figure 3.1). The filter should objectively select MJO events that clearly interact with the Maritime Continent region (Table 3.1). As a result of that interaction, the MJO might be weakened over the MC region or continue to move eastward. The first problem of this kind of investigation is finding a method to capture the propagation of MJO in three dimensions, i.e., time, latitude, and longitude. Most of the MJO monitoring methods relied on averaging information along the latitude. However, the latitudinal shift is necessary to differentiate between MJO that actually passes through the Maritime Continent or only detours without interacting with MC islands. One method suits this need, i.e., Large-scale Precipitation Tracking (Kerns & Chen, 2016, 2020).

The classification method work as expected (Figure 3.5), categorizing each MJO into MJO that is blocked by the Maritime Continent (MJO-B), or the MJO that passes through the Maritime Continent (MJO-C) with necessary statistical distribution (Figure 3.6). The other type is reserved for MJO, which does not interact with the Maritime Continent. The result of the classification showed that around 40% of the MJO is blocked by the MC (Figure 3.3 and 3.7). These results confirmed previous studies that found similar values for MJO-B (Kerns & Chen, 2016; Zhang & Ling, 2017). MJO-B and MJO-C, that was selected in this stage, were further analyzed to investigate the connection between the land surface condition and MJO propagation.

We used land surface data from ERA5-Land to analyze the relationship between land surface temperature, surface soil moisture, and the passage of the Madden-Julian Oscillation (MJO) through two different conditions: MJO-B (when the MJO is blocked) and MJO-C (when the MJO crosses over the Maritime Continent). When the MJO is blocked (MJO-B), we found that the composite of land surface temperature shows cooler-than-average temperatures. Conversely, during MJO-C, the composite of land surface temperature indicates slightly warmer conditions. By subtracting these two conditions, we discovered that land surface conditions and surface soil mois-

ture in the Maritime Continent might contribute to blocking the propagation of the MJO. Further analysis revealed that anomalously warmer land surface temperatures and drier soil moisture, particularly in the central and western parts of the Maritime Continent, tend to precede the crossing of the MJO (MJO-C). Additionally, the composite of soil moisture during MJO-B and MJO-C suggests that drier soil moisture might be a precursor for the MJO to cross over the Indonesian Maritime Continent and vice versa. For a visual representation, please refer to Figure 3.8 for the land surface temperature anomaly and Figure 3.9 for the surface soil moisture anomaly.

To test the significant difference between the two composites of land surface properties, i.e., a couple of days before MJO-B vs. a couple of days before MJO-C, we performed a two-tailed t-test using a 95% confidence level. The locations with significant differences between the two composites are marked by stippling (two-tailed t-test) and presented in Figures 3.10 to 3.17. The figures are presented by each main island to clearly shows significant regions.

We proposed that the MJO convection center might be crossed or blocked by the Indonesian Maritime Continent due to the redistribution of convection over the main islands. This might also be related to the strength of sea-breeze circulation. A strong sea breeze might redistribute convection to be more inland. Then, more intensive convection over the main islands of the Maritime Continent will redistribute the convection and further weaken the MJO convection, which is aligned with previous studies that found suppressed precipitation over the ocean increase the possibility of MJO to propagating through the Maritime Continent (Zhang & Ling, 2017). Surface temperature and surface soil moisture provide indications of the near-surface energy and distribution of convection over the Indonesian Maritime Continent. We hypothesized that the distribution of convection over the main islands of the Maritime Continent could distribute the MJO convection center, further weakening the MJO.

Furthermore, surface temperature and surface soil moisture provide indications of the near-surface energy and distribution of convection over the Indonesian Maritime Continent. Surface temperature is linked to the redistribution of convection due to the land-sea temperature gradient; this is also linked to the sea-breeze circulation by altering the near-surface pressure gradient that drives onshore-offshore wind. Meanwhile, soil moisture is linked to the onshore wind, which will

enhance convection over land, while offshore wind will enhance convection over the ocean. Convection over the ocean tends to strengthen and continuation of MJO convection over the Maritime Continent. Therefore, redistribution of convection is a proposed mechanism that possibly affects the behavior of MJO when crossing the Maritime Continent.

3.5 Conclusion

This study investigated the potential influence of land-atmosphere interaction over the Indonesian Maritime Continent on the propagation and behavior of the Madden-Julian Oscillation (MJO). By designing a classification method to objectively select MJO events that interact with the MC region, the study found that approximately 40% of MJOs are blocked by the MC. The study then analyzed the connection between land surface conditions and MJO propagation, revealing that the anomalously warmer land surface temperatures and drier soil moisture over parts of the Indonesian Maritime Continent ($p < 0.05$) tend to precede MJOs that pass through the MC. These findings suggest that land surface conditions over the Maritime Continent might play a role in blocking or allowing MJO propagation and highlight the need for further investigation of land-atmosphere interactions in intraseasonal variability.

Tables

Table 3.1: Parameters used for the objective classification to obtain MJO-C and MJO-B that interacted with the Maritime Continent

Parameter	Value	Reference/Notes
Propagation speed	1–9 m s^{-1}	Chen and Wang (2020)
Initiation location	Indian Ocean (40°E–95°E and 50°S–50°N)	Resembling phases 1–3 of the RMM index
Termination locations MJO-B	Maritime Continent (100°E–150°E and 10°S–10°N) and 5° extension* to the north, west, and south of the MC	Resembling phases 4–5 of the RMM index
Termination locations MJO-C	Pacific Ocean (160°E–0° and 50°S–50°N)	Resembling phases 6-8 of the RMM index
Allowed latitude or longitude jump of the centroid	Less than 20° for MJO-C	Centroid jump for over 20° is considered as a different event
First contact longitude	100°E	The time when the trajectory first approached this longitude is considered as the first contact with MC

*Five degree (latitude or longitude) extension is added to accomodate MJO that dissipated and deflected not too far after interacting with the Maritime Continent.

Table 3.2: Validation of the objective classification based on expert judgement.

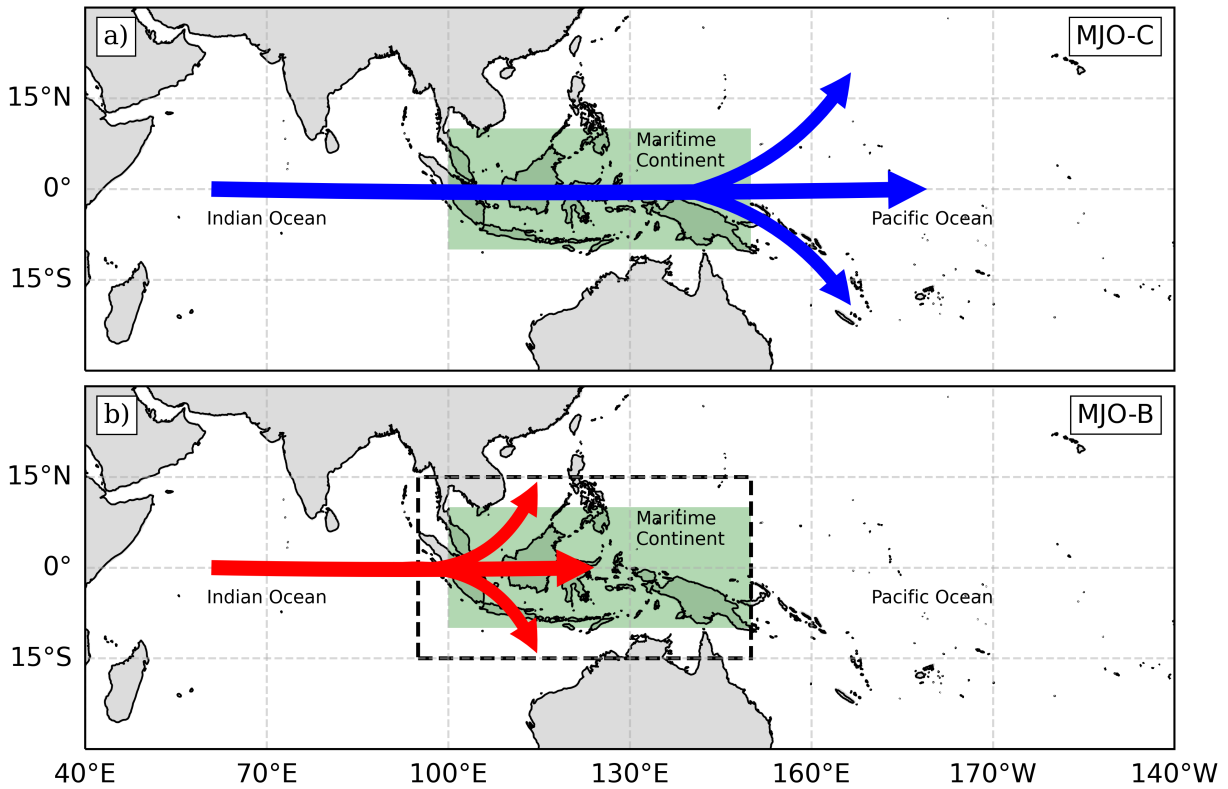| Class	Precision	Recall	F1-score	Support
MJO-C	1.00	0.83	0.91	18
MJO-B	0.95	0.9	0.92	41
Unrelated	0.95	0.99	0.97	140

Figures

Figure 3.1: Schematic illustration of the propagation of the Madden-Julian Oscillation (MJO) to indicate: a) MJO-C and b) MJO-B. MJO-C, or "MJO-Crossed," is the MJO event that initiated over the Indian Ocean (40°E–95°E and 50°N–50°S), propagated eastward, crossed over the Maritime Continent (MC) region (100°E–150°E and 10°N–10°S), and eventually reached and terminated over the western Pacific (>160°E), as illustrated by blue arrows. Meanwhile, MJO-B, or "MJO-Blocked," is the MJO event that initiated over the Indian Ocean, propagated eastward, but dissipated either over or nearby the MC region (95°E–150°E and 15°N–15°S), as illustrated by red arrows and the dashed line.
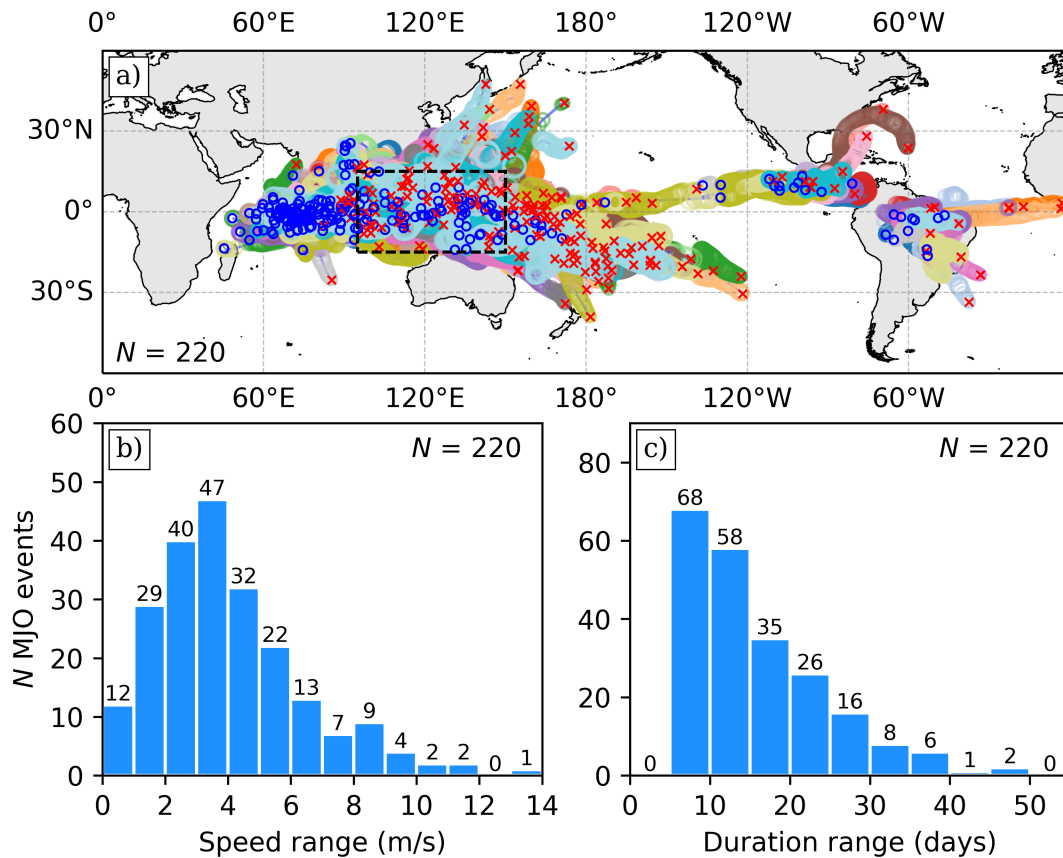
Figure 3.2: Global distribution of the Madden-Julian Oscillation: a) trajectories, b) speed (m s^{-1}), and c) duration (days), from June 1998 to June 2018, using the Large-scale Precipitation Tracking (LPT) method (Kerns & Chen, 2016, 2020). The trajectories shown above are the eastward propagating MJO using the 12-mm d^{-1} threshold. Rectangle with dashed lines on subplot a) denotes Maritime Continent region.
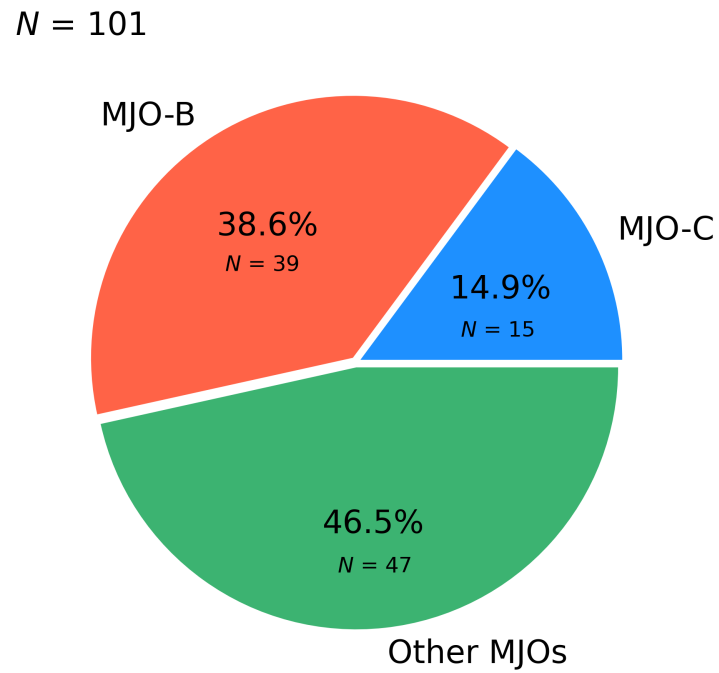
Figure 3.3: Aggregated results of the MJO classification

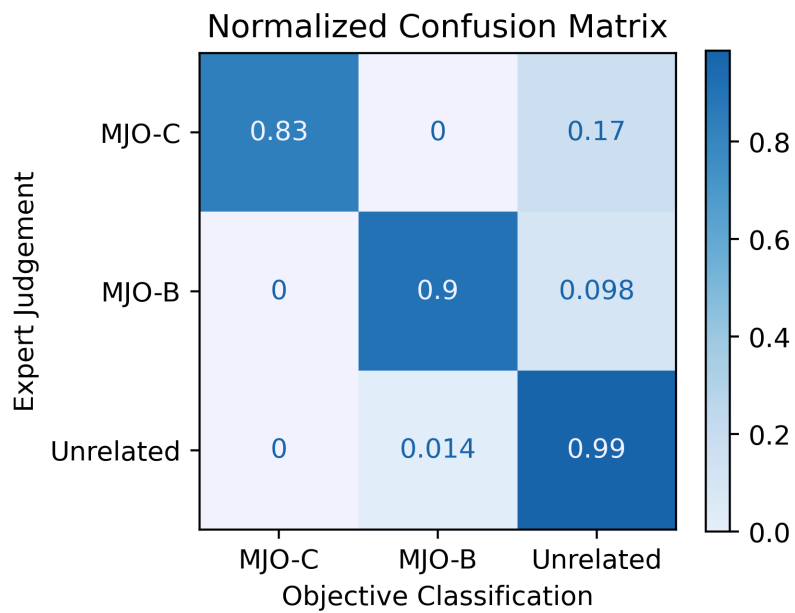Figure 3.4: Normalize confusion matrix from the comparison between objective MJO classification and the expert judgment.

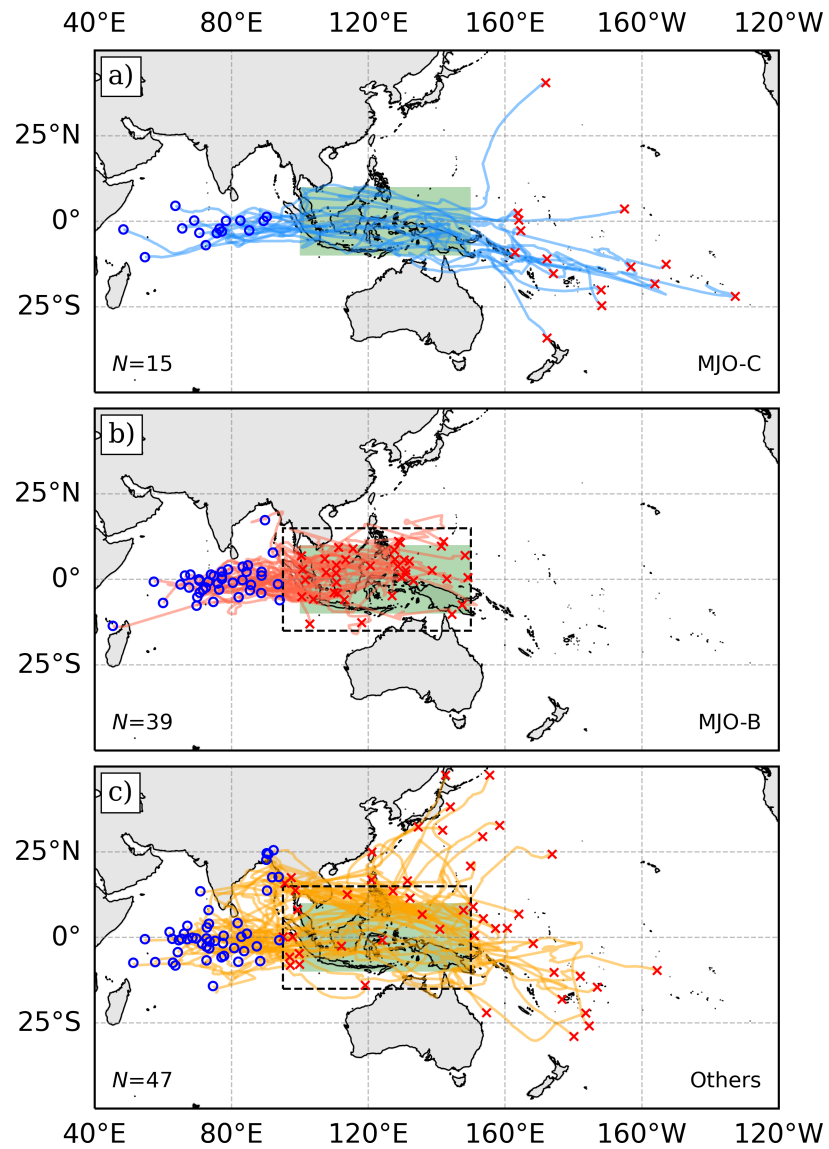Figure 3.5: MJO tracks of the classified MJO: a) MJO-C, b) MJO-B, and c) Other MJOs.
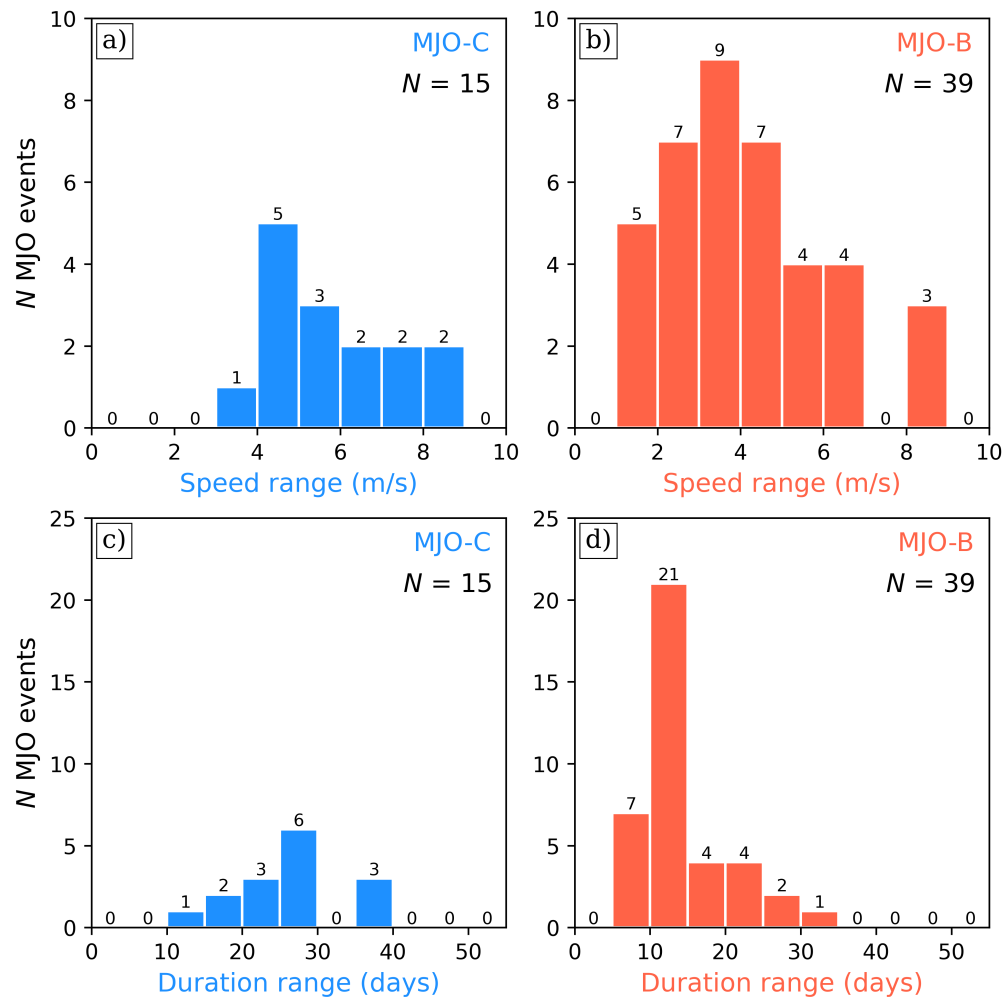
Figure 3.6: Histogram of speed and duration of MJO-C and MJO-B.
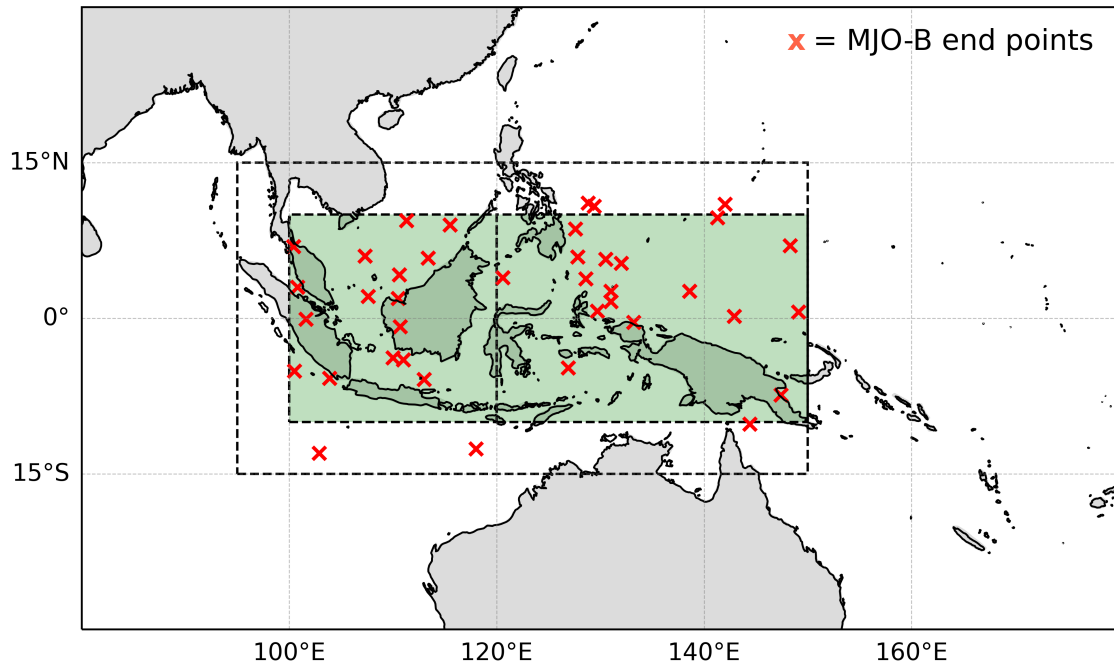
Figure 3.7: MJO-B endpoints over the Maritime Continent.
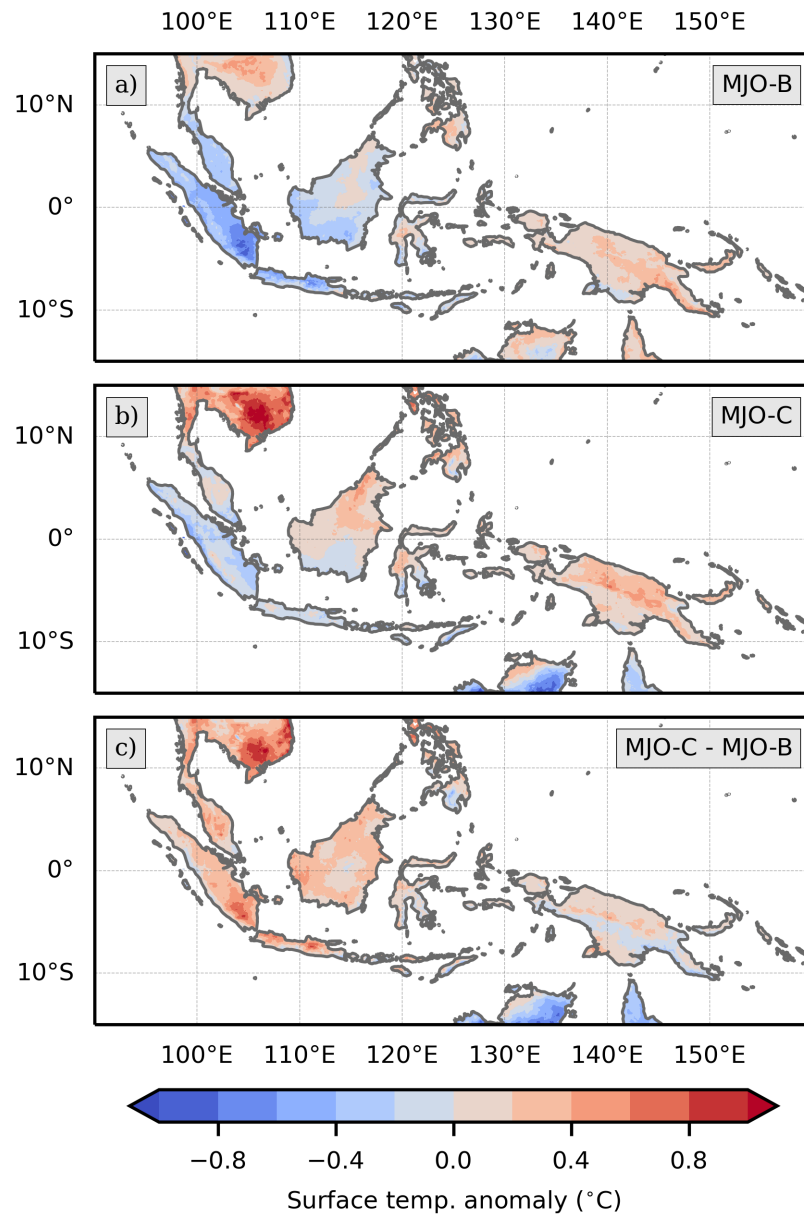
Figure 3.8: Surface skin temperature ERA5-Land during MJO-C, MJO-B, and the difference MJO-C minus MJO-B.
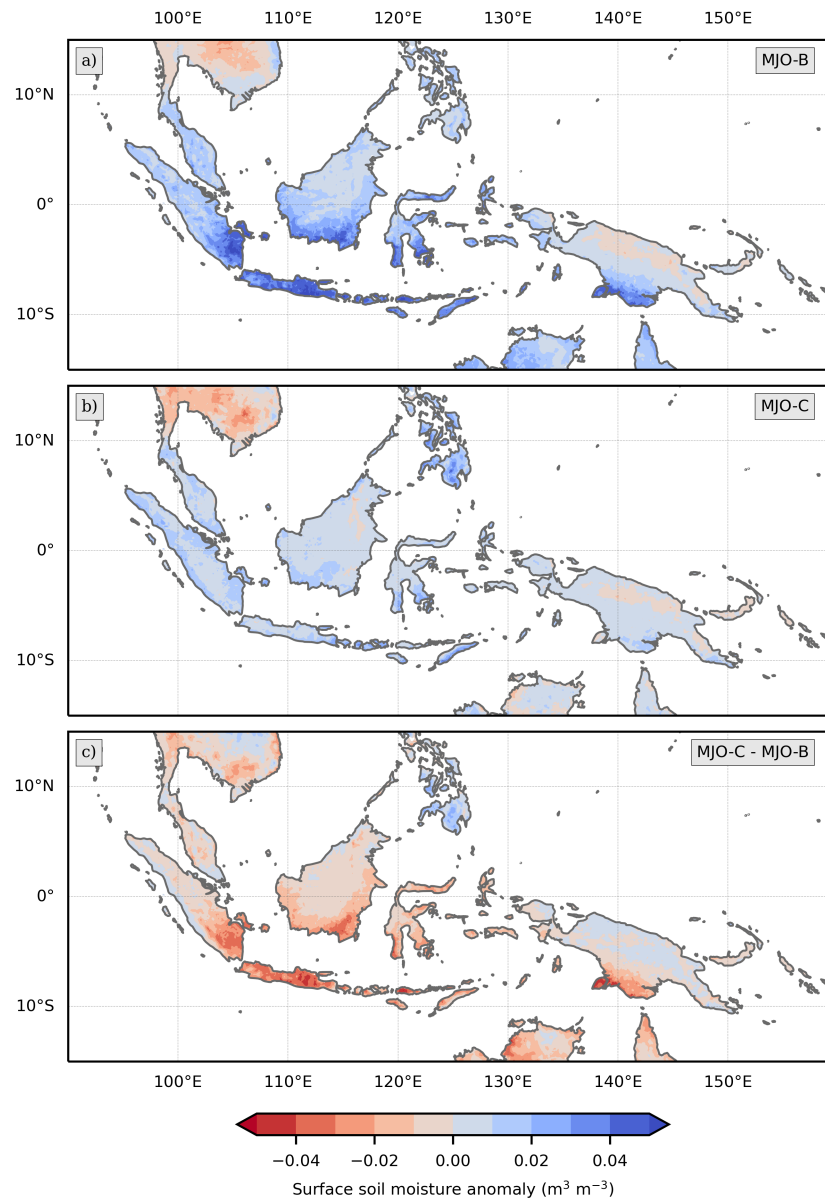
Figure 3.9: Surface soil moisture during MJO-C, MJO-B, and the difference MJO-C minus MJO-B.

Figure 3.10: Surface skin temperature difference (MJO-C minus MJO-B) over Sumatra. The stippling on the map shows a significant difference between the two composite means (MJO-C vs. MJO-B) at a 95% confidence level using a two-tailed t-test.
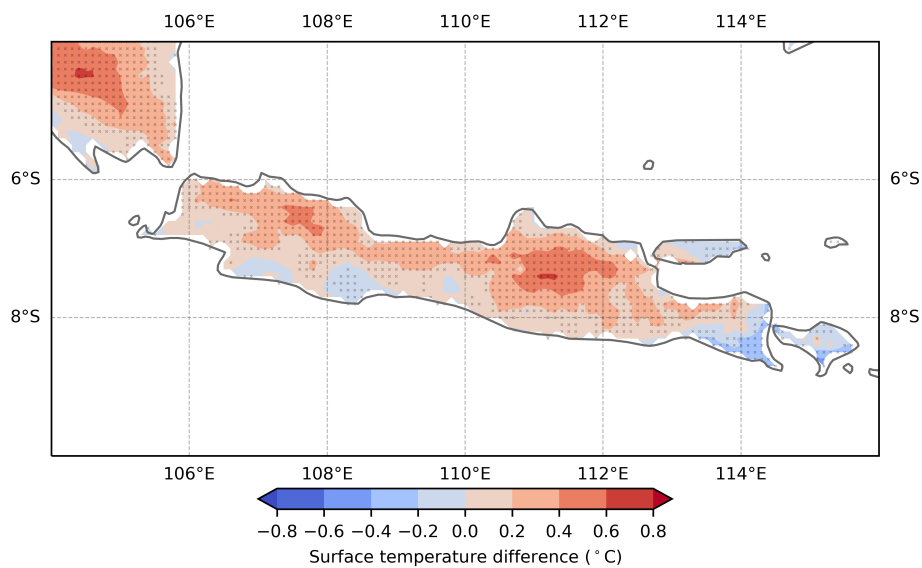
Figure 3.11: Surface skin temperature difference (MJO-C minus MJO-B) over Java. The stippling on the map shows a significant difference between the two composite means (MJO-C vs. MJO-B) at a 95% confidence level using a two-tailed t-test.
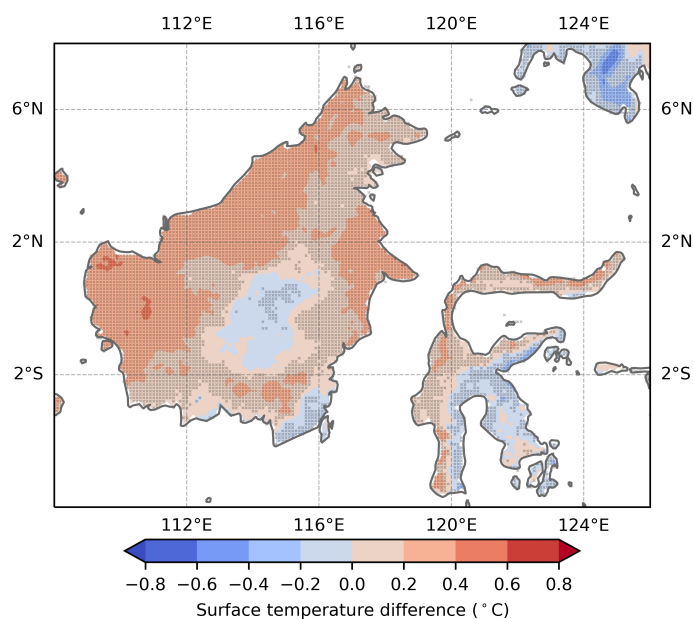
Figure 3.12: Surface skin temperature difference (MJO-C minus MJO-B) over Borneo and Sulawesi. The stippling on the map shows a significant difference between the two composite means (MJO-C vs. MJO-B) at a 95% confidence level using a two-tailed t-test.
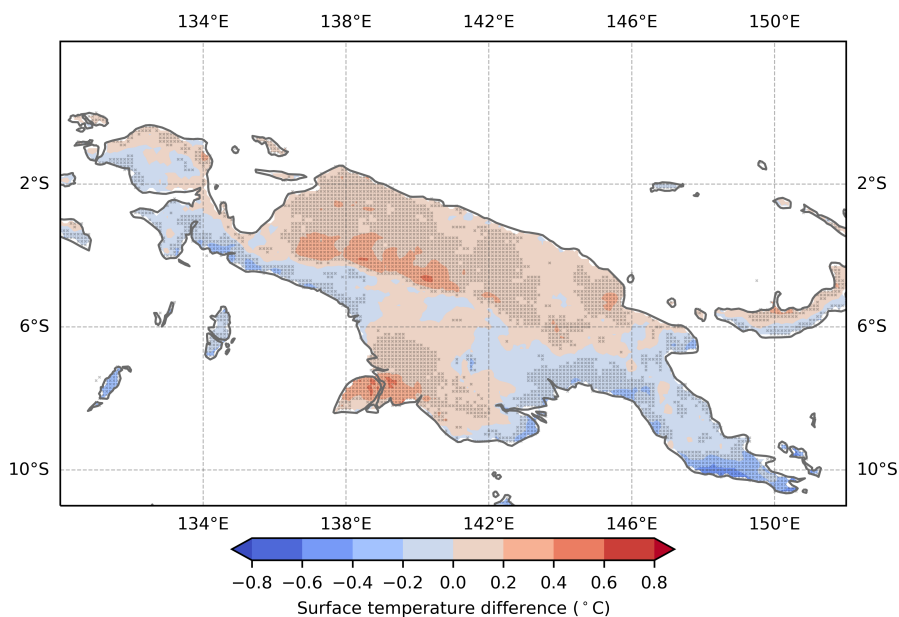
Figure 3.13: Surface skin temperature difference (MJO-C minus MJO-B) over Papua. The stippling on the map shows a significant difference between the two composite means (MJO-C vs. MJO-B) at a 95% confidence level using a two-tailed t-test.
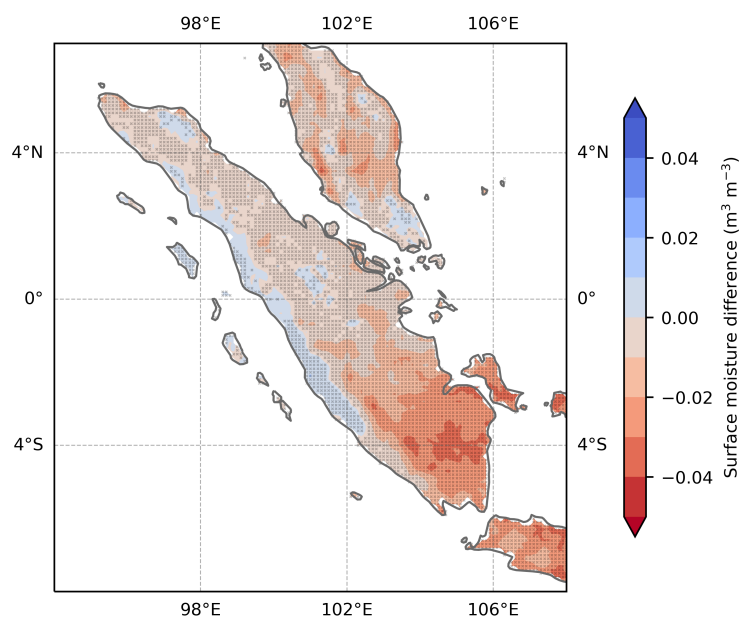
Figure 3.14: Soil moisture difference (MJO-C minus MJO-B) over Sumatra. The stippling on the map shows a significant difference between the two composite means (MJO-C vs. MJO-B) at a 95% confidence level using a two-tailed t-test.
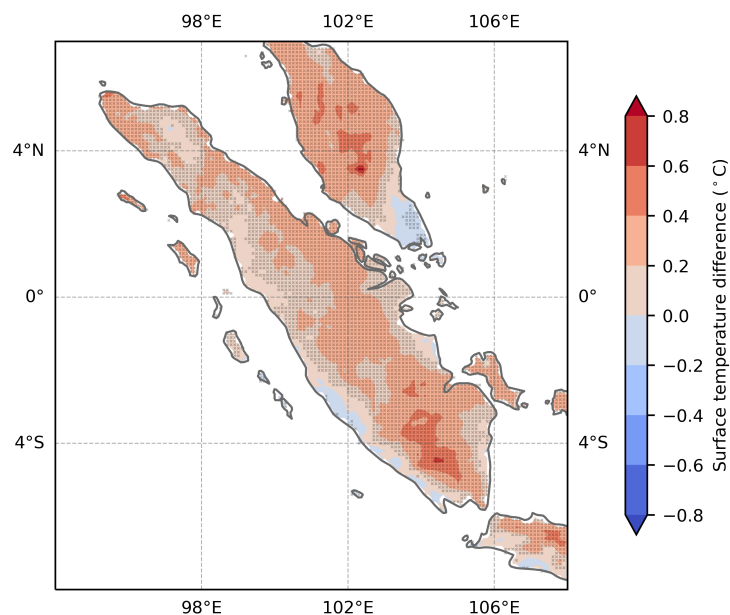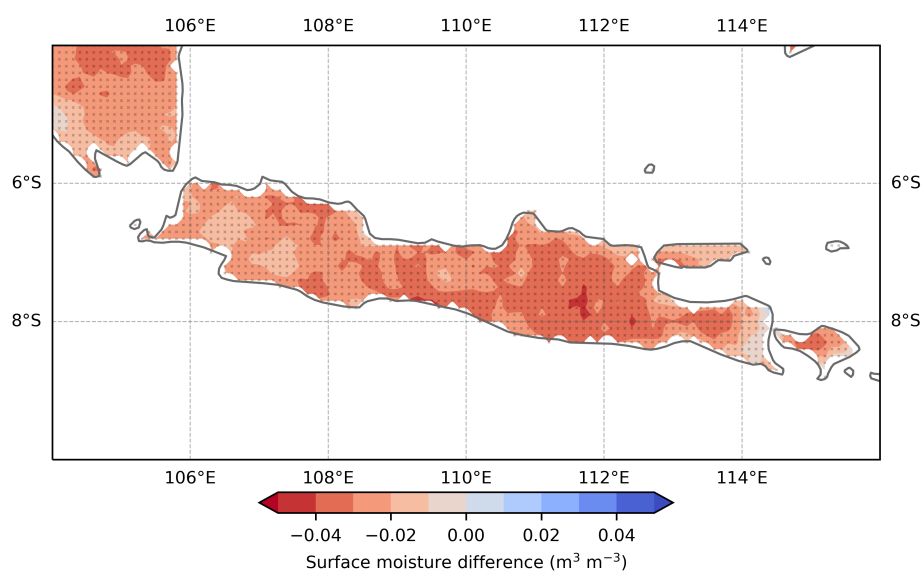

Figure 3.15: Soil moisture difference (MJO-C minus MJO-B) over Java. The stippling on the map shows a significant difference between the two composite means (MJO-C vs. MJO-B) at a 95% confidence level using a two-tailed t-test.

Figure 3.16: Soil moisture difference (MJO-C minus MJO-B) over Borneo and Sulawesi. The stippling on the map shows a significant difference between the two composite means (MJO-C vs. MJO-B) at a 95% confidence level using a two-tailed t-test.

Figure 3.17: Soil moisture difference (MJO-C minus MJO-B) over Papua. The stippling on the map shows a significant difference between the two composite means (MJO-C vs. MJO-B) at a 95% confidence level using a two-tailed t-test.
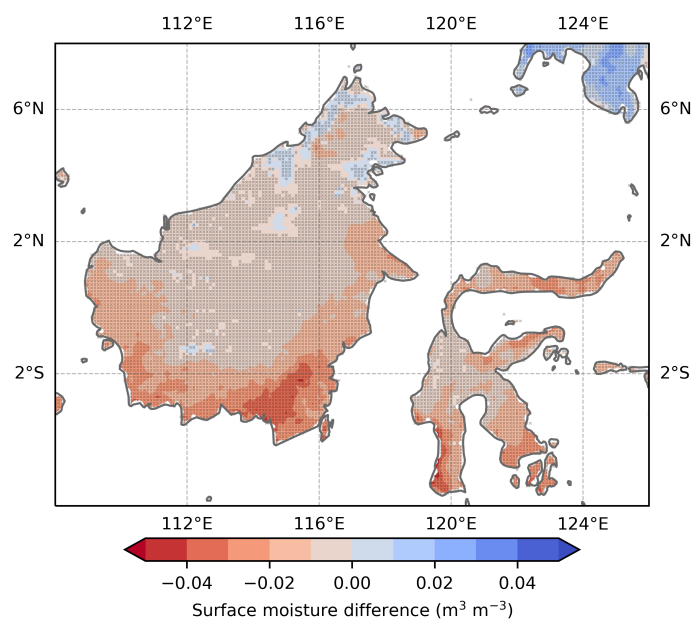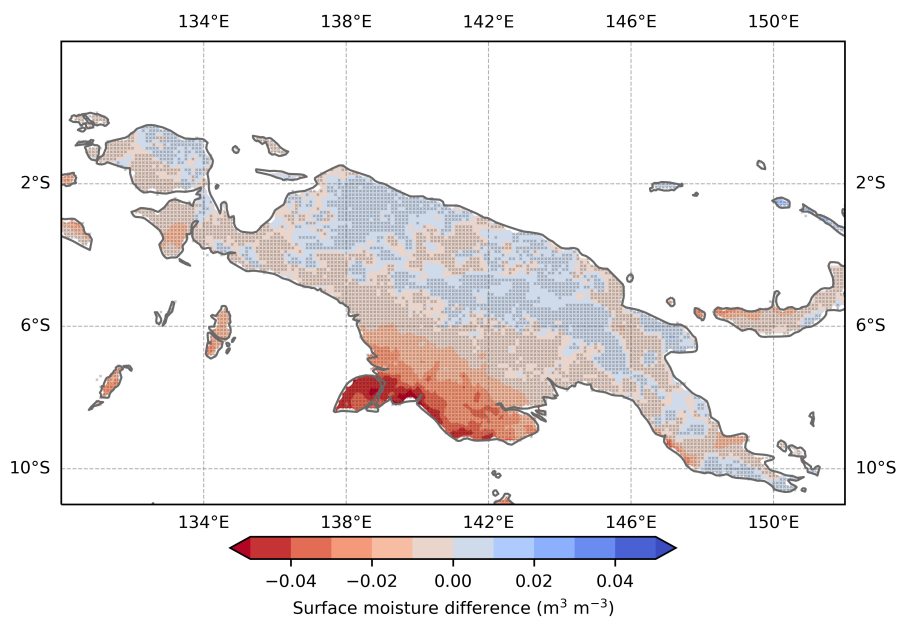
References

Adames, Á. F., Kim, D., Maloney, E. D., & Sobel, A. H. (2020). The Moisture Mode Framework of the Madden-Julian Oscillation. In C.-P. Chang, K.-J. Ha, R. H. Johnson, D. Kim, G. N. C. Lau, & B. Wang (Eds.), *The Multiscale Global Monsoon System* (pp. 273–287). World Scientific. https://doi.org/10.1142/9789811216602_0022

Baldocchi, D., Falge, E., Gu, L., Olson, R., Hollinger, D., Running, S., Anthoni, P., Bernhofer, C., Davis, K., Evans, R., Fuentes, J., Glodstein, A., Katul, G., Law, B., Lee, X., Malhi, Y., Meyers, T., Munger, W., U., W. O. K. T. P., . . . Wofsy, S. (2001). FLUXNET: A new tool to study the temporal and spatial variability of ecosystem-scale carbon dioxide, water vapor, and energy flux densities. *Bull. Am. Meteorolo. Soc*, *82*(11), 2415–2434. https://doi.org/10.1175/1520-0477(2001)082⟨2415:FANTTS⟩2.3.CO;2

Baranowski, D. B., Flatau, M. K., Flatau, P. J., Karnawati, D., Barabsz, K., Labuz, M., Latos, B., Schimdt, J. M., Paski, J. A. I., & Marzuki. (2020). Social-media and newspaper reports reveal large-scale meteorological drivers of floods on Sumatra. *Nat. Commun.*, *11*(2503). https://doi.org/10.1038/s41467-020-16171-2

Chen, G., & Wang, B. (2020). Circulation factors determining the propagation speed of the Madden-Julian Oscillation. *J. Clim.*, *33*(8), 3367–3380. https://doi.org/10.1175/JCLI-D-19-0661.1

Cowan, T., Wheeler, M., Alves, O., Narsey, S., de Burgh-Day, C., Griffiths, M., Jarvis, C., Cobon, D., & Hawcroft, M. (2019). Forecasting the extreme rainfall, low temperatures, and strong winds associated with the northern queensland floods of february 2019. *Weather and Climate Extremes*, *26*, 100232. https://doi.org/10.1016/j.wace.2019.100232

Da Silva, N. A., & Matthews, A. J. (2021). Impact of the Madden-Julian Oscillation on extreme precipitation over the western Maritime Continent and Southeast Asia. *Q. J. R. Meteorol. Soc.*, *147*, 3434–3453. https://doi.org/10.1002/qj.4136

Eltahir, E. A. B. (1998). A soil moisture-rainfall feedback mechanism: 1. theory and observations. *Water Resour. Res.*, *34*(4), 765–776. https://doi.org/10.1029/97WR03499

Feng, J., Li, T., & Zhu, W. (2015). Propagating and Nonpropagating MJO Events over Maritime Continent. *Journal of Climate*, *28*(21), 8430–8449. https://doi.org/10.1175/JCLI-D-15-0085.1

Gerken, T., Ruddell, B. L., Yu, R., Stoy, P. C., & Drewry, D. T. (2019). Robust Observations of Land-to-Atmosphere Feedbacks using the Information Flows of FLUXNET. *npj Climate and Atmospheric Science*, *2*. https://doi.org/10.1038/s41612-019-0094-4

Hand, E. (2015). How two pioneers took the tropics' pulse. *Science*, *350*(6256), 25. https://doi.org/10.1126/science.350.6256.25

Henderson, S. A., & Maloney, E. D. (2018). The Impact of the Madden–Julian Oscillation on High-Latitude Winter Blocking during El Niño–Southern Oscillation Events. *Journal of Climate*, *31*(13), 5293–5318. https://doi.org/10.1175/JCLI-D-17-0721.1

Henderson, S. A., Maloney, E. D., & Barnes, E. A. (2016). The influence of the Madden-Julian Oscillation on Northern Hemisphere winter blocking. *J. Clim.*, *29*(12), 4597–4616. https://doi.org/10.1175/JCLI-D-15-0502.1

Hirata, F. E., Webster, P. J., & Toma, V. E. (2013). Distinct Manifestations of Austral Summer Tropical Intraseasonal Oscillations. *Geophysical Research Letters*, *40*(12), 3337–3341. https://doi.org/10.1002/grl.50632

Kerns, B. W., & Chen, S. S. (2016). Large-Scale Precipitation Tracking and the MJO over the Maritime Continent and Indo-Pacific Warm Pool. *Journal of Geophysical Research: Atmospheres*, *121*(15), 8755–8776. https://doi.org/10.1002/2015JD024661

Kerns, B. W., & Chen, S. S. (2020). A 20-Year Climatology of Madden-Julian Oscillation Convection: Large-Scale Precipitation Tracking from TRMM-GPM Rainfall. *Journal of Geophysical Research: Atmospheres*, *125*(7), 1–21. https://doi.org/10.1029/2019JD032142

Kiladis, G. N., Dias, J., Straub, K. H., Wheeler, M. C., Tulich, S. N., Kikuchi, K., Weickmann, K. M., & Ventrice, M. J. (2014). A comparison of OLR and circulation-based indices for tracking the MJO. *Mon. Wea. Rev.*, *142*(5), 1697–1715. https://doi.org/10.1175/MWR-D-13-00301.1

Kim, D., Kim, H., & Lee, M.-I. (2017). Why does the MJO detour the Maritime Continent during austral summer? *Geophys. Res. Lett.*, *44*(5), 2579–2587. https://doi.org/10.1002/2017GL072643

Kim, D., Kug, J.-S., & Sobel, A. H. (2014). Propagating versus Nonpropagating Madden-Julian Oscillation Events. *Journal of Climate*, *27*(1), 111–125. https://doi.org/10.1175/JCLI-D-13-00084.1

Kim, D., Maloney, E. D., & Zhang, C. (2020). Review: MJO Propagation over the Maritime Continent. In C.-P. Chang, K.-J. Ha, R. H. Johnson, D. Kim, G. N. C. Lau, & B. Wang (Eds.), *The Multiscale Global Monsoon System* (pp. 261–272). World Scientific. https://doi.org/10.1142/9789811216602_0021

Ling, J., Bauer, P., Bechtold, P., Beljaars, A., Forbes, R., Vitart, F., Ulate, M., & Zhang, C. (2014). Global versus local MJO forecast skill of the ECMWF model during DYNAMO. *Mon. Wea. Rev.*, *142*(6), 2228–2247. https://doi.org/10.1175/MWR-D-13-00292.1

Ling, J., Zhao, Y., & Chen, G. (2019). Barrier Effect on MJO propagation by the Maritime Continent in the MJO Task Force/GEWEX Atmospheric System Study Models. *J. Clim.*, *32*(17), 5529–5547. https://doi.org/10.1175/JCLI-D-18-0870.1

Madden, R. A., & Julian, P. R. (1971). Detection of a 40–50 Day Oscillation in the Zonal Wind in the Tropical Pacific. *Journal of the Atmospheric Sciences*, *28*(5), 702–708. https://doi.org/10.1175/1520-0469(1971)028⟨0702:DOADOI⟩2.0.CO;2

Madden, R. A., & Julian, P. R. (1972). Description of Global-Scale Circulation Cells in the Tropics with a 40–50 Day Period. *Journal of the Atmospheric Sciences*, *29*(6), 1109–1123. https://doi.org/10.1175/1520-0469(1972)029⟨1109:DOGSCC⟩2.0.CO;2

Muhammad, F. R., Lubis, S. W., & Setiawan, S. (2020). Impacts of the madden-julian oscillation on precipitation extremes in indonesia. *Int. J. Climatol.*, *41*(3), 1970–1984. https://doi.org/10.1002/joc.6941

Muñoz-Sabater, J., Dutra, E., Agustí-Panareda, A., Albergel, C., Arduini, G., Balsamo, G., Boussetta, S., Choulga, M., Harrigan, S., Hersbach, H., Martens, B., Miralles, D. G., Piles, M., Rodríguez-Fernández, N. J., Zsoter, E., Buontempo, C., & Thépaut, J.-N. (2021). ERA5-Land: A state-of-the-art global reanalysis dataset for land applications. *Earth Syst. Sci. Data*, *13*(9), 4349–4383. https://doi.org/10.5194/essd-13-4349-2021

Taylor, C. M., de Jeu, R. A. M., Guichard, F., Harris, P. P., & Dorigo, W. A. (2012). Afternoon rain more likely over drier soils. *Nature*, *489*, 423–426. https://doi.org/10.1038/nature11377

Wheeler, M. C., Hendon, H., Cleland, S., Meinke, H., & Donald, A. (2009). Impacts of the Madden-Julian Oscillation on Australian rainfall and circulation. *J. Clim.*, *22*(6), 1482–1498. https://doi.org/10.1175/2008JCLI2595.1

Wheeler, M. C., & Hendon, H. H. (2004). An All-season Real-time Multivariate MJO index: Development of and index for monitoring and prediction. *Mon. Wea. Rev.*, *132*(8), 1917–1932. https://doi.org/10.1175/1520-0493(2004)132⟨1917:AARMMI⟩2.0.CO;2

Zhang, C., & Ling, J. (2017). Barrier Effect of the Indo-Pacific Maritime Continent on the MJO: Perspectives from Tracking MJO Precipitation. *Journal of Climate*, *30*(9), 3439–3459. https://doi.org/10.1175/JCLI-D-16-0614.1

Zhou, Y., Wang, S., Fang, J., & Yang, D. (2022). The Maritime Continent barrier effect on the MJO teleconnections during the boreal winter seasons in the northern hemisphere. *J. Clim.*, *36*(1), 171–192. https://doi.org/10.1175/JCLI-D-21-0492.1

Chapter 4

The Role of Land-Atmosphere Feedback on Monsoon Onset over the Maritime Continent

Abstract

The monsoon onset over the Maritime Continent (MC) gradually follows the Northwest-Southeast progression, with the Northwestern region experiencing the onset earlier than the remaining region. Onset variations over MC are also known to be affected by large-scale climate variabilities such as ENSO and Indian Ocean Dipole (IOD). While large-scale climate variabilities significantly shifted the monsoon onset, the influence of local land-atmosphere feedback on the onset variation is less explored. This study investigates the relationship between land surface conditions over the west part of MC and monsoon onset variation over four regions, i.e., South Sumatra, South Borneo, and Java Island. These regions are the most affected and benefited by monsoonal rainfall for agriculture and crop production. The monsoon onset was calculated and determined for 20 years (2000–2020) using IMERG GPM precipitation. The onset variation was observed, and the relationship between this variation and the variation in land surface conditions was explored using the ERA5-Land dataset. The land surface temperature and soil moisture composite during early and delayed onset were analyzed, revealing that local land surface conditions contribute to the 1-2 weeks variation of monsoon onset. Specifically, the land surface temperature of nearby islands moderately contributes

to the onset variation in South Sumatra and East Java, while soil moisture over neighboring islands contributes to the onset variation in South Borneo and West/Central Java. Overall, this study highlights the importance of local land surface conditions in affecting monsoon onset variations.

Plain Language Summary

Monsoon onset in the Maritime Continent follows a pattern in which the Northwestern region experiences the onset earlier than the other regions. Large-scale climate factors like the El Niño-Southern Oscillation (ENSO) and the Indian Ocean Dipole (IOD) are known to influence monsoon onset. However, accurate prediction of the onset remains a challenge, causing issues for farmers who rely on this information to decide when to plant their crops. This study examines the impact of local land conditions on monsoon onset in areas that are heavily dependent on rainfall for agriculture and crop production, specifically South Sumatra, South Borneo, and Java Island. By analyzing rainfall and land surface data from 2000 to 2020, the researchers discovered that local land surface conditions, such as temperature and soil moisture, can significantly influence the timing of monsoon onset. The study found that higher land surface temperatures and drier soil conditions on Java Island led to a delay in monsoon onset in the surrounding regions. This suggests that the influence of local land conditions should be taken into account when attempting to predict monsoon onset. By incorporating these factors, the accuracy of onset predictions could potentially be improved, leading to better agricultural planning and management. Ultimately, this could help farmers make more informed decisions about when to plant their crops and minimize the negative impacts of monsoon onset variations on crop production.

4.1 Introduction

The Maritime Continent (MC), especially Indonesia, experiences a unique monsoon season, which is affected by the Asian and Australian monsoon, and monsoon rainfall is essential for the region's agricultural production. Moron et al. (2010) found that monsoon onset over the MC generally shifts from Northwest to Southeast of the equator, followed by a more zonal propagation south of the

equator (Hamada et al., 2002). The onset of the monsoon season is crucial for agriculture because it provides the necessary moisture for seed germination and crop growth. Therefore, accurate information about the timing and duration of the monsoon season is imperative for farmers to ensure favorable crop yields (Moron et al., 2010). However, changes in rainfall patterns, especially the onset of the wet season and the temporal distribution of rainfall, can severely affect agriculture in Indonesia (Apriyana et al., 2021).

Extended periods of dry conditions following the initial precipitation can have detrimental effects on crops, particularly during critical developmental phases. A study conducted by (Naylor et al., 2007) examined the potential impact of climate change and variability on rice agriculture and found that the timing of the monsoon onset would significantly influence agriculture in Java and Bali, Indonesia. The study predicted a 30-40% chance of a 30-day delay in monsoon onset in 2050 compared to a 9-18% chance in 2007. Such delays could lead to considerable alterations in the annual precipitation cycle, affecting agricultural practices and productivity in these regions. In particular, rice yields could be reduced, but this can be mitigated by adjusting planting time to match rainfall patterns and improving irrigation practices (Amale et al., 2023).

The predictability of wet season rainfall in the Maritime Continent has been a long-standing issue (Haylock & McBride, 2001), with the western region of the area experiencing substantial forecast errors during the boreal winter monsoon season (Chang et al., 2020). This problem is compounded by "false rains," where isolated rainfall events around the expected onset date do not signal sustained monsoon onset, causing difficulty for farmers in Indonesia (Moron et al., 2009). Similarly, in Northern Australia, false onsets of wet season rainfall occur between 20 and 30% of wet seasons, with increased likelihood during La Niña patterns and negative Indian Ocean Dipole, and can lead to flash droughts that are disruptive and costly for agriculture and fire management (Lisonbee et al., 2022).

There are primarily two techniques for determining the onset of monsoons: methods that operate on a local level and those that function on a regional to extensive scale. Similarly, the factors influencing the variability in the timing of monsoons can be divided into two categories: those that stem from local-scale sources and those that originate from large-scale sources (Bombardi et al.,

2019). Most studies have primarily investigated large-scale influences on monsoon onset, such as the impact of El Niño and La Niña events on monsoon onset variation. For example, Robertson et al. (2011) found that monsoon onset is delayed during El Niño years, and interannual variability of onset date is largely in-phase across the monsoonal region of Indonesia (Moron et al., 2010). Meanwhile, extreme La Niña events usually coincide with an early onset and (Lisonbee & Ribbe, 2021). However, land surface changes, such as soil moisture, vegetation, and anthropogenic land cover change, can significantly impact the Asian monsoon climate and its variability through land-atmosphere and in-situ feedback processes (Yasunari, 2007). Recent studies used regional climate model and observation to explore the land surface feedback on the Australian monsoon system (Notaro et al., 2017; Yu & Notaro, 2020), demonstrating the need to accurately represent land surface characteristics and associated feedbacks of the global monsoon systems. As a result, this research seeks to delve deeper into the role of land-atmosphere feedback in monsoon onset variability over the monsoonal region of the Maritime Continent. We hypothesize that land surface properties over parts of the Maritime Continent affect local monsoon onset variation over the monsoonal region of the MC.

4.2 Methodology

4.2.1 Study Area

Indonesia is characterized by three distinct climatic regions (A, B, and C) with distinct characteristics and shows both strong annual and semi-annual variability in these regions. Region A, also known as the "monsoonal" region, is the dominant pattern over Indonesia (see Figure 2 in Aldrian & Susanto, 2003). This region experiences strong influences of two monsoons, the wet northwest (NW) and the dry southeast (SE) monsoon, which covers south and central Indonesia. This study will focus on the monsoon onset over the monsoonal region of Indonesia, i.e., South Sumatra (102°E–106°E and 6°S–2°S), West/Central Java (106°E–110°E and 8°S–6°S), East Java (110°E–116°E and 9°S–7°S), and South Borneo (110°E–116°E and 4°S–2°S), with the land surface analysis over the western Maritime Continent (95°E–120°E and 12°S–10°N) (Figure 4.1). These

regions are among the most impacted by the monsoon, the most inhabited regions, and the largest contributor to agriculture and crop production. We hypothesized that land surface conditions over the West Maritime Continent (WMC) or parts of the WMC contribute to the monsoon onset variation over the region.

4.2.2   Definition of Monsoon Onset

The main methods used to detect the timing of monsoons are divided into two categories: local-scale methods and regional to large-scale methods. Bombardi et al. (2019) found that spatial aggregation usually reduces the noise and enhances the regional monsoonal signal. Therefore, this study will use the regional-scale method to quantify the monsoon onset by performing the area average of daily precipitation over the selected study area. The precipitation uses GPM IMERG Final Precipitation L3 1 day $0.1° \times 0.1°$ V06 accessed from NASA Goddard Earth Sciences Data and Information Services Centre (GES DISC) (Huffman et al., 2019). To define the monsoon onset, we took a similar approach with Naylor et al. (2007) by defining the onset as the number of days past August 1 when accumulated rainfall equals 200 mm, the amount of moisture needed for crop establishment.

Meanwhile, the termination date is the latest day when the accumulated precipitation reach or exceeds 90% of total rainfall in that year. The onset and termination are calculated from the gridded precipitation averaged over the selected regions, i.e., South Sumatra, South Borneo, and Java, for 20 years (2000–2020). This method provides a straightforward way to calculate the onset as this does not include an additional calculation but is still reliable for determining the onset date. The most prominent method used in this region is the BMKG method (Meteorology, Climatology, and Geophysical Agency), which uses the three consecutive 10-day with a 50 mm threshold for each period after September 1 (Marjuki et al., 2016). However, we chose the Naylor et al. (2007) method due to the simplicity and more significant threshold for the crop requirements compared to the other method.

4.2.3   Land-Atmosphere Feedback Analysis on Monsoon Onset

Land-atmosphere feedback on monsoon onset over the "monsoonal" region of the West Maritime Continent utilizes a high-resolution land surface dataset ($0.1° \times 0.1°$) from ERA5-Land (Hersbach et al., 2020), accessed from the Climate Data Store (CDS) from ECMWF, which includes land surface temperature (K) and soil moisture (m^3/m^3). After the onset date was calculated and the onset variation was determined (early or delayed onset), the land surface properties were composited over early and delayed onset. The "early onset" in this study was determined as an onset date that is 5–15 days earlier than the mean monsoon onset (calculated from the base period 2000–2020). Meanwhile, "delay onset" was determined as an onset that is 5–15 days later than the mean monsoon onset. The earliest and the latest monsoon onset can reach 60 days or two months in advance or two months delayed from the mean onset date. This range (5–15 days) is selected to avoid large-scale climate effects on monsoon onset variations. The large-scale climatic disturbance that significantly contributes to the monsoon onset includes El-Niño Southern Oscillation, La Niña, and Indian Ocean Dipole. Avoiding these primary sources of significant onset variation will provide a chance to explore the local or regional effects of land surface properties on monsoon onset variation, which particularly become the concern of this study. The land surface conditions were then averaged from 30-15 days prior to the onset date for each region and subsequently area-averaged for each respective region.

4.3   Results

4.3.1   Characteristics of Monsoon Onset and Duration

Figure 4.2 presents the long-term mean (2000–2020) of the monsoon onset and duration over the four selected regions of the West Maritime Continent. First, the onset date was calculated from IMERG GPM daily precipitation that averaged over the selected regions (see Figure 4.1b). Next, the monsoon onset was calculated following the method by Naylor et al. (2007). "Monsoon onset" was defined as the date after August 1 when the cumulative precipitation exceeds 200 mm. Over

2000-2020, the onset dates and variation were then calculated and averaged to get the box plots of onset dates (top panel of Figure 4.2). Next, the termination date was calculated by defining when the cumulative precipitation reached 90% of the total year precipitation. Finally, the duration of the monsoon is simply the number of days between the onset date and the termination date. The average value of the monsoon duration is then presented on the bottom panel of Figure 4.2.

The long-term mean of the onset date provides an apparent shifting of the onset date from the earliest around late September, i.e., South Sumatra, to the latest around late November (East Java and Bali). This pattern clearly shows that the monsoon over the West Maritime Continent is propagated from the Northwest to the Southeast, confirming previous studies and validating the monsoon onset calculation method. Most regions exhibit considerable variation of the onset date as depicted by the tails of the box plots, except for East Java and Bali region, which has a shorter distribution of early onset, but with two outliers. Meanwhile, the long-term mean of the monsoon duration has another noticeable trend, which shows that the monsoon duration is decreasing. At the same time, it propagates Southeastward over the West Maritime Continent. South Sumatra, on average, experienced more than 250 days (more than eight months) of wet monsoon season, while East Java only experienced less than six months of the monsoon season.

4.3.2   Interannual Variation of Monsoon Onset

Interannual variation of monsoon onset over the West Maritime Continent is presented in Figure 4.3 using a bar chart that deviated from a mean value. The long-term mean of the onset date is depicted as a horizontal line with a value of zero, which can be different for different regions. Four panels on the figure present each region of interest (South Sumatra, South Borneo, West/Central Java, and East Java/Bali). The x-axis of each figure is the year range during the period of interest, from 2000 to 2020, while the y-axis is the onset date anomaly (in days). The mean onset value can be found in the bottom-left corner for each figure. Positive deviation from the mean onset (red bars) is the onset date that comes later after the mean onset date or the "delay", while negative deviation means "early" onset. The onset deviation can generally reach two months, either early or delayed. For example, in 2010, East Java/Bali experienced monsoon onset two months earlier

than usual due to an intense La Niña event (Zhang et al., 2013). On the other hand, in 2019, South Sumatra experienced two months delay in the monsoon onset, which coincides with the extremely positive Indian Ocean Dipole (Ratna et al., 2020).

As we can see from Figure 4.3, all regions exhibit a general pattern of the monsoon onset variation. The La Niña effect in 2010 affected not only South Sumatra but also affecting the other regions, with slightly different intensities. Also, 2019 +IOD influenced monsoon onset over the regions with varying responses. Other than that, there were years with significant onset variations that were clearly affected by large-scale interannual climate variations. Therefore, the further analysis excludes years with an apparent signal from such large-scale disturbance by applying a 5–15 days threshold for the onset days, presented as two dashed lines above and below the horizontal line at zero y-value. Any onset variation that falls inside the threshold is assumed to be free from large-scale effect and further explored to find the relationship between land-surface properties over the West Maritime Continent and the onset variation over the region.

Monsoon onset variation that excludes the large-scale effect is then grouped into early onset years and delayed onset years for each region. This subset of years will be further used to explain the possible connection between land surface properties and monsoon onset variation over the Maritime Continent.

4.3.3 Land Surface Feedback on Monsoon Onset Variation

Figure 4.4 shows the composite of land surface properties, i.e., land surface temperature and soil moisture content, during early and delayed onset. Note that the large-scale influence on the onset variation was filtered out. This figure focuses on the South Sumatra monsoon onset variation with a dashed line displaying the region boundary for calculating the onset from precipitation. The early onset years for this region were 2000, 2003, 2009, and 2017, and the delayed onset year was 2007. Referring back to Figure 4.3, 2004 was not considered a delayed onset year since the delay is less than five days; hence it is considered a normal variation of monsoon onset. Therefore, there was only one year, 2007, when the delay fell inside the threshold to be considered as the year of onset delay.

Land surface properties in Figure 4.4 were averaged from 1 month to two weeks before the onset date, describing the "pre-onset" conditions. From this figure, we can see that drier pre-onset soil moisture over South Sumatra and dominant parts of Java preceded early onset, while this signal is not clear for the land surface temperature. For the delayed onset, a noticeable difference is the warmer than usual over Thailand, Cambodia, and Vietnam, to the north of the area of interest. Overall, the analysis of land surface properties in Figure 4.4 reveals essential patterns related to the timing of monsoon onset over the West Maritime Continent. Specifically, the data suggests that drier pre-onset soil moisture over South Sumatra and parts of Java are associated with early onset. In contrast, the pre-onset land surface temperature does not show a clear signal. In contrast, delayed onset is characterized by warmer-than-usual temperatures over Thailand, Cambodia, and Vietnam, north of the study area. These findings highlight the potential value of using land surface properties to predict monsoon onset and suggest that variations in soil moisture and temperature may play an essential role in the onset of the monsoon over the West Maritime Continent.

Figure 4.5 shows the pre-onset land surface properties before the onset dates over West/Central Java. The shaded line indicated the location where the onset dates were calculated. For this region, years with early onset are 2000, 2003, and 2008 and years with delayed onset include 2004, 2007, 2011, and 2012. The figure shows that drier soil moisture and warmer land surface temperature over South Sumatra lead to early onset. Meanwhile, there was no apparent difference for the delayed onset, except that drier and warmer land surface conditions over parts of Java island led to the delayed onset. In summary, early onset was associated with drier soil moisture and warmer land surface temperature over South Sumatra. At the same time, no clear difference was observed for delayed onset, except for drier and warmer land surface conditions over parts of Java island.

Pre-onset land surface properties preceding the monsoon onset for East Java/Bali are presented in Figure 4.6. Similar to the previous two figures, the figure consisted of land surface temperature conditions for the early and delayed onset for the left panels and soil moisture conditions for the early and delayed onset for the right panels. From the land surface temperature, we can observe that warmer pre-onset condition of land surface temperature over Sumatra, Malay Peninsula, and Borneo shows a clear difference between early and delayed onset, i.e., warmer surface temperature

over these three islands leads to delayed onset. Moisture condition seems to support the delay when the mentioned islands have drier conditions. Therefore, we might conclude that warmer and drier adjacent islands lead to delayed monsoon onset over East Java.

Figure 4.7 shows the land surface condition prior to the monsoon onset variation at South Borneo. It is clear that drier and slightly warmer soil over Sumatra leads to the early onset of the wet season at South Borneo. Meanwhile, delayed onset is preceded by warmer and drier soil over Java and South Sumatra. In summary, the pre-onset land surface condition over South Borneo indicates that drier and slightly warmer soil over Sumatra is associated with early onset, while delayed onset is related to warmer and drier soil over Java and South Sumatra.

4.4   Discussion

This study investigates the possible effect of pre-onset land surface conditions on monsoon onset variation over the monsoonal region of the West Maritime Continent. We hypothesized that land surface conditions over the West Maritime Continent (WMC) might contribute to the variation of monsoon onset over the region. To examine this hypothesis, we carefully select the study area that is affected by monsoon and has great importance in utilizing the water supply brought by the monsoon for agriculture and crop production and management (Figure 4.1).

Four regions, or provinces, for the land-atmosphere feedback analysis in this study are South Sumatra, South Borneo, and Java Island. For each of the regions, we calculate the onset by simply averaging daily rainfall from IMERG GPM and then defining the onset and termination dates by following Naylor et al. (2007). Another information that can be obtained is the duration of the monsoon season, which clearly indicated by the onset and termination date. Twenty years of onset, termination, and duration were analyzed. The 20-year mean onset, as well as the yearly onset variation, were obtained. Monsoon season is gradually shifted following the Northwest-Southeast pattern (Hamada et al., 2002) and the duration of monsoon season is decreased along the path (Figure 4.2), requiring careful consideration to manage the agriculture and water resources (Amale et al., 2023). We also found that the mean onset dates are generally shifted to be earlier (Naylor

et al., 2007) while this study confirms late vs early years (Moron et al., 2010).

To explore the connection between the land surface condition and monsoon onset variation, we calculated the interannual variation of monsoon onset and observed that the delayed onset could be as severe as a couple of months, significantly affecting farmers who relied on rainfed agriculture and pushing others to manage water resources for agriculture and crop production over the region. These huge variations stem from the large-scale climate variabilities such as ENSO and IOD, indicated by similar patterns over the four regions (Figure 4.3). We then learned that applying a threshold on the monsoon onset could filter out such large-scale effects. The threshold is then used to define which years can be categorized as early onset years and which years as delayed onset years. This will be useful in grouping the land surface condition and seeing the connection between the land surface and the possible association with the onset variations.

From the land surface temperature and soil moisture composite during early and delayed onset, we can see that land surface patterns related to the timing of monsoon onset over the West Maritime Continent with varying conditions for different regions, highlighting the importance of local land surface contribution on affecting the 1-2 weeks variation of monsoon onset. For South Sumatra and East Java, the land surface temperature of the nearby islands seems moderately contribute to the onset variation. Meanwhile, for South Borneo and West/Central Java, soil moisture over neighboring islands appeared to contribute to the onset variations. This might occur due to the alteration of local circulation that alter or enhance the gradual propagation of monsoon onset over the Maritime Continent.

4.5   Conclusion

In conclusion, this study aimed to investigate the possible impact of land surface conditions on monsoon onset variation over the West Maritime Continent. The study focused on four regions, namely South Sumatra, South Borneo, West Java, and Central Java. The onset and termination dates of the monsoon were calculated based on the daily rainfall from IMERG GPM. The inter-annual variation of monsoon onset was observed, and a threshold was applied to filter out the

large-scale climate variabilities such as ENSO and IOD. The land surface temperature and soil moisture composite during early and delayed onset were analyzed, revealing that local land surface conditions contribute to the 1-2 weeks variation of monsoon onset. Specifically, the land surface temperature of nearby islands moderately contributes to the onset variation in South Sumatra and East Java, while soil moisture over neighboring islands contributes to the onset variation in South Borneo and West/Central Java. Overall, this study highlights the importance of local land surface conditions in affecting monsoon onset variations and could aid in managing water resources and agriculture production over the region.
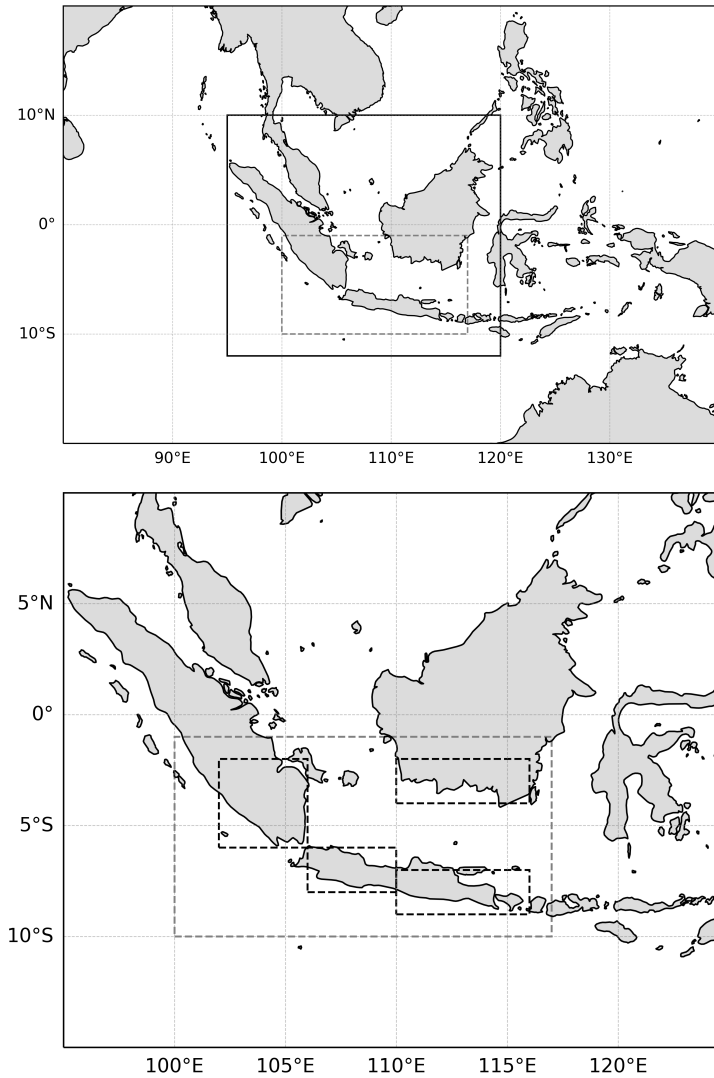
Figures

Figure 4.1: Study area for the land-atmosphere feedback on monsoon onset analysis: (top panel) depicting the West Maritime Continent (WMC) that bounded by a solid line to explore land surface conditions that might be essential in altering monsoon onset over four regions (bottom panel), which include South Sumatra (102°E–106°E and 6°S–2S), West/Central Java (106°E–110°E and 8°S–6°S), East Java (110°E–116°E and 9°S–7°S), and South Borneo (110°E–116°E and 4°S–2°S).
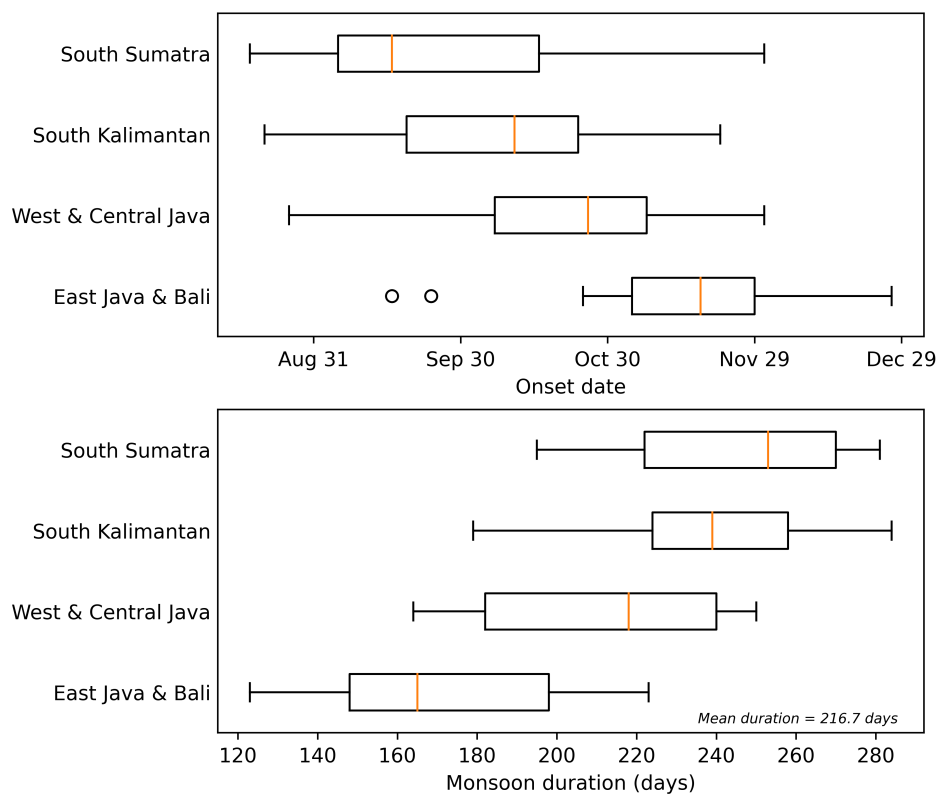
Figure 4.2: Long-term average of monsoon onset and duration over the West Maritime Continent.
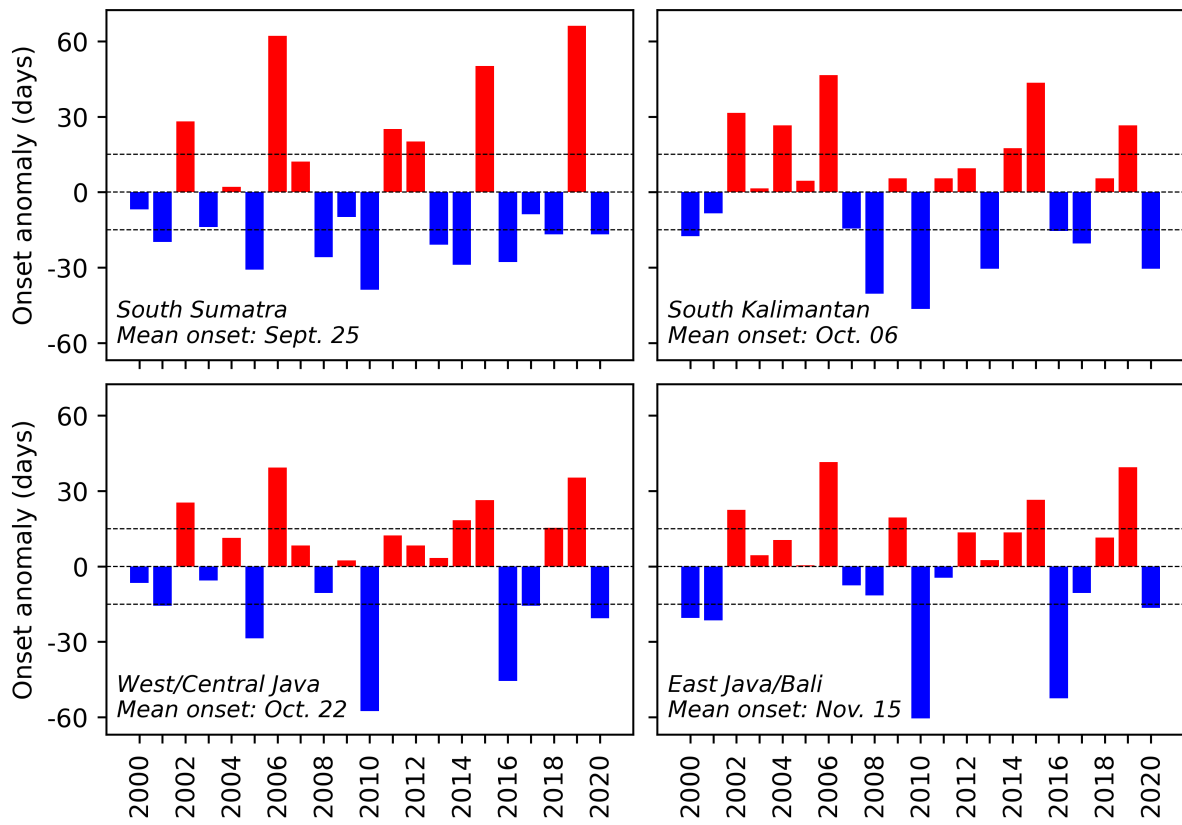
Figure 4.3: Monsoon onset variation at four monsoonal regions (see Figure 4.1) over the West Maritime Continent.

South Sumatra

Figure 4.4: Composite of land surface temperature and soil moisture over the West Maritime Continent during pre-onset for the early and delayed onset at South Sumatra.

Figure 4.5: Composite of land surface temperature and soil moisture over the West Maritime Continent during pre-onset for the early and delayed onset at West/Central Java.

Figure 4.6: Composite of land surface temperature and soil moisture over the West Maritime Continent during pre-onset for the early and delayed onset at East Java/Bali.
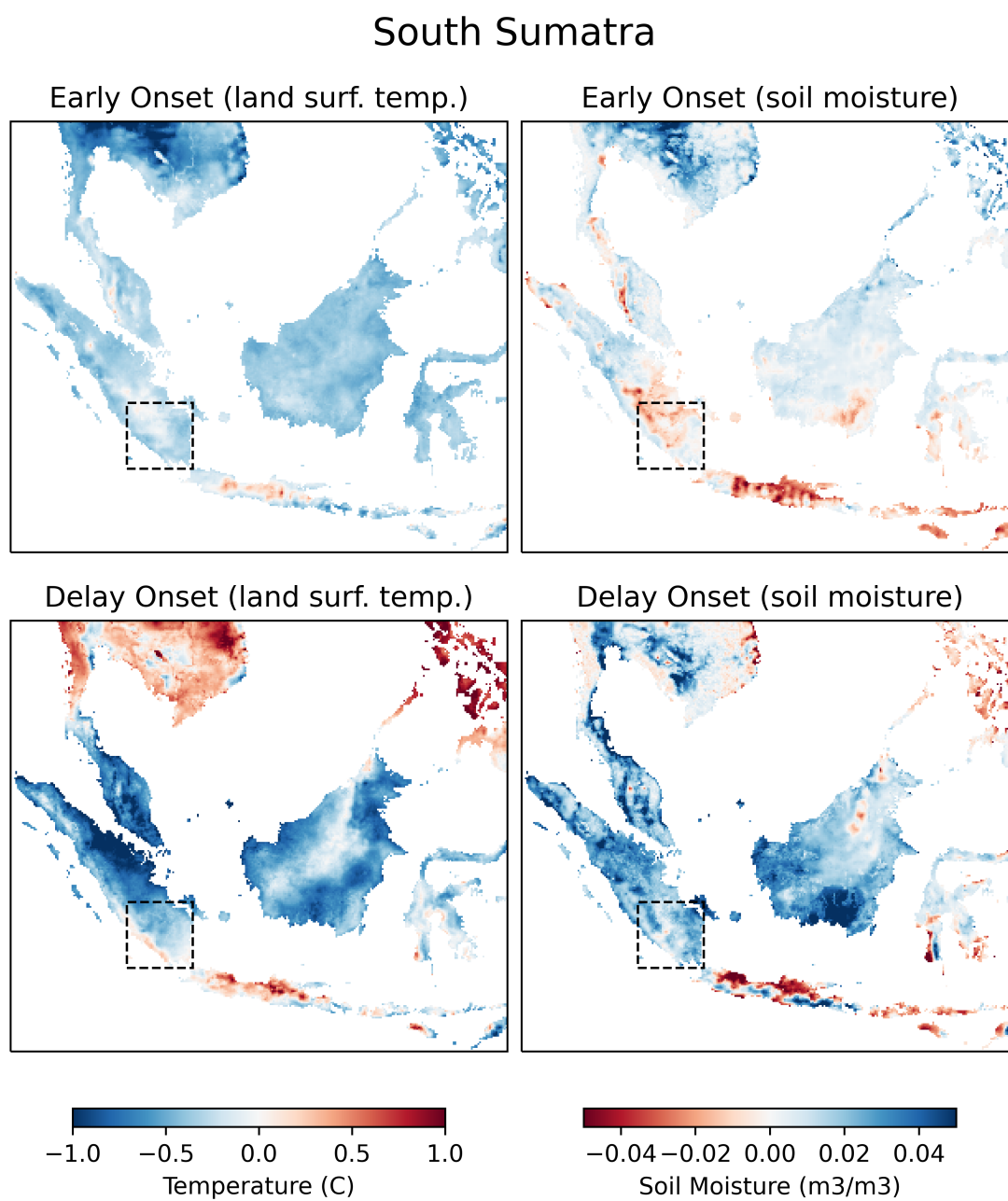
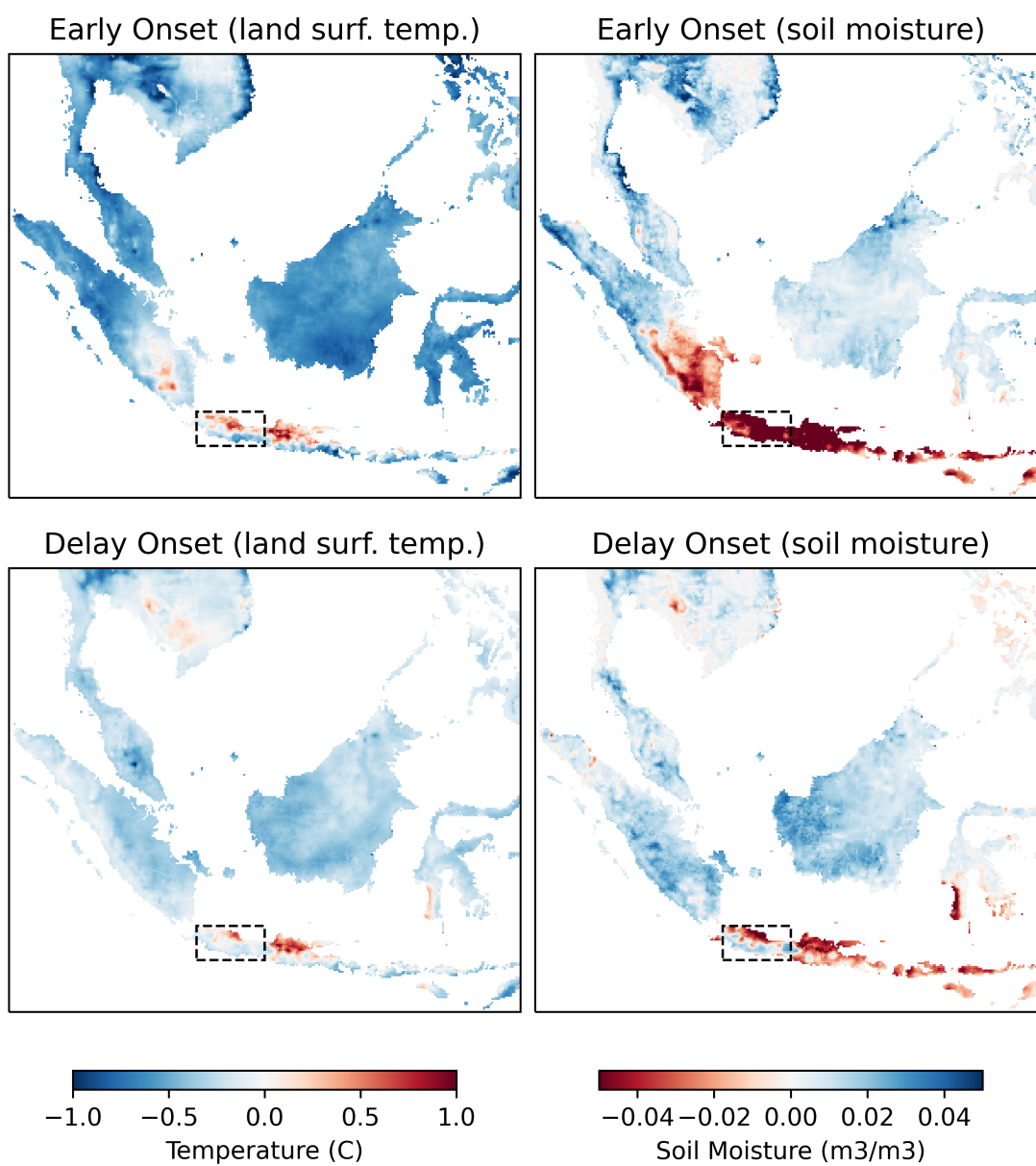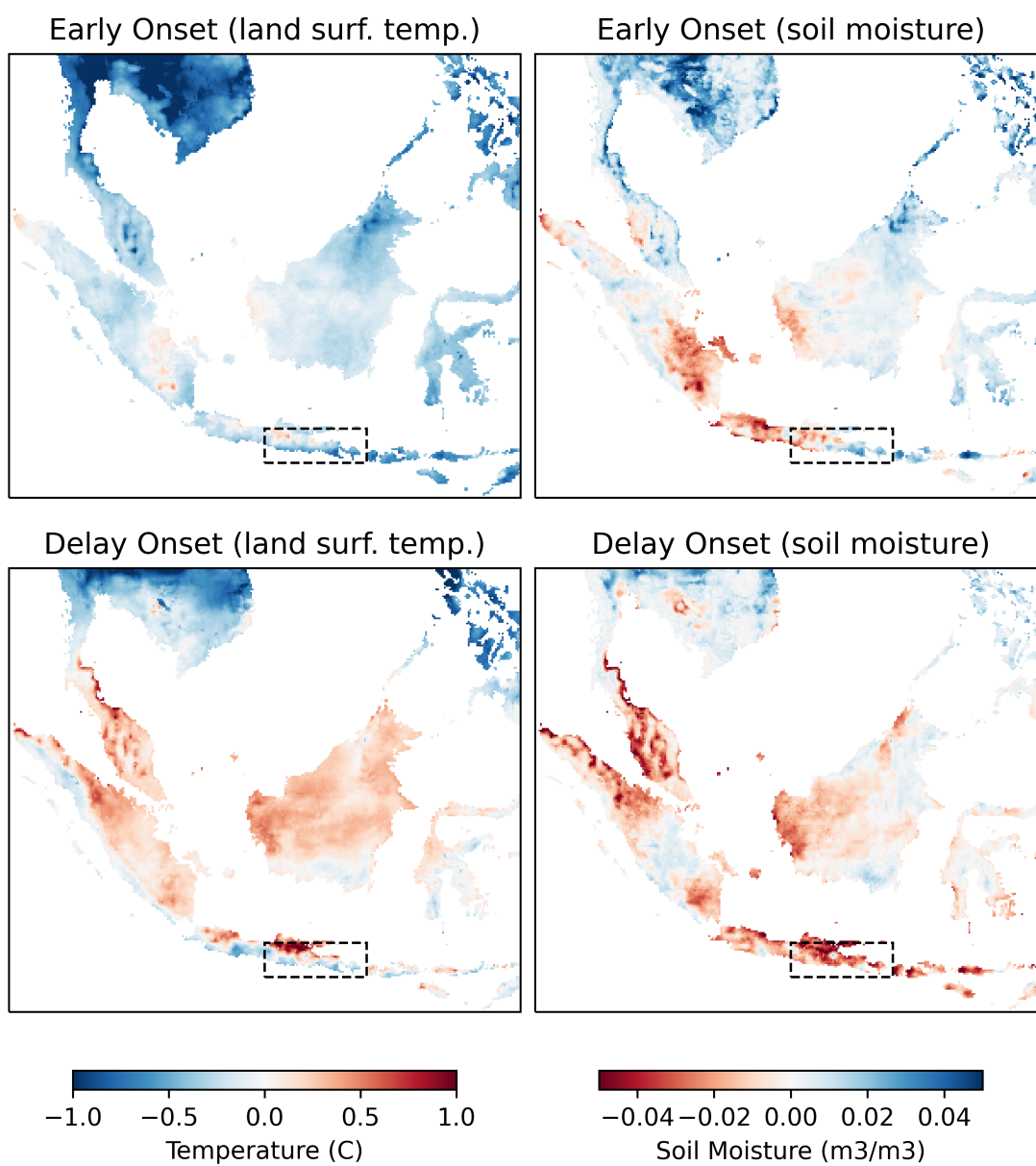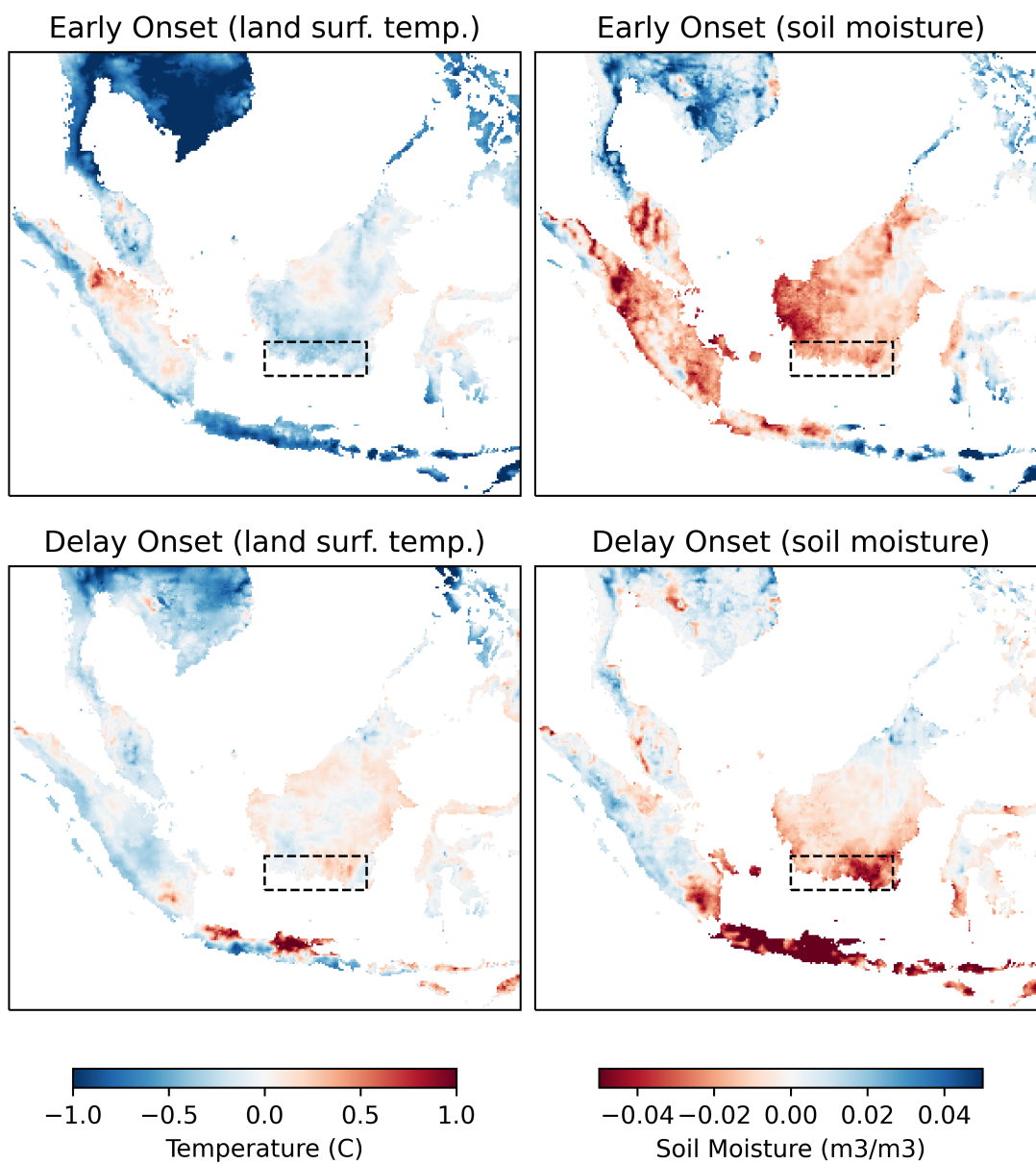# South Kalimantan

Figure 4.7: Composite of land surface temperature and soil moisture over the West Maritime Continent during pre-onset for the early and delayed onset at South Borneo.

References

Aldrian, E., & Susanto, R. D. (2003). Identification of three dominant rainfall regions within indonesia and their relationship to sea surface temperature. *International Journal of Cliamtology*, *23*(12), 1435–1452. https://doi.org/10.1002/joc.950

Amale, H. S., Birthal, P. S., & Negi, D. S. (2023). Delayed monsoon, irrigation and crop yields. *Agricultural Economics*, *54*(1), 77–94. https://doi.org/10.1111/agec.12746

Apriyana, Y., Surmaini, E., Estiningtyas, W., Pramudia, A., Ramadhani, F., Suciantini, S., Susanti, E., Purnamayani, R., & Syahbuddin, H. (2021). The Integrated Cropping Calendar Information System: A Coping Mechanism to Climate Variability for Sustainable Agriculture in Indonesia. *Sustainability*, *13*(11). https://doi.org/10.3390/su13116495

Bombardi, R. J., Moron, V., & Goodnight, J. S. (2019). Detection, Variability, and Predictability of Monsoon Onset and Withdrawal Dates: A Review. *International Journal of Climatology*, *40*(2), 641–667. https://doi.org/10.1002/joc.6264

Chang, C.-P., Li, T., & Yang, S. (2020). Monsoon rainfall prediction problem in the western Maritime Continent. In C.-P. Chang, K.-J. Ha, R. H. Johnson, D. Kim, G. N. C. Lau, & B. Wang (Eds.), *The Multiscale Global Monsoon System* (pp. 103–110). World Scientific. https://doi.org/10.1142/9789811216602_0009

Hamada, J.-I., Yamanaka, M. D., Matsumoto, J., Fukao, S., Winarso, P. A., & Sribimawati, T. (2002). Spatial and Temporal Variations of the Rainy Season over Indonesia and their Link to ENSO. *Journal of the Meteorological Society of Japan Ser II*, *80*(2), 285–310. https://doi.org/10.2151/jmsj.80.285

Haylock, M., & McBride, J. (2001). Spatial coherence and predictability of indonesian wet season rainfall. *Journal of Climate*, *14*(18), 3882–3887. https://doi.org/10.1175/1520-0442(2001)014⟨3882:SCAPOI⟩2.0.CO;2

Hersbach, H., Bell, B., Berrisford, P., Hirahara, S., Horányi, A., Muñoz-Sabater, J., Nicolas, J., Peubey, C., Radu, R., Schepers, D., Simmons, A., Soci, C., Abdalla, S., Abellan, X., Balsamo, G., Bechtold, P., Biavati, G., Bidlot, J., Bonavita, M., . . . Thépaut, J.-N. (2020). The ERA5 global reanalysis. *Quarterly Journal of the Royal Meteorological Society*, *146*(730), 1999–2049. https://doi.org/10.1002/qj.3803

Huffman, G. J., Stocker, E. F., Bolvin, D. T., Nelkin, E. J., & Tan, J. (2019). Gpm imerg final precipitation l3 1 day 0.1 degree x 0.1 degree v06 [Edited by Andrey Savtachenko, Greenbelt, MD, Goddard Earth Sciences Data and Information Services Center (GES DISC), Accessed: 19 April 2023, https://doi.org/10.5067/GPM/IMERGDF/DAY/06].

Lisonbee, J., & Ribbe, J. (2021). Seasonal climate influence on the timing of the australian monsoon onset. *Weather and Climate Dynamics*, *2*(2), 489–506. https://doi.org/10.5194/wcd-2-489-2021

Lisonbee, J., Ribbe, J., Otkin, J. A., & Pudmenzky, C. (2022). Wet season rainfall onset and flash drought: The case of the northern australian wet season. *International Journal of Climatology*, *42*(12), 6499–6514. https://doi.org/10.1002/joc.7609

Marjuki, van der Schrier, G., Tank, A. M. G. K., van den Besselaar, E. J. M., Nurhayati, & Swarinoto, Y. S. (2016). Observed Trends and Variability in Climate Indices Relevant for Crop Yields in Southeast Asia. *Journal of Climate*, *29*(7), 2651–2669. https://doi.org/10.1175/JCLI-D-14-00574.1

Moron, V., Robertson, A. W., & Boer, R. (2009). Spatial Coherence and Seasonal Predictability of Monsoon Onset over Indonesia. *Journal of Climate*, *22*(3), 840–850. https://doi.org/10.1175/2008JCLI2435.1

Moron, V., Robertson, A. W., & Qian, J.-H. (2010). Local versus regional-scale characteristics of monsoon onset and post-onset rainfall over indonesia. *Climate Dynamics*, *34*, 281–299. https://doi.org/10.1007/s00382-009-0547-2

Naylor, R. L., Battisti, D. S., Vimont, D. J., Falcon, W. P., & Burke, M. B. (2007). Assessing Risks of Climate Variability and Climate Change for Indonesian Rice Agriculture. *Proceedings of the National Academy of Sciences*, *104*(19), 7752–7757. https://doi.org/10.1073/pnas.0701825104

Notaro, M., Chen, G., Yu, Y., Wang, F., & Tawfik, A. (2017). Regional Climate Modeling of vegetation feedbacks on the Asian-Australian Monsoon systems. *Journal of Climate*, *30*(5), 1553–1582. https://doi.org/10.1175/JCLI-D-16-0669.1

Ratna, S. B., Cherchi, A., Osborn, T. J., Joshi, M., & Uppara, U. (2020). The extreme positive Indian Ocean Dipole of 2019 and associated Indian Summer Monsoon rainfall response. *Geophysical Research Letters*, *48*(2). https://doi.org/10.1029/2020GL091497

Robertson, A. W., Moron, V., Qian, J.-H., Chang, C.-P., Tangang, F., Alrdian, E., Koh, T. Y., & Liew, J. (2011). The Maritime Continent Monsoon. In C.-P. Chang, Y. Ding, N.-C. Lau, R. H. Johnson, B. Wang, & T. Yasunari (Eds.), *The Global Monsoon System, Research and Forecast 2nd Edition* (pp. 85–98). World Scientific. https://doi.org/10.1142/9789814343411_0006

Yasunari, T. (2007). Role of land-atmosphere interaction on asian monsoon climate. *Journal of the Meteorological Society of Japan*, *85B*, 55–75. https://doi.org/10.2151/jmsj.85B.55

Yu, Y., & Notaro, M. (2020). Observed land surface feedbacks on the Australian monsoon system. *Climate Dynamics*, *54*, 3021–3040. https://doi.org/10.1007/s00382-020-05154-0

Zhang, R.-H., Zhang, F., Zu, J., & Wang, Z. (2013). A successful real-time forecast of the 2010-2011 la niña event. *Scientific Reports*, *3*(1108). https://doi.org/10.1038/srep01108

Chapter 5

Conclusions

5.1 Key findings and implications

This dissertation has investigated the role of land-atmosphere feedback on various aspects of the Indonesian Maritime Continent (MC) complex system. The research questions addressed three key topics: the role of land surface properties on sea breeze circulations, the role of land-atmosphere interactions on the propagation of the Madden-Julian Oscillation (MJO) across the MC, and the role of land-atmosphere feedback on monsoon onset over the Maritime Continent.

Sea-breeze Analysis

The first research question addressed the effect of land surface properties on sea breeze circulation over the Indonesian Maritime Continent. Our study reveals that some regions exhibit strong sea breeze signals, i.e., the southwest coast of Sumatra, most of the coastline of Java, and most parts of Sulawesi, while Borneo and Papua mostly have weak sea-breeze signals. Our findings also highlight the importance of land surface properties in influencing sea breeze intensity. Using Granger causality analysis, we discovered a statistically significant causality between soil moisture and sea breeze intensity (F-test, $p < 0.05$). It means that past values of soil moisture (3 hours in advance) contain information that is useful for predicting sea breeze circulation intensity, providing a better understanding of the land-atmosphere interactions that drive sea breeze circulations over

the Indonesian Maritime Continent.

MJO Propagation across the Maritime Continent

The second research question addressed the role of the Indonesian Maritime Continent (MC) land-masses in the propagation of the Madden-Julian Oscillation (MJO) across the MC region. This study investigated the potential influence of land-atmosphere interaction over the Indonesian Maritime Continent on the propagation and behavior of the Madden-Julian Oscillation (MJO). The study analyzed the connection between land surface conditions and MJO propagation, revealing that the anomalously warmer land surface temperatures and drier soil moisture over parts of the Indonesian Maritime Continent (t-test, $p < 0.05$) tend to precede MJOs that pass through the MC. These findings suggest that land surface conditions over the Maritime Continent might play a role in blocking or allowing MJO propagation and highlight the need for further investigation of land-atmosphere interactions in intraseasonal variability.

Monsoon Onset

The third research question addressed the relationship between land surface conditions and monsoon onset variation over the western part of the MC. The land surface temperature and soil moisture composite during early and delayed onset years were analyzed, revealing that local land surface conditions contribute to the 1-2 weeks variation of monsoon onset. Specifically, the land surface temperature of nearby islands moderately contributes to the onset variation in South Sumatra and East Java, while soil moisture over neighboring islands contributes to the onset variation in South Borneo and West/Central Java. Overall, this study highlights the importance of local land surface conditions in affecting monsoon onset variations.

Implications

Our findings have several implications for improving our understanding of the MC complex system and its associated impacts on weather and climate. First, the results of the first research question suggest that an accurate representation of land-atmosphere feedback processes is essential

for improving regional climate modeling and weather forecasting, particularly in the MC region. Second, the results of the second research question highlight the importance of understanding land-atmosphere interactions and the role of the MC landmasses in the propagation of the MJO through the MC region. Better forecasting of the MJO could lead to improved predictions of weather and climate impacts associated with the MJO. Third, the results of the third research question provide valuable insights into the factors that drive monsoon onset variation over the western part of the MC, which can help improve the accuracy of monsoon onset predictions and better agricultural planning in the region.

5.2   Limitations and future work

Sea-breeze Analysis

The potential limitation of the sea breeze analysis is the reliance on the available data (ERA5 and ERA5-land). While the study incorporated a range of datasets and analytical techniques, there may be other data sources or analytical approaches that could be used to further improve the accuracy and resolution of the analysis. In addition, the determination of segments along the coastline was based on visual observation, which may limit the level of detail that can be achieved. These limitations may impact the generalizability of the findings and limit the scope of the analysis.

There are several potential areas for future work on the sea breeze analysis. One potential avenue for future research is to develop a more objective method for determining segments along the coastline. Currently, the determination of segments relies on visual observation, which may limit the level of detail that can be achieved. Using machine learning algorithms to learn the coastline shape and determine segments could provide a more objective and accurate approach to identifying segments, allowing for more detailed analyses of sea breeze circulation patterns.

Finally, future work on this chapter could include additional causality analyses beyond the Granger causality analysis that was used in the current study. Other approaches, such as machine learning-based causality analyses or Bayesian network modeling, could provide a more nuanced understanding of the causal relationships among land surface fluxes, sea breeze circulation, and

diurnal rainfall patterns along pre-defined transects. These alternative approaches could also be used to investigate the sensitivity of sea breeze circulation to different land surface variables and land use types, providing valuable insights for regional climate modeling and weather forecasting.

MJO Propagation

One potential limitation of the MJO propagation chapter is the limited sample size after MJO classification. While the current study focused on MJO events that interacted with the Maritime Continent region, excluding events that detoured around the region, this may have resulted in a relatively small sample size for the analysis. This could limit the statistical significance of the results and reduce the generalizability of the findings.

Despite these limitations, there are several potential areas for future work on the MJO propagation chapter. One potential avenue for future research is to expand the analysis to a longer period of time, allowing for a more comprehensive assessment of MJO variability and dynamics. This could help to address the issue of limited sample size and improve the statistical significance and generalizability of the findings. Additionally, future research could focus on refining the classification of MJO events and their interaction with the Maritime Continent region, taking into account a range of factors, such as MJO amplitude, intensity, and trajectory.

Furthermore, future work on this chapter could explore the role of land-atmosphere feedback in MJO propagation using more advanced modeling techniques, such as regional climate models. These models could incorporate a range of land surface variables and processes, such as vegetation cover, soil moisture, and surface temperature, to better capture the complex interactions between the land and atmosphere that influence MJO propagation.

Monsoon Onset

Future research on the monsoon onset analysis could investigate the specific processes and mechanisms that drive the relationship between land surface conditions and monsoon onset, using more advanced modeling techniques, such as regional climate models. This could lead to a better understanding of the underlying physical processes that drive monsoon onset variation and improve the

accuracy of monsoon onset predictions. Finally, future work could explore the potential impacts of climate change on monsoon onset and associated agricultural productivity, which is of particular importance for the many small-scale farmers who rely on monsoon rains for their livelihoods.